Curriculum Vitae

Megan Carmell Moorer
Molecular Medicine PhD student
University of Maryland, Baltimore
School of Medicine

DATE

May 3, 2018

CONTACT INFORMATION

EMAIL: moorer.megan@gmail.com

EDUCATION

August 2013 – May 2018	University of Maryland, School of Medicine; Graduate Program in Life Sciences; Molecular Medicine, PhD; GPA: 3.82
Graduated May 2011	Auburn University at Montgomery; Montgomery, AL; B.S. Biology, Concentration in Molecular Biology, Minor in Chemistry; GPA: 3.5

COURSEWORK

Graduate:

2013	Mechanisms in Biomedical Sciences: Core Course	GPILS 601
2013	Current topics in Genetics and Genomics	GPILS 692
2014	Cell and Systems Physiology	GPILS 645
2014	Advanced Cancer Biology	GPILS 790
2014	Topics in Molecular Medicine	GPILS 750
2014	Research Ethics	CIPP 907
2015	Bio statistical Methods	PREV 621
2015	Molecular Mechanisms of Signal Transduction	GPILS 616
2015	Molecular Medicine Survival Skills	GPILS 647

Undergraduate:

Biology 1 and 2
Chemistry 1 and 2
Organic Chemistry 1 and 2
Biochemistry
General Microbiology
Genetics
Developmental Biology
Histology
Cell Biology
Immunology
Epidemiology
Molecular Genetics

EXPERIENCE

University of Maryland, School of Medicine (UMB)

PhD Thesis: Joseph Stains, Ph.D.
June 30 2014 – present
Project title: Connexins as Active Regulators of Signal Transduction in Bone

Auburn University of Montgomery

Mentor: **Dr. Robert Estes,** Undergraduate Directed Research
June 2010 to May 2011

TECHNICAL EXPERTISE

1. Primary and cell line cell culture including transient transfections
2. qRT-PCR
3. Micro-computed Tomography (Micro CT)
4. Histology
5. Luciferase assays
6. Western blotting
7. Co-Immunoprecipitations
8. Immunofluorescence
9. Mouse colony maintenance
10. Mineralization assays

PROFESSIONAL SOCIETY MEMBERSHIPS

2015-present	American Society for Bone and Mineral Research

HONORS AND AWARDS

2011	Undergraduate Research Symposium participant
2015	Young Investigator Travel Award, ASBMR
2016	Young Investigator Travel Award, ASBMR
2016	Awarded "APS select Distinction in Scholarship" award for manuscript [PMID: 27605453]
2018	UMB Graduate Research Conference– Poster session Winner

INSTITUTIONAL SERVICE

2016	Molecular Medicine Program Recruitment, University of Maryland School of Medicine
2016	Molecular Medicine Research Retreat committee, University of Maryland School of Medicine
2016	Poster Session Judge, Molecular Medicine Research Retreat, University of Maryland School of Medicine
2016/2017	Graduate Student Association (GSA) Molecular Medicine Program Representative

2017/2018	Graduate Student Association (GSA) Vice President
2017/2018	USGA Graduate School Primary Senator

PUBLICATIONS

First Author

1. **Moorer MC**, Buo AM, Garcia-Pelagio K, Stains JP, Bloch RJ (2016) Deficiency of the intermediate filament synemin reduces bone mass in vivo. Am J Physiol Cell Physiol. [PMID: 27605453] ***This work was highlighted by an Editorial Focus***.
2. **Moorer MC**, Hebert C, Tomlinson RE, Liu S, Chason M, Stains JP (2017). Truncation of the Cx43 C terminal domain leads to a skeletal phenotype resembling deletion of full length Cx43. Journal of Cell Science. [PMID: 28049723]
3. **Moorer MC**, Stains JP (2017). Connexin43 and the intercellular signaling network regulating skeletal remodeling. Current Osteoporosis Reports. [PMID: 28181063]

Contributing author

1. Gupta A, Anderson H, Buo AM, **Moorer MC**, Ren M, Stains JP (2016) Communication of cAMP by connexin43 gap junctions regulates osteoblast signaling and gene expression. Cell Signal [PMCID: PMC4899183].

SUBMITTED PUBLICATIONS

1. Diminished activity of canonical WNT/β-catenin signaling during osteogenic differentiation impedes skeletal development in progeria. Ji Young Choi, Jim K Lai, Zheng-Mei Xiong, Margaret Ren, **Megan C Moorer**, Joseph P Stains, Kan Cao. Aging Cell, **submitted** 12/5/17.

ABSTRACTS

1. **Moorer MC**, Hebert C, Stains JP (2015) Structure-Function Analysis of Connexins as Active Regulators of Signal Transduction in Osteoblasts. American Society for Bone and Mineral Research, Seattle WA. *Oral presentation and Plenary poster. Young Investigator Travel Award Winner (MCM)*.

2. **Moorer MC**, Hebert C, Stains JP (2015) Structure-Function Analysis of Connexins as Active Regulators of Signal Transduction in Osteoblasts. University of Maryland, Baltimore Graduate Research Conference. *Poster presentation.*

3. **Moorer MC**, Hebert C, Tomlinson RE, Liu S, Chason M, Stains JP (2016) Truncation of the Cx43 C-terminal domain disrupts multiple signaling pathways and recapitulates the skeletal phenotype of full length Cx43 conditional deletion in the osteoblast lineage. American Society for Bone and Mineral Research, Atlanta GA. *Plenary poster. Young Investigator Travel Award Winner (MCM).*

4. **Moorer MC**, Hebert C, Tomlinson RE, Liu S, Chason M, Stains JP (2016) Truncation of the Cx43 C-terminal domain disrupts multiple signaling pathways and recapitulates the skeletal phenotype of full length Cx43 conditional deletion in the osteoblast lineage. Molecular Medicine PhD program retreat, University of Maryland, Baltimore. *Poster presentation.*

5. **Moorer MC**, Hebert C, Tomlinson RE, Liu S, Chason M, Stains JP (2017) Truncation of the Cx43 C-terminal domain disrupts multiple signaling pathways and recapitulates the skeletal phenotype of full length Cx43 conditional deletion in the osteoblast lineage. University of Maryland, Baltimore Graduate Research Conference. *Poster presentation.*

6. **Moorer MC**, Hebert C, Joca HC, Stains JP (2017) Connexins form distinct complexes with signaling machinery that differentially affect osteoblast signaling and gene expression. American Society for Bone and Mineral Research, Denver, CO. *Poster presentation (*presented by another lab member)*.

7. **Moorer MC**, Hebert C, Joca HC, Stains JP (2018) Connexins form distinct complexes with signaling machinery that differentially affect osteoblast signaling and gene expression. University of Maryland, Baltimore Graduate Research Conference. *Poster presentation*.

8. **Moorer MC**, Hebert C, Joca HC, Stains JP (2018) Connexins form distinct complexes with signaling machinery that differentially affect osteoblast signaling and gene expression. University of Maryland, Baltimore. Training Program in Integrative Membrane Biology Retreat. *Poster presentation*.

PROPOSALS/GRANTS

1. 1F-31AR072445-01. (NIH/NIAMS) Structure-Function Analysis of Connexins as Active Regulators of Signal Transduction in Osteoblasts. PI: **Moorer MC**. Submitted December 8, 2016. Not funded.

MANUSCRIPT REVIEW

1. *Ad Hoc* reviewer – Cellular Physiology and Biochemistry, 2017.
2. *Ad Hoc* reviewer – Journal of Bone and mineral Research, 2018.

SEMINARS

1. **Megan C. Moorer**. “Gap junctions, Signaling, and Bone”. University of Utah. Salt Lake City, UT, January 19, 2018.

2. **Megan C. Moorer**. “Gap junctions, Signaling, and Bone”. Johns Hopkins University. Baltimore, MD, February 9, 2018.

3. **Megan C. Moorer**. “Gap junctions, Signaling, and Bone”. University of Western Ontario. London, Ontario, Canada, March 26, 2018.

Abstract

Title: Connexins as Active Regulators of Signal Transduction in Bone

Megan Carmell Moorer, Doctor of Philosophy 2018

Dissertation Directed by: Joseph P. Stains, PhD., Associate Professor, Department of Orthopedics

Intercellular communication by gap junctions plays an important role in achieving peak bone mass and determining bone quality. Deletion of the gap junction protein connexin43 (Cx43) in mice impairs bone quality (osteopenia), and results in a cortical structure resembling aging and disuse. Although it is clear that Cx43 plays a role in osteoblast function and bone mineralization, the molecular mechanism underlying the specific roles of Cx43 are not well defined. Contrastingly, osteoblasts also express connexin45 (Cx45) and its role in osteoblasts has not been extensively studied and nothing is known about its role in skeletal tissue *in vivo*. Cx43 and Cx45 form gap junctions with different molecular permeability, or pore sizes (<1kD <0.3kD) and seem to have opposing functions in bone biology. While gap junctions are generally thought of as passive conduits for small molecules to be shared between cells, growing evidence indicates that connexins actively contribute to downstream signaling. Modulation of Cx43 expression impacts PKCδ, ERK1/2 and β-catenin signaling pathways i*n vitro*, which influence osteoblast gene expression and function. The regulation of signal transduction downstream of intercellular communication may involve assembly of a specific subset of effectors to the gap junction. The work presented

in this thesis examines the influence of the C-terminus (CT) of connexins on osteoblast signaling and function through physical interactions with effectors like β-catenin, ERK(1/2), CREB, and PKCδ, both *in vivo* and *in vitro*. The **central hypothesis** of this work is that in addition to having distinct molecular permeability, each connexin can assemble a unique "interactome" of locally recruited signaling machinery that can affect downstream signaling from the gap junction and ultimately, bone cell function. We characterized the skeletal phenotype of a Cx43 truncation mouse model. The absence of the Cx43 CT in mice resulted in an osteopenic skeletal phenotype analogous to osteoblast conditional deletion of the entire Cx43 gene including cortical thinning and increased cross-sectional area, defective signaling, reduced gene expression, and altered collagen processing. These data imply that Cx43-containing gap junctions not only exchange signals, but also recruit signaling machinery to the Cx43 CT domain to optimally affect cell signaling, cell function, and bone acquisition. We also determined the requirement for both pore permeability (pore function) and signal effector protein recruitment (tail function) to Cx43 and Cx45 in osteoblast signaling and function using chimeric constructs composed of portions of Cx43 and Cx45. By luciferase reporter assays, western blot analysis, and qPCR, we found that, in general, both the Cx43 pore and Cx43 tail are required for optimal osteoblast signaling and gene expression, as Cx45 overexpression was ineffective or inhibitory in all aspects, while Cx43 overexpression stimulated signaling and gene expression. The chimeras largely mimicked Cx45 or had an intermediate effect. We also further defined the interactomes of Cx43 and Cx45 to determine their requirement for affecting osteoblast function. Through co-immunoprecipitation, our data shows binding of ERK(1/2), CAMKII, and β-catenin to

Cx43 but not to Cx45, which is consistent with the idea of differential interactomes. In total, these data imply that each connexin can differentially regulate downstream signaling and gene expression from the gap junction by local recruitment of different signaling effector molecules to each connexin's CT in order to affect bone cell function and bone modeling and remodeling.

Connexins as Active Regulators of Signal Transduction in Bone

by
Megan C. Moorer

Dissertation submitted to the Faculty of the Graduate School of the
University of Maryland, Baltimore in partial fulfillment
Of the requirements for the degree of
Doctor of Philosophy
2018

Acknowledgements

I would like to acknowledge all the wonderful people who have been supportive of me through the years to reach this priceless moment in my life.

First, I would like to thank my mentor, Dr. Joseph P. Stains, for his support through the years. Dr. Stains has always encouraged me to push beyond my comfort zone and reach new heights. He taught me invaluable amounts through lessons and knowledge concerning science, independence, and patience. His belief in me as a person and scientist has contributed to the person and scientist I am today. He has allowed me to flourish scientifically, making my self-confidence to be a successful, independent researcher a reality.

Secondly, I would like to thank my committee members, Dr. Doug DiGirolamo, Dr. Brian Mathur, Dr. Paul Shapiro, Dr. Dudley Strickland, and Dr. Bruce Vogel, for their continued support and advice through the last few years. I am forever grateful to each one of them for their guidance. My committee has always come with great suggestions for furthering the investigation of my thesis work.

Last, but certainly not least, I would like to thank my family and friends, for all the moral support and love I've consistently received through the process of graduate school. It's been a long road to travel, and my family and friends have always been there to keep me company and keep me focused on the goal at hand.

Table of contents

List of Figures

Tables

List of Abbreviations

ALP – alkaline phosphatase

BV – bone volume

BFR – bone formation rate

BMSC – bone marrow stromal cell

BSP – Bone sialoprotein

CAMKII – Calcium/calmodulin dependent protein kinase II

cAMP – cyclic adenosine monophosphate

CCD – cleidocranial dysplasia

CCK-8 – Cell Counting Kit -8 (colorimetric assay)

cKO – conditional knock out

CMD – craniometaphyseal dysplasia

Co-IP – co-immunoprecipitation

Col1α1 – Type I collagen

CT – C terminal domain/tail

Cx43 – connexin43

Cx43 CT – Cx43 C terminus

Ct.Th – Cross-sectional thickness

CTX – collagen 1 C-terminal telopeptide

Cx45 – connexin45

Cx37 – connexin37

DMP1 – dentin matrix acidic phosphoprotein 1

Ec.Pm – endosteal perimeter

FGF2 – fibroblast growth factor 2

Gja1 – gap junction alpha protein (Connexin 43 gene)

ERK – Extracellular signal-related kinase

HSP47 – heat shock protein 47

i.p. – intraperitoneal

IP3 – inositol triphosphate

IP7 – inositol polyphosphate

kDa – kilo Dalton

Lox – lysyl oxidase

MAR – Mineral apposition rate

Micro CT – Micro computed tomography

MMA – methylmethacrylate

MMI – Mean polar moment of inertia

MSC – mesenchymal stem cell

Ob. N – osteoblast number

Ob.S/BS – osteoblast surface per bone surface

OCN - osteocalcin

ODDD – oculodentodigital dysplasia

Oc. N – osteoclast number

Oc.S/BS - osteoclast surface per bone surface

OPG – osteoprotegerin

Osx – Osterix

PGE2 – Prostaglandin E2

PKCδ – Protein Kinase C-delta

P1NP – total procollagen type 1 N-terminal peptide

Ps.Pm – periosteal perimeter

PTH – parathyroid hormone

qRT-PCR – quantitative reverse transcription polymerase chain reaction

RANKL – receptor activator of nuclear factor kappa B ligand

Runx2 – Runt-related transcription factor 2

SOST - Sclerostin

trabecular BV/TV – trabecular bone volume per tissue volume

Tb.N, - trabecular number

Tb.Th. – trabecular thickness

TbSp – trabecular spacing

TRAP – tartrate resistant acid phosphatase

TV – tissue volume

WT – wild type

ZO-1 – zona-occludens 1

Chapter 1: Connexin43 and the Intercellular Signaling Network Regulating Skeletal Remodeling.[1]

1. *Basic Bone Biology*

The skeletal system is an evolutionary adaptation becoming the distinguishable difference between vertebrates and invertebrates. The skeleton of an organism is composed of a mineralized biological composite material, consisting of mostly cartilage and bone. Most would think of bones as just playing a protective and structural role, but bones have many other physiological roles. They serve as leverage for movement, a niche for hematopoiesis, along with regulating glucose and circulating phosphate and calcium levels. Like most organs, bone is a biologically active tissue that is constantly formed and remodeled to help maintain structural integrity. Furthermore, mechanical strain, hormones and growth factors dynamically regulate bone turnover. Through this process of tissue remodeling, the human skeleton is effectively "replaced" every ten years on average.

Bone can take many shapes, in order to accommodate specific anatomic functions. There are several types of bone: long, flat, short, irregular, and sesamoid. Long bones such as the femur, tibia, and humerus are located in the arms and legs and are cylindrical, with a hollow shaft and mineralized outer shell. The shaft is called the diaphysis and the ends of long bones are termed the epiphyses of the bone. Short bones, such as the wrist and ankle bones, have a cube-shape. Flat bones such as the skull bones are thinner but have many surfaces of muscle attachments. Sesamoid bones are unique in that only form

[1] Moorer MC, Stains JP. Connexin43 and the intercellular signaling network regulating skeletal remodeling. *Current osteoporosis reports*. 2017;15(1):24-31. doi:10.1007/s11914-017-0345-4.

in locations where there are fair amounts of tension and stress, such as the patella. Irregular bones are bone that cannot be classified as long, short or flat bones. Examples of irregular bones are the hyoid bone, the pelvis, and vertebrae surrounding the spinal cord. They serve a protective function, and their shape represents the need for skeletal tissue to morph into appropriate shapes to protect and maintain internal structural integrity within the organism.

Developmentally, bone is formed through two mechanisms: endochondral ossification and intramembranous ossification. In endochondral ossification, bone is formed by osteochondral progenitors differentiating into chondrocytes, forming the template (or anlage) for future bone formation. These chondorcytes also eventually contribute to the growth plates of long bones, permitting longitudinal growth. Endochondral ossification occurs in long bones and most other bones within the human body. During embryogenesis, a bone collar is formed around the cartilaginous model. A primary ossification center becomes apparent at the shaft or middle of long bones as blood vessels move into the developing tissue. At birth, a secondary ossification center is formed at the two ends, or epiphyses of long bones. Appositional growth occurs, allowing diameter increases of the cortical shell in bone, as well as growth in length of long bones from the growth plate. Endochondral ossification also occurs after a skeletal fracture. Intramembranous ossification is more direct, where the osteochondral progenitors aggregate and directly differentiate into osteoblasts, without a cartilaginous intermediate, to form skeletal tissue. Mesenchymal stem cells form a cluster and change morphologically, becoming osteoprogenitor cells. Intramembranous ossification occurs in the bones of the skull and jaw as well as the clavicle.

Long bones are the primary focus of this project. Most long bones are composed of two types: cortical and trabecular bone. Cortical bone is the outer shell of long bones. It is dense, compact and, and more involved in the protective and structural functions. Trabecular bone is found in the marrow cavity, is more porous than cortical bone, and is involved in the metabolic function and hematopoietic support. Bone tissue is composed of two main components: organic content and mineral content. The organic content of bone consists of extracellular matrix, named osteoid in this context, and cellular content. Osteoid is mostly made up of Type I Collagen, which is a triple helix of 2 alpha-1 chains and 1 alpha-2 chain. The mineral content, composed of hydroxyapatite crystals and other crystalline salts, forms on the osteoid matrix, like rebar and concrete, giving bone great compressive, tensile and torsional strength.

Bone is composed of mainly four cell types: osteoblasts, osteocytes, osteoclasts, and bone lining cells. Osteoblasts form new bone by depositing collagen rich osteoid that will eventually nucleate the hydroxyapatite crystals. When osteoblasts become embedded in the calcified matrix, they become osteocytes and are the most abundant cell type in bone tissue. Osteocytes play an integral role in regulating bone turnover, allowing signaling to osteoblasts and osteoclasts for either bone formation or resorption. Bone lining cells are considered quiescent cells and may serve as a source of osteoblast progenitor cells. Osteoclasts are macrophage like cells with multiple nuclei that dissolve and break down bone by secreting acids and proteolytic enzymes to dissolve and degrade the calcified matrix and organic osteoid, respectively [[1]]. A balance of bone formation and resorption contributes to bone quality. Therefore, a defect in this balance may lead to disease, such as osteoporosis.

2. Bone is a tissue requiring exquisite intercellular coordination

Bone is a dynamically regulated tissue involving cross-talk between cells to coordinate tissue formation, remodeling, and repair. As such, the cells of bone form an extensive interconnected network. Bone embedded osteocytes link up with each other and with surface osteoblasts and osteoprogenitors via long dendritic processes that pass through the bone canalicular system. These osteocytes orchestrate the tightly controlled process of bone remodeling by directing the differentiation and activity of surface osteoblasts and osteoclasts to synthesize, resorb, and repair skeletal tissue ([2–4]). In the absence of tight coordination of this network of cells, bone quality can be diminished, leading to skeletal fragility. Osteocytes are permanent cells in bone, surviving for decades encased in bone, while osteoblasts and osteoclasts are transient, only becoming active on demand from cues such as growth factors, and hormones and mechanical load. So, an important question in the field is how do these osteocytes, which are encased in bone and distally removed from the bone surface, influence the surface osteoblasts and osteoclasts? One proposed mechanism is that osteocytes influence bone turnover through direct intercellular communication with cells on the surface of bone through gap junctions.

3. Osteogenesis

Osteogenesis has five major steps starting with mesenchymal stem cells and ending with a mature osteocyte (**Figure 1.1**). Once a mesenchymal stem cell expresses the transcription factor, Runx2, it becomes a pre-osteoblast/osteochondral progenitor.

Runx2 is a master regulator of osteogenesis. Deletion of Runx2 in mice leads to mice born with no bones and an absence of osteoblasts ([5]). Mutations of a single allele of Runx2 cause a disease called CCD, or cleidocranial dysplasia in humans, and is characterized by an under mineralized skeleton among other skeletal defects. Markers for pre-osteoblast/osteochondral progenitors are low levels of alkaline phosphatase and Type I Collagen, and fibronectin expression. The cell will become differentiated into a matrix depositing osteoblast once the transcription factor, osterix, is expressed and the cell becomes more cuboidal. Osterix deficiency also results in mice born without a mineralized skeleton and no osteoblasts, and mutations in osterix lead to a form on osteogenesis imperfecta, or brittle bone disease, in humans ([6]). Markers for matrix depositing osteoblasts are osterix expression and high levels of Type I collagen and alkaline phosphatase. The next stage is a mineralizing osteoblast which express markers like bone sialoprotein (BSP), osteocalcin (OCN), alkaline phosphatase (ALP) and osterix (OSX). These cells are associated with the production of an ossified extracellular matrix. The last stage is a mature osteocyte, which is encased in bone with long dendritic processes that extend through bone by canalicular networks. These dendritic processes interconnect osteocytes with each other and with osteoblasts and osteoclasts on the surface of bone, forming an interconnected cell network. Lineage markers for osteocytes include osteocalcin (OCN), dentin matrix protein 1(DMP1), RANKL, FGF23, and sclerostin (SOST). Disruption of osteogenesis leads to malformation and diseases such as osteoporosis, rickets, osteogenesis imperfecta, and oculodentodigital dysplasia [[1,7]].

4. Gap junctions: conduits on the information superhighway

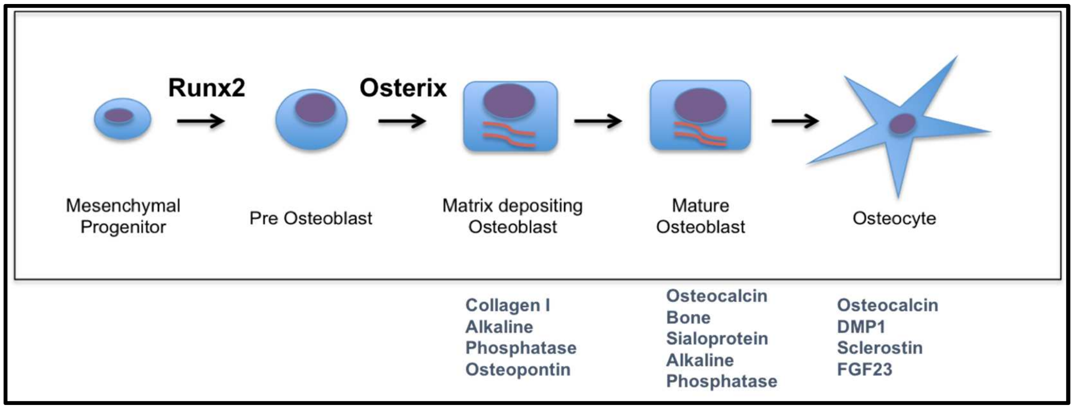

Figure 1.1. Osteoblastogenesis: the process of osteoblast differentiation. Osteoblasts are derived from mesenchymal stem cells.
Runx2 is a transcription factor that commits a cell to become a bone cell. Osterix is a transcription factor that allows further differentiation of the cell, causing osteoblasts to make and deposit extracellular matrix. Without these two transcription factors, mineralized bone will not form. As cell progress through the lineage, the cells express certain proteins, such as Type 1 collagen, Alkaline Phosphatase and osteocalcin, which are used as markers for each stage. A terminally differentiated osteoblast becomes an osteocyte.

One method bone cells coordinate their actions is by intercellular communication through gap junctions. Gap junctions form aqueous channels that allow the direct exchange of small ions, molecules, and second messengers between cells. This allows for efficient intercellular communication and functional coordination through an interconnected cellular network. A useful analogy is to think of the gap junction-coupled cellular network as a telecommunications network, with gap junctions being the point of *data* exchange between components that allow efficient communication, comparable perhaps to the *modem/router* (**Figure 1.2A)**.

To extend this analogy in bone, the osteocytic cell processes are comparable to the *cables* and *wires* connecting the different cells of the bone communication network (**Figure 1.2A**). At the intersection of two osteocyte cell processes or where osteocytes and osteoblast lineage cells touch, gap junctions form and facilitate direct cell-to-cell communication (**Figure 1.2B)**. The osteocyte itself would be comparable to the *server*, sending out information to the *workstations* (e.g., osteoblasts and their progenitors) on the bone surface. As such, the gap junction plays important roles in permitting, regulating and responding to the shared *data* in the form of small molecules, ions, and second messengers.

It is becoming increasingly accepted that gap junctions regulate the *data* they permit to be communicated and acted on in numerous ways, including the monomeric composition of the gap junction channel, the relative abundance of the connexins, and the local recruitment of signaling machinery to the gap junction plaque. Gap junctions form from the assembly of connexin monomers (**Figure 1.3**). Each connexin has four transmembrane domains, 2 extracellular loops, and intracellular N and C terminal domains. Connexin protein hexamers in the plasma membrane form a hemi-channel, also called a connexon. When a hemichannel in one cell aligns with a hemichannel in a neighboring cell, a gap junction pore is formed, creating an aqueous channel between the cytoplasm of the coupled cells. These gap junctions aggregate into larger gap junction plaques, composed of hundreds to thousands of gap junction channels ([8,9]).

Humans have 21 genes encoding connexin proteins, and the specific connexin composition of a gap junction influences the size and charge selective permeability as well as the open/closed state probability of the channel ([9,10]). Further, most tissues, including bone, express multiple connexins and these can interact to form both hexameric (*e.g.*, mixed channels of connexin43 and connexin45) and heterotypic gap junctions (*e.g.*, a connexin43 containing hemichannel docked to a connexin45 hemichannel ([11]). Thus, there is great plasticity in the molecules that can be exchanged by gap junctions. Another way that gap junctions can regulate intercellular communication is by regulating the relative abundance of connexins in a plaque, effectively tuning the *bandwidth* of the communication network with increasing gap junctions enhancing the efficiency of communication ([12]).

Furthermore, emerging data support a model in which gap junctions not only serve as passive conduits for the intercellular exchange of small molecules, but gap junction also assemble large complexes of signaling machinery. These signaling complexes not only regulate the open/closed state probability of the channel (affecting *bandwidth*), but may also serve as a docking scaffold for recruiting effectors of downstream signaling ([13–15]).

As with any effective communication, there must be a process to receive the communicated information. This pre-assembled complex of signaling machinery at the

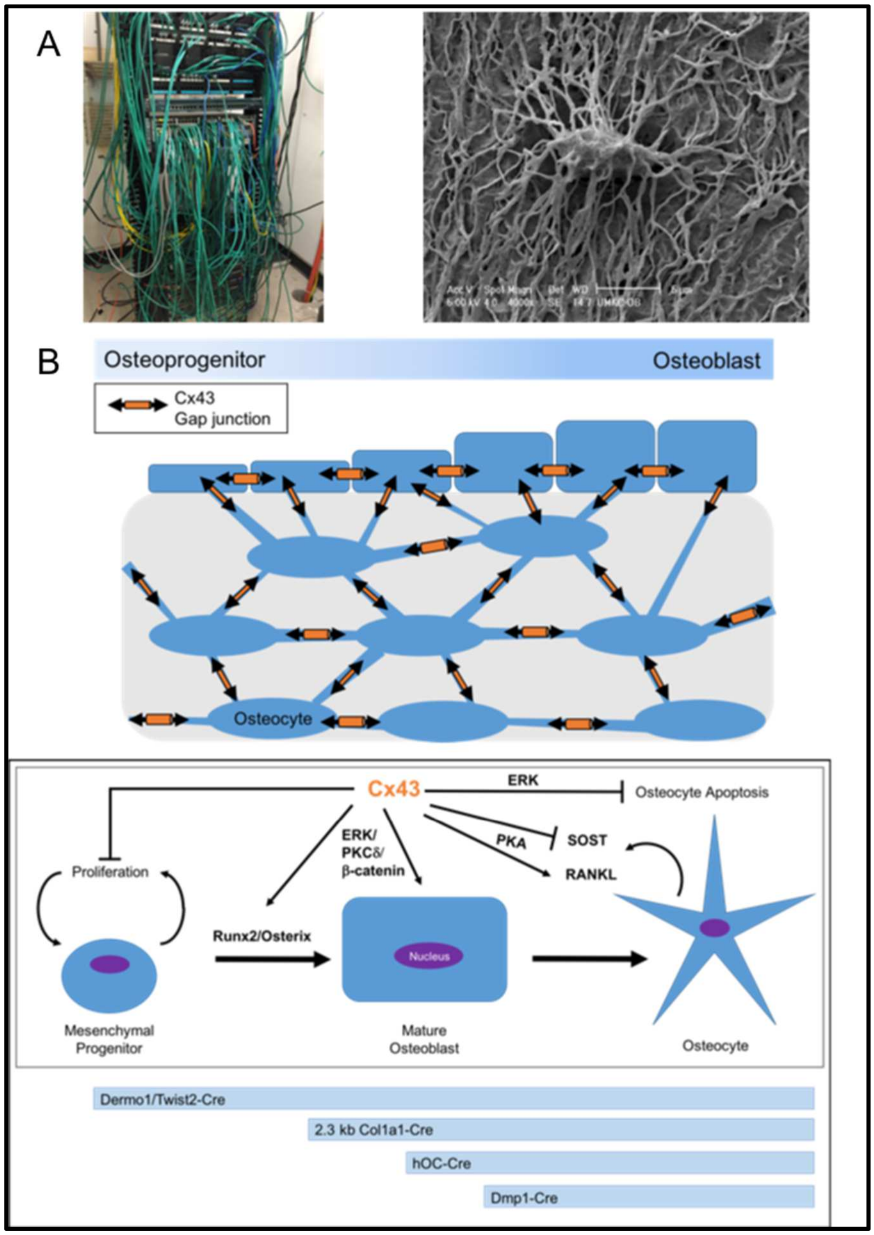

Figure 1.2. A. Left, image of IT network cables. Right, back-scatter scanning electron micrograph of an acid-etched resin embedded murine femoral cortical bone sample showing a resin-filled osteocyte lacunae and the many resin filled osteocyte canaliculi (Image provided by Lynda Bonewald, IUPUI). We propose the basic analogy of the osteocyte-osteoblast network to a telecommunication/IT network. **B**. Model of the interconnected cellular network within bone by gap junctions, containing osteoprogenitors, osteoblasts, and osteocytes. **C**. Top, osteoblastogenesis model and the influence of connexin43 on various aspects of the differentiation/survival program of these cells. Below, timeline of expression of promoters used in osteoblast-lineage conditional knockout models.

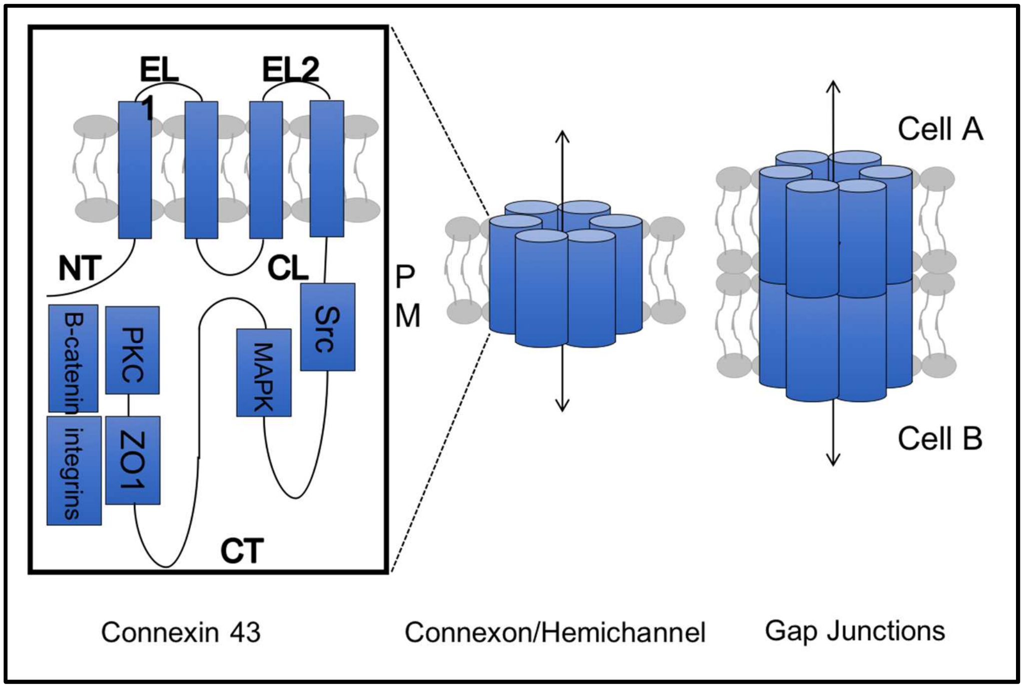

Figure 1.3. Structure of connexins and gap junctions. NT: N-terminus. EL1: extracellular loop 1. EL2: extracellular loop 2. CL: cytoplasmic loop. CT: C-terminus. PM: plasma membrane. Boxes on CT indicate binding sites for proteins.

connexin43 plaque may serve this purpose. In addition, the assembly of specific signaling effectors to the gap junction permits even more specificity and control in regulating the *data* exchanged through this intercellular network.

5. Gap Junctions in bone: the skeletal information network

Connexin43 is the most abundant (and most studied) connexin present in the osteoblast lineage and allows passages of molecules and second messengers less than ~1.2 kDa, with a preference for negatively charged molecules ([16–19]).

There is growing evidence that connexin43 may be able to pass larger molecules, including siRNA or miRNAs with shapes permissive of traversing the gap junction channel ([20,21]). Other connexins are also expressed in osteoblast lineage cells, including connexin45, connexin46 and connexin37 ([22–25]), but a critical role for these other connexins in the osteoblast lineage has not been established. The gap junctions that form from connexin monomers occur not only between osteoblasts and osteoprogenitors on the bone surface, but also at the long dendritic cell processes of osteocytes that extends through the canalicular network. The result is a functional syncytium of cells throughout bone. It is through this network of cells that information is passed between cells in a gap junction-dependent manner to affect bone formation and resorption to ultimately impact bone quality. While much of what is known about connexin biology in the skeleton has been studied in cells of the osteoblast lineage, osteoclasts also express several gap junction proteins, including connexin37 and connexin43 ([25–27]). A skeletal phenotype has been reported in osteoclast-lineage knockouts connexin37 *in vivo* ([25]). Interestingly, despite overlap in connexin expression, there is little evidence that the osteoblasts and osteoclasts directly communicate via gap junctions. Since the connexin in these bone resorbing osteoclasts do not appear to be directly *plugged in* to the intercellular communication syncytium of osteoblasts, osteocytes and their progenitors, we will not focus on them here.

6. Taking the bone cellular network offline: models of connexin-mutation or deficiency

The fundamental observations that connexins, and connexin43 in particular, play an important role in bone function has come from several loss of function studies performed in animal models. These findings have been confirmed by the observation of a role for connexin43 in human diseases with musculoskeletal involvement, including oculodentodigital dysplasia and craniometaphyseal dysplasia ([28,29]). When the bone intercellular communication network is "*taken offline*" by connexin43 gene deletion in healthy mice, the consequences for the skeleton are reproducibly poor, leading to defective osteoblast differentiation. Point mutations in Gja1, the gene encoding human Connexin 43, cause ODDD, or oculodentodigital dysplasia. This is an autosomal dominant disorder affecting the skeletal structure and architecture in patients, resulting in long, tubular bones; syndactly of the hands and feet; and craniofacial abnormalities ([28]). Syndactly is the soft tissue fusion between phalanges. At the molecular level, the mutant gap junctions formed make it to the plasma membrane, but are thought to act in a dominant negative manner because the intercellular channel formed is faulty ([30]). While detailed skeletal characterizations haven't really been studied in detail in these patients, mouse models of ODDD have been developed.

Three models of ODDD exist to characterize Connexin 43's role in the skeletal development and maintenance. The first model is called $Gja1^{jrt}$, which has a mutation that isn't actually present in human disease. This mutation (G60S) was found through a N-ethyl-N-nitrosurea screen and pheno-copies ODDD in humans, resulting in syndactly, and craniofacial abnormalities. The $Gja1^{jrt}$ mice also have low bone mineral density, decreased trabecular bone volume, and reduced mechanical strength; indicative of osteopenia, or low bone mass. Micro CT images of these mutant mice display cortical thinning and increased marrow diameter in the femoral diaphysis ([31]). A second mouse model of ODDD that has been studied is the Gja1 G138R mutant mouse, which has a ubiquitously expressed conditional replacement of one GJA1 allele with a G138R allele, a known mutation in humans with ODDD. These mice also have craniofacial anomalies and decreased trabecular bone volume ([32]). In order to determine if the Cx43 mutation in the osteoblasts leads to their skeletal phenotype of ODDD, the third model conditional replacement of the G138R allele was performed using Dermo1/Twist2-Cre, which began expression at E9.5 in osteoprogenitor populations. These mice also have a severe skeletal phenotype including reduced whole BMD, cortical thinning and increased marrow cavity area, resulting in a broad, tubular shaped bone ([33]). Similar observations of cortical thinning and increased marrow area are also present in aging and disuse, suggesting Cx43 as a regulator of normal bone patho-physiology.

Connexin43 global knock out mice exhibit delayed mineralization and brittle bones in the axial and appendicular skeleton, craniofacial abnormalities and a cell autonomous osteoblast dysfunction, including a failure to progress through differentiation ([34]). These mice die at birth due to a cardiac defect ([35]). This role for connexin43 in bone is evolutionarily conserved in zebrafish, in which gain and loss of function of connexin43 regulate fin ray segment length ([36–39]).

In order to assess post-natal connexin43 gene deletion, conditional deletion knockout mouse models have been generated using four different promoters to drive Cre recombinase at progressively later stages of osteoblast differentiation (**Figure 1.2C**). The Dermo1/Twist2-Cre mouse line was used to conditionally delete connexin43 in cells of the early chondro-osteoblast lineage (cKO^{TW2})([33]). cKO^{TW2} mice have smaller and hypo-mineralized skulls at birth, reduced chest cavity from shortened ribs, and a 12% reduction in whole body BMD (bone mineral density). cKO^{TW2} mice have a striking cortical, but no trabecular phenotype, including a more than 40% increase in cross sectional area of the long bones at the mid-diaphysis. This is a result of increased periosteal osteoblast activity, leading to periosteal expansion; cortical thinning, and increased marrow cavity area due to a concomitant increase in endocortical osteoclast activation. This demonstrated that deletion of connexin43 early in the osteoblast lineage not only affects the activity of osteoblasts, which had a cell autonomous differentiation defect, enhanced proliferation and produced a disorganized collagenous matrix, but can also affect osteoclast formation and function. Similar, slightly milder results were observed using the 2.3 kb Col1a1-Cre mice to genetically delete connexin43 at a later stage in the osteoblast-lineage (cKO^{Col1}; **Figure 1.2C**). cKO^{Col1} mice have a 5% reduction whole body BMD, cortical thinning, and a 20% increase in the cross sectional area at the diaphysis ([40,41]). These animals had a similar cell autonomous osteoblast differentiation defect and enhanced support of osteoclastogenesis ([40]). Indeed, much of the cortical phenotype could be restored by administering anti-resorptive bisphosphonates to these animals, indicating that the role of connexin43 in bone is not only to coordinate osteoblast differentiation and function, but also that communicating networks of bone cells are needed to suppress osteoclast activation ([42]). Conditional knock outs using the human osteocalcin-Cre mice (cKO^{hOC}) allowed connexin43 knock out to be restricted to mineralizing (late-stage) osteoblasts and osteocytes (**Figure 1.2C**). Consistent with the progressively less pronounced skeletal phenotype when connexin43 deletion occurred later in the osteoblast differentiation stage, these cKO^{hOC} mice had only slightly diminished BMD (albeit only ~4%) and only a ~25% increase in cross sectional area at the diaphysis, but without cortical thinning in cKO^{hOC} mice compared to wild type mice ([43,44]). The fourth conditional knock out model was generated using the 8 kb DMP1-Cre mice (cKO^{DMP1}), which is expressed almost exclusively in mature osteoblasts/osteocytes (**Figure 1.2C**) ([43,44]).The $cKO^{DMP1\ mice}$ have no cortical thinning or decrease in whole body BMD along with no trabecular phenotype. cKO^{DMP1} mice do exhibit a 20% increase in diaphysis cross-sectional area resulting from increased osteoclast number. This model also exhibits a disorganized collagenous extracellular matrix with inferior material properties ([44,45]). Enhanced osteocyte apoptosis was observed in this model, underscoring an additional role for connexin43 in osteocyte cell survival ([44]). Notably, mouse models of oculodentodigital dysplasia, a disease caused by loss of function mutations in connexin43, have largely recapitulated the findings of connexin43 conditional deletion models, including osteopenia, an expanded cortical cross sectional area with a widened marrow cavity, and bone with impaired material properties ([30–33]).

A common theme in these models of connexin43 deficiency in the osteoblastic lineage is reduced bone mass, cortical widening, and reduced cortical thickness. Another consistent finding is an increase in bone resorption, caused by alterations in the production of osteoclastogenic factors by osteoblasts and osteocytes. These findings confirm connexin43 as an important regulator of osteoblastogenesis and the production of osteoclastogenic factors by osteoblasts and osteocytes, especially in cortical bone. It is also notable that aspects of the phenotype are more pronounced the earlier in differentiation that connexin43 is deleted. The demonstration of the altered proliferative capacity of osteo-progenitors in the cKO^{TW2} model is unique among the osteoblast-lineage conditional knockout models and implies that connexin43 plays a role in restraining proliferation in early osteoprogenitor populations (**Figure 1.2C**) ([33]). A cell autonomous defect in osteoblast differentiation was exclusive to the models of connexin43 deletion early in the lineage (i.e., cKO^{Col1} and $cKO^{TW2)}$ (**Figure 1.2C**)([33,40]). In the cKO^{DMP1} model, connexin43 expression is obligated for osteocyte cell survival, as osteocyte apoptosis was substantially increased in connexin43 deleted cells (**Figure 1.2C**) ([44]). A similar observation of connexin43-dependent support of osteocyte survival was made in cKO^{hOC} mice ([46]). In addition, loss of connexin43 in this model promoted osteocytic osteolysis in this model ([47]). Interestingly, aspects of the skeletal phenotypes in these mice are similar to osteocyte ablation studies (e.g., fragile bones with increased cortical porosity, decreased cortical BMD, and osteoblast dysfunction) ([48–51]). A computer simulation of the intercellular communication between osteocytes and bone cells on the bone surface predicted that even a modest 5-9% level of osteocyte apoptosis would have a 25-37% reduction in the signaling received at the cell surface ([52]). This suggests that at least some signals communicated through this cellular network travel through osteocytes to target the effector cells (i.e., osteoblasts, osteoclasts and their progenitors). Not only that, the osteoblast-stage specific progressive skeletal phenotype supports a role for connexin43 throughout the lineage, including osteo-progenitors, osteoblasts, and osteocytes, underscoring bone as a coordinated remodeling unit.

The effects of defective intercellular communication caused by loss of connexin43 in bone become more complex in aging, loading and disuse (reviewed ([53–55]). Thus, it is clear that *data* exchanged through this intercellular communication network is dynamic. The signals passed in a healthy animal likely fundamentally differ from those in an aged animal, under mechanical load stimuli, or in disuse. Understanding the *code* of communicating anabolic and catabolic *data* signals will allow us to *hack* the systems to modulate bone responses.

7. **Connexin43's mechanisms of action: identifying *data* packets and downstream effectors**

The need for this elaborate communication network in bone is most evident in the coordinated bone formation process, in which hundreds of osteoblasts in a local area become activated to deposit and mineralize the extracellular matrix. One of the key roles of connexin43 in this process is likely the ability to detect, amplify and coordinately respond to subtle signals relative to background noise. This concept has been beautifully demonstrated in mammary epithelial cells, where gap junctional communication among cells was shown to enable detection of shallow concentration gradients of epidermal growth factor that could not be sensed by a single cell by improving the efficiency of the signaling relay among cells ([56]). In this context, the exchanged *data* was in the form of Ca^{2+} signaling. Indeed, bone cell networks of osteocytes and osteoblasts have been shown to exchange Ca^{2+}-dependent signals in response to hormonal, growth factor and mechanical cues ([57–60]). But, Ca^{2+} is not the only *data* that this network exchanges. Connexin43 has been shown to be involved directly or indirectly in the regulation of signaling cascades involving low molecular weight second messengers, like cAMP, inositol polyphosphates and ATP release ([61–64]). Interestingly, ATP release and the release of prostaglandin E2 have been shown to occur through unpaired hemichannels of connexin43([63,65,66]). In a transgenic model of mutant connexin43 overexpression in osteocytes, a dominant negative connexin43 construct (connexin43 Δ130-136) that blocked both gap junctions and hemichannels recapitulated the increase in cortical cross-sectional area, endocortical resorption and osteocyte apoptosis that is observed in models of connexin43 deficiency([67]). These phenotypes were not observed when a dominant negative construct (connexin43 R76W) that only blocked gap junctional communication, not hemichannels was expressed in osteocytes. These data strongly indicate that connexin43 hemichannel activity is a driving force behind osteocytic signaling in this context. This interpretation is not without controversy as closely related pannexin channels have also been implicated in ATP release from these cells ([68]).

The downstream effectors of connexin43 in bone include various signaling pathways, including ERK, PKCδ, β-catenin and protein kinase A ([12,61,69–72]) (**Figure 1.2C**). The connexin43-dependent effect on ERK and PKCδ regulate the transcriptional activity of Runx2, a master regulator of osteoblast differentiation, with increased connexin43 levels promoting Runx2 activity driving the expression of several osteoblast genes and vice versa (**Figure 1.2C**) ([12,62,69,70]). Similarly, the connexin43-dependent effect on ERK impact the recruitment and activity of the transcriptional activator Sp1, the required osteoblast transcription factor, osterix/Sp7, and osteocyte survival (**Figure 1.2C**) ([71,73–76]). Loss of osteocyte connexin43 has been shown to increase β-catenin, which has been speculated to prime endocortical bone formation in response to mechanical load ([72]). Communication of cAMP through connexin43 gap junctions activates protein kinase A-dependent cascades to increase expression of the pro-osteoclastogenic signal, RANKL, and suppress sclerostin, an inhibitor of osteogenesis through the Wnt/ β-catenin pathway (**Figure 1.2C**) ([61]). Consistent with this finding, loss of connexin43 in vivo has been shown to attenuate the bone anabolic actions of parathyroid hormone, which acts in part via the cAMP/ protein kinase pathway ([40]). The role of connexin43 in this effect appears to be more in the osteoblasts than osteocytes, as this effect is observed in connexin43 deficiency in osteoblasts and osteocytes (cKO^{Col1}), but not in cKO^{DMP1} mice lacking connexin43 only in the mature osteoblast/osteocyte compartment ([40,45]).

Undoubtedly, these second messengers and signaling pathways are not comprehensive, nor is it likely they are all operant under all conditions. Different stimuli are likely to elicit very different second messengers and signaling cascades. Indeed, such diversity in signals likely explains the differential roles for connexin43 in load, aging, disuse, hormonal signal, fracture healing, and even differences in function on the periosteal versus endocortical surfaces of bone. Regardless, in healthy adult animals, the role of connexin43 in the osteoblast lineage seems to be to inhibit osteoclastogenesis, suppress osteoblast proliferation, support early osteogenic differentiation, and promote osteocyte survival (**Figure 1.2C**). In the absence of connexin43, there is an expansion of the progenitor pool and a bottleneck as these cells fail to differentiate effectively, this combined with the deposition of a disorganized collagenous extracellular matrix leads to poor bone quality.

8. Connexin43 and its assembled interactome

One means by which cell-cell communication through Cx43 gap junctions can translate second messengers into function is by locally recruiting a specific signaling effector proteins, or a Cx43-specific "interactome". An interactome consists of all proteins interactions with a molecule, in this case Cx43. The C-terminal domain of Cx43 (Cx43 CT) binds numerous proteins and signaling molecules, but the consequences of these interactions are unclear ([14]). These interactions have been shown to regulate the open/closed state of the pore and/or data are building that suggests these interactions regulate downstream signaling from the gap junction. The research presented in this dissertation focuses on the latter concept of regulation of downstream signaling through the local recruitment of signaling effectors to the connexin C terminus. Here is a schematic of multiple interactions of signaling molecules with the Cx43 CT, for example (**Figure 1.4**). We hypothesize that it is not only the charge and size selective permeability of a gap junction pore that determines the channel's biologic activity, but also the unique profile of signal molecules that are recruited to the gap junction channel, and this may be specific for each connexin. The relevance of the interactome of C termini within the connexin family is allowing for efficient signaling downstream of the gap junction through the local recruitment of effector molecules to the gap junction.

9. Connexin43 as a docking platform: a firewall for regulating which communicated data is acted on

While gap junctions are generally thought of as passive conduits for small molecules to be shared between cells, growing evidence indicates that connexins actively contribute to downstream signaling. Numerous protein complexes, including kinases associated with signal transduction cascades, assemble on the connexin43 C-terminus ([13–15]). This led to the intriguing notion that, in order for efficient signaling to occur following the exchange of small molecules through the gap junction pore, the signal machinery must be spatially recruited to the gap junction plaque to be available to initiate a response. This also implies an additional level of control where *data* can be communicated, but not responded to if the appropriate signaling machinery is not present at the gap junction plaque. In support of this model, several of the signaling molecules involved in osteoblasts and osteocyte signaling have been shown to bind to the connexin43 C-terminus. In MC3T3 osteoblasts, PKCδ transiently binds to the connexin43 C-terminus and upon stimulation translocates to the nucleus where it can regulate Runx2 transcriptional activity ([62]). In OB-6 cells, interactions between connexin43 C-terminus and β-arrestin allow survival from apoptosis from PTH, by sequestering β-arrestin and allowing cAMP-dependent cascades to be activated ([77]). Lastly, in MLO-Y4 osteocyte like cells, the connexin43 C-terminus interacts with α5β1 integrin, which controls opening and closing of the hemi channels by causing a conformational change in the extracellular domain of the integrin in response to mechanical load, leading to activation of AKT signaling ([78]).

Further validating this model of the local recruitment of signaling machinery to the connexin43 C-terminus for efficient signal transduction, the connexin43 C-terminus is required (necessary but not sufficient) for the efficient activation of the ERK and PKCδ

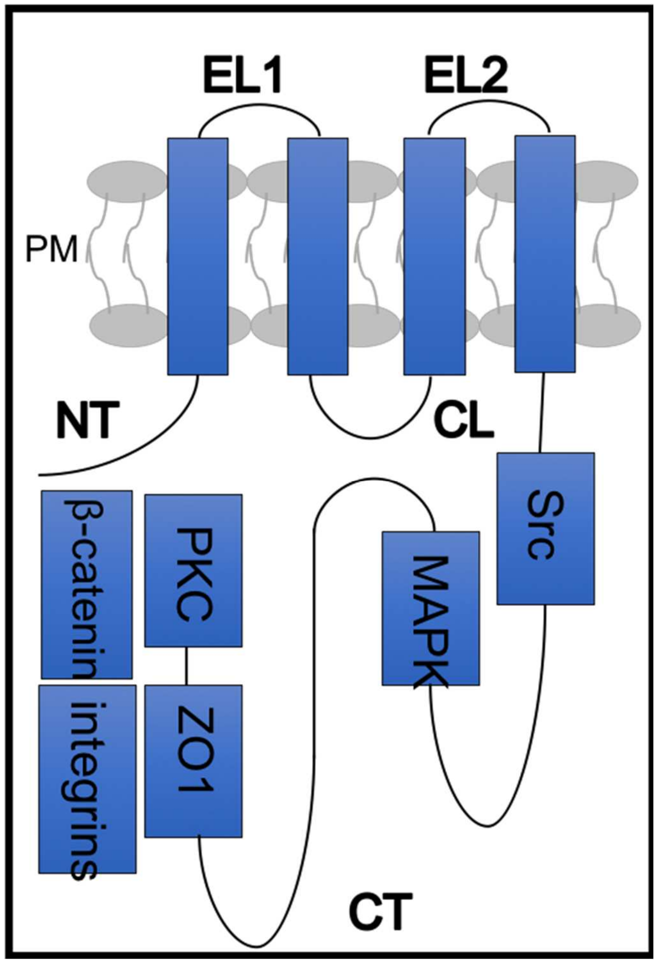

Figure 1.4. Cx43 interactome. Schematic of multiple interactions of signaling molecules with the Cx43 CT, for example. . NT: N-terminus. EL1: extracellular loop 1. EL2: extracellular loop 2. CL: cytoplasmic loop. CT: C-terminus. PM: plasma membrane. Boxes on CT indicate binding sites for proteins. Binding sites are not necessarily spatially accurate.

signaling cascades, activation of Runx2 transcriptional activity, and the expression of osteoblast genes ([12]). An *in vivo* model of connexin43 C-terminal truncation (connexin43 K258Stop) had reduced trabecular bone, but surprisingly no changes in cortical cross-sectional area or marrow area in female mice ([79]). Careful inspection did reveal a cortical phenotype in these mice that included decreased crystallinity and fracture toughness ([80]).

10. <u>Hacking the network: modulating communicated molecules to impact bone quality</u>

Bone forms an elaborate communication network with osteoblast, osteocytes and osteoprogenitors sharing *data*. The communication of this *data* throughout the network plays a key role in how bone modeling and remodeling occurs. It has become clear that taking the cellular network *offline* by loss of connexin43 function has negative consequences for the skeleton, at least in healthy mice. But the mechanisms leading to these effects are less clear. We have only begun to scratch the surface of the actual *data* being communicated through these cells. Cracking the *code* of the *data* passing through this network will have obvious implications into bone therapeutic targets. For example, if we can *hack* the communication network to communicate *data* informing the skeleton that it is under load, even during disuse, we can have a profound impact on skeletal fragility and the maintenance of bone mass. The emerging data that this communicated *data* is diverse, with multiple targets, acting differently in distinct skeletal compartments, and in response to a broad array of extracellular cues only enhances the need to understand this fundamental process in bone homeostasis.

Chapter 2 : Defective signaling, osteoblastogenesis, and bone remodeling in a mouse model of connexin 43 C-terminal truncation[1]

1. ***Abstract***

In skeletal tissue, loss or mutation of the gap junction protein connexin 43 (Cx43, also known as GJA1) in cells of the osteoblast lineage leads to a profound cortical bone phenotype and defective tissue remodeling. There is mounting evidence in bone cells that the C-terminus (CT) of Cx43 is a docking platform for signaling effectors and is required for efficient downstream signaling. Here, we examined this function, using a mouse model of Cx43 CT-truncation (*Gja1 K258Stop*). Relative to *Gja1*$^{+/-}$ controls, male *Gja1*$^{-/K258Stop}$ mice have a cortical bone phenotype that is remarkably similar to those reported for deletion of the entire Cx43 gene in osteoblasts. Furthermore, we show that the Cx43 CT binds several signaling proteins that are required for optimal osteoblast function, including PKCδ, ERK1 and ERK2 (ERK1/2, also known as MAPK3 and MAPK1, respectively) and β-catenin. Deletion of the Cx43 CT domain affects these signaling cascades, impacting osteoblast proliferation, differentiation, and collagen processing and organization. These data imply that, at least in bone, Cx43 gap junctions not only exchange signals, but also recruit the appropriate effector molecules to the Cx43 CT in order to efficiently activate signaling cascades that affect cell function and bone acquisition.

2. ***Introduction***

---

[1] Moorer MC, Hebert C, Tomlinson RE, Iyer SR, Chason M, Stains JP. Defective signaling, osteoblastogenesis and bone remodeling in a mouse model of connexin 43 C-terminal truncation. *Journal of Cell Science*. 2017;130(3):531-540. doi:10.1242/jcs.197285.

The gap junction protein, connexin43 (Cx43), is broadly expressed in many tissues of the body, including the skeleton. Other connexins expressed in bone are Cx45 and Cx37. Previous studies have revealed that gap junction communication is important to physiologic function, and changes in gap junctions underpin many diseases ([81,82]). Accumulating data indicate an important role for intercellular communication by Cx43-containing gap junctions among the extensive interconnected network of bone cells (i.e., osteoblast, osteocytes and osteoprogenitor cells). ([33–35,40,43,44,83,84]). However, details of the molecular mechanisms by which Cx43 affects osteoblast function and bone remodeling are unclear.

While the biophysical properties of the permeability of each of these connexins often functionally overlap, the C-terminal (CT) domain of these connexins is the least conserved region within the protein family, as discussed previously in the introduction ([15]). The C-terminal domain of connexins is the target of many signaling pathways that regulate the gap junction channel open/closed states ([15,85]). Further, numerous signaling proteins exist in a complex with the Cx43 CT ([13–15]). In osteoblasts, a growing body of evidence suggests that protein-protein interactions with the Cx43 CT domain are important for the spatio-temporal recruitment of signaling proteins to gap junctions for efficient downstream signaling ([12,77,78,86]). Hebert et. al. showed that the Cx43 CT domain was necessary but not sufficient to activate downstream signaling, *in vitro*. We speculated that signaling proteins, such as ERK, PKCδ and β-catenin, are locally recruited to the gap junction plaque via their interaction with the Cx43 CT domain. As ions and second messengers are communicated through the gap junction pore, the locally assembled signaling machinery can be efficiently activated to affect bone cell function.

Using a mouse model of Cx43 CT-truncation (*Gja1 K258Stop*), we tested the hypothesis that the Cx43 CT is a docking platform for signaling proteins and is required for efficient downstream signaling in bone. In this mouse model, the endogenous *Gja1* allele was replaced with a truncation mutant, lacking much of the CT domain (amino acids 258-382 removed) downstream of the microtubule interaction domain ([87]). The resultant truncated Cx43 traffics to the plasma membrane and forms functional gap junctions with single channel properties similar to intact Cx43 gap junctions ([88]). However, the Cx43 K258Stop gap junction plaques tend to be larger in size and fewer in number ([88]). In contrast to *Gja1*$^{-/-}$ mice ([35,83]), there is no lethal obstruction of the cardiac ventricular outflow tract in homozygous *Gja1*$^{K258Stop/K258stop}$ mice, though these mice die as a result of a postnatal epidermal barrier defect ([87]). In contrast, *Gja1*$^{-/K258stop}$ mice, which have just a single copy of the truncated Cx43 allele, are viable and healthy with no overt phenotype ([88]). *Here, w*e show that 6-week-old *Gja1*$^{-/K258stop}$ male mice have an obvious skeletal phenotype that includes increased femoral diaphyseal marrow cavity area, enhanced periosteal apposition and endosteal resorption, increased cortical porosity, and cortical thinning relative to *Gja1*$^{+/-}$ controls. Truncation of Cx43 reduced the mRNA levels of genes involved in osteoblast proliferation, differentiation and collagen processing. Further, truncation of the Cx43 CT resulted in reduced levels of pPKCδ, pERK, and active β-catenin, signaling effectors that bind the Cx43 CT and play roles in osteoblast function. These data suggest that the Cx43 CT serves as a docking platform for signaling proteins and is required for efficient signal pathway activation to affect cell proliferation, differentiation and function.

3. __Results__

2.3.1 Cx43 CT interacts with signaling proteins

In osteoblasts, Cx43 is in a complex with several proteins, including PKCδ, β-arrestin, ZO-1, and α5β1 integrins ([14,77,78,86]). Further, alteration of Cx43 abundance regulates the activation of ERK and PKCδ signaling cascades ([62,69,70]). *In vitro*, overexpression of a full length, intact Cx43, but not a Cx43 S244Stop CT-truncation mutant, increases signal transduction through the PKCδ and ERK pathways and elevates mRNA levels of osteoblast associated genes, even though both constructs support similar levels of intercellular communication ([12]).

In order to establish that the Cx43 CT interacts with signaling proteins that are known to be affected by Cx43 abundance and are relevant to bone biology, we performed co-immunoprecipitations in UMR106 osteoblast-like cells (**Figure 2.1**). Immunoprecipitation of ERK1/2, PKCδ and β-catenin resulted in the co-precipitation of Cx43 (**Figure 2.1A**). Conversely, overexpression of just a FLAG-tagged Cx43 CT domain (aa 236-382) reduced the binding of the full length Cx43 to these signaling proteins. When the reverse co-immunoprecipitation was performed, these signaling effectors were found in complex with the overexpressed FLAG-Cx43 CT construct (**Figure 2.1B**). These data show that PKCδ, ERK and β-catenin are in a complex with Cx43 and suggest that the overexpressed Cx43 CT competes for binding of the signaling proteins with the endogenous, intact Cx43.

2.3.2 Male Gja1$^{-/K258Stop}$ mice have no overt morphological phenotype

Given the accumulated *in vitro* data showing that the Cx43 CT binds numerous signaling proteins to affect signaling and cell function, we analyzed the consequence of Cx43 CT truncation *in vivo*. Specifically, we examined the skeletal phenotype of 6 week

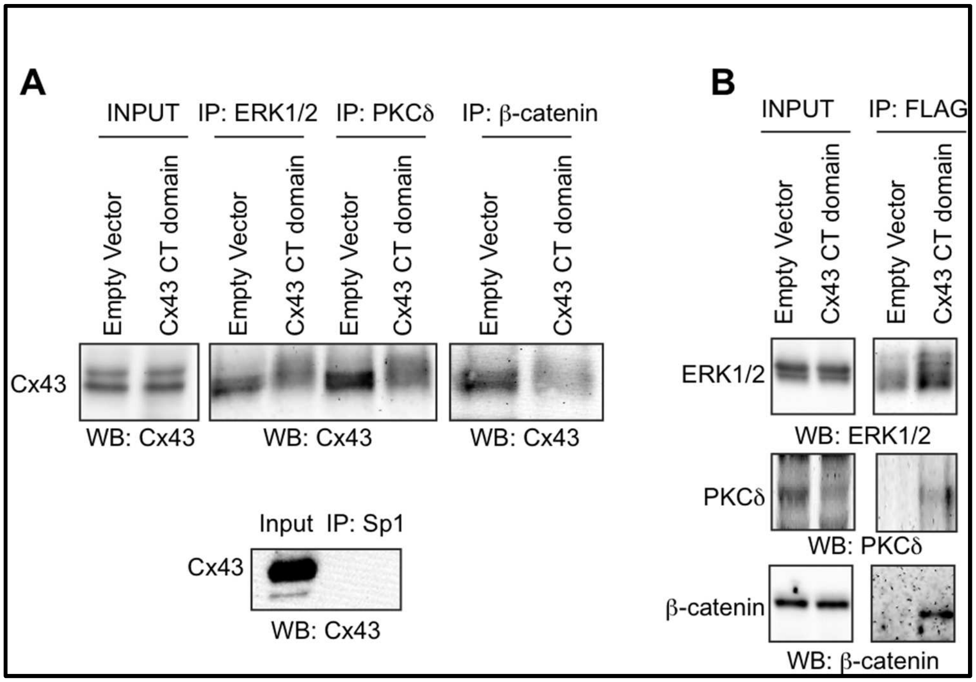

Figure 2.1. Overexpression of the Cx43 CT domain competes for binding of signaling proteins with the intact Cx43 protein. Co-immunoprecipitations (co-IP) were performed to assess protein-protein interactions between indicated signaling proteins and the Cx43 C terminus. UMR106 cells were transfected with a construct encoding the CT domain of Cx43 (FLAG-tagged) or with an empty vector control. (A) Input and bead fractions are shown for IPs performed with anti-ERK, anti-PKCδ, and anti β-catenin antibodies and blotted with anti-Cx43 antibodies. (B) IPs were performed for the Cx43 C terminus (by anti-FLAG), and then blotted for the indicated signaling proteins.

old, male *Gja1*$^{-/K258stop}$ mice, expressing a single allele of the Cx43 gene that lacks the majority of the Cx43 CT domain, relative to *Gja1*$^{+/-}$ mice expressing a single allele of the intact Cx43 gene (**Figure 2.2**). X-rays show no gross skeletal differences between male *Gja1*$^{-/K258Stop}$ mice and *Gja1*$^{+/-}$ littermate controls (**Figure 2.2A**). Further, there were no differences in body length or body weight between genotypes (**Figure 2.2B**).Using an antibody recognizing a C-terminal epitope of Cx43, we confirmed absence of the Cx43 CT in the *Gja1*$^{-/K258stop}$ mice. Quantitative real time PCR performed on cDNA from tibial extracts confirmed a loss of *Gja1* mRNA in the *Gja1*$^{-/K258stop}$ mice as compared to the heterozygous controls (**Figure 2.2C**). In contrast, the mRNA expression of *Gjc1* (Cx45), the second most abundant connexin expressed in bone, was unchanged. A prior report had shown a compensatory upregulation of Cx45 in *Gja1*$^{-/-}$ animals ([34]).

2.3.3 Altered cortical bone in male Gja1$^{-/K258Stop}$ **mice**

Despite gross morphological similarity, microcomputed tomography (microCT) revealed a cortical bone phenotype in the femurs of male *Gja1*$^{-/K258stop}$ mice (**Figure 2.3**). At the femoral mid-diaphysis, there was a pronounced expansion of the cross-sectional area, with an increase in the periosteal (15%) and endosteal (26%) bone perimeter in *Gja1*$^{-/K258stop}$ mice relative to age and gender matched littermate *Gja1*$^{+/-}$ controls. In addition, *Gja1*$^{-/K258stop}$ mice demonstrated cortical thinning and a 3.7-fold increase in cortical porosity. The changes in cortical bone geometry resulted in a 48% increase in mean polar moment of inertia. In contrast, there was no trabecular bone phenotype detected in 6-week-old male *Gja1*$^{-/K258stop}$ mice relative to controls, despite an overall increase in cross-sectional volume in the distal femur (**Table 1**).

			-/Stop		+/-		
			mean	sd	mean	sd	p-value
Tissue volume	TV	mm^3	5.30	0.95	3.83	0.31	0.001
Bone volume	BV	mm^3	0.69	0.14	0.53	0.14	0.027
Percent bone volume	BV/TV	%	13.17	2.12	13.73	2.70	0.652
Trabecular thickness	Tb.Th	mm	0.05	0.00	0.05	0.00	0.234
Trabecular number	Tb.N	1/mm	2.54	0.36	2.74	0.47	0.365
Trabecular separation	Tb.Sp	mm	0.22	0.02	0.23	0.04	0.414

Table 1. 6-week old male trabecular bone parameters at the distal femur by microCT. (*Gja1*$^{-/Stop}$ *n*=8, Gja1$^{+/-}$ *n*=11)**.**

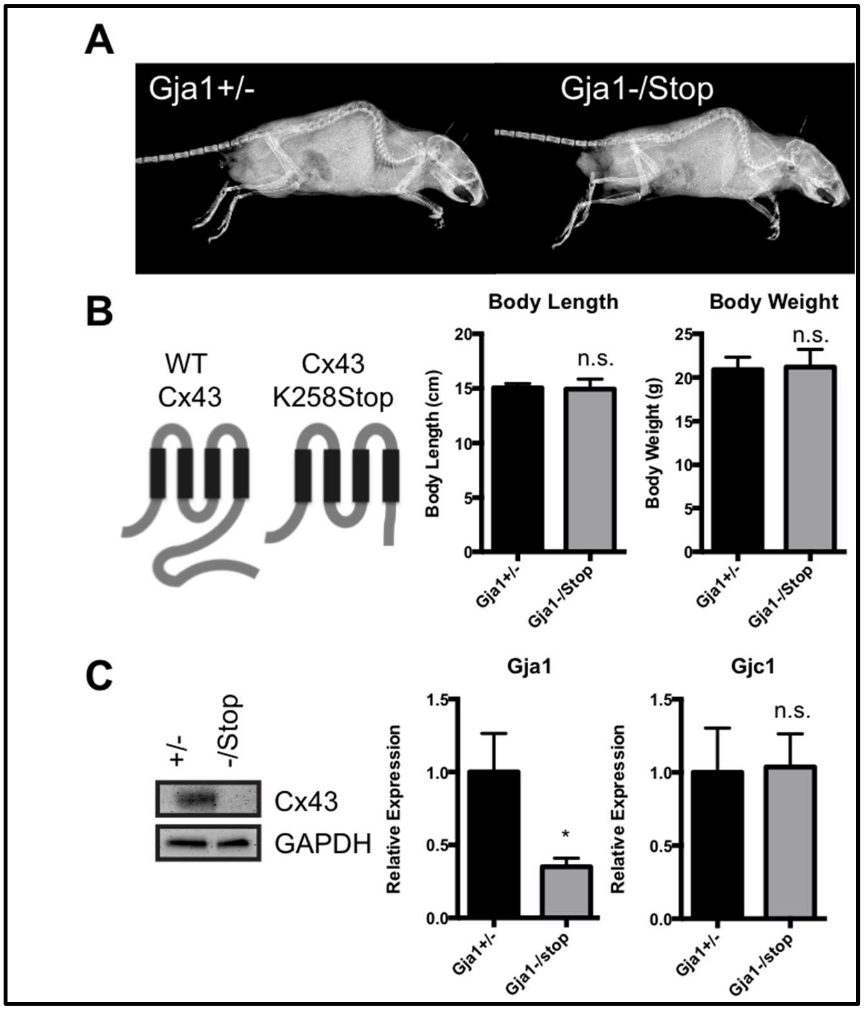

Figure 2.2. No apparent morphological defects are observed in mice with truncation of the Cx43 CT. (A) Digital x-rays, (B) body length and weight measurements in 6-week-old, male *Gja1*$^{+/-}$ (*n*=11) and *Gja1*$^{-/K258stop}$ (*n*=8) mice. (B) Schematic of full length (WT Cx43) and truncated Cx43 (Cx43K258Stop) proteins, showing deletion of most of the C terminus. (C) Western blot performed in tibial extracts (marrow flushed) and immunoblotted for Cx43 (C terminal epitope). qPCR from RNA isolated from tibia (marrow flushed) of the indicated genotype was performed for *Gja1*/Cx43 (3' primers to the C-terminal encoding region) and *Gjc1*/Cx45 mRNA expression. (*n*=7 for *Gja1*$^{+/-}$ and *n*=5 for *Gja1*$^{-/K258stop}$). Graphs depict mean±SD. * = p<0.05, n.s. = not significant.

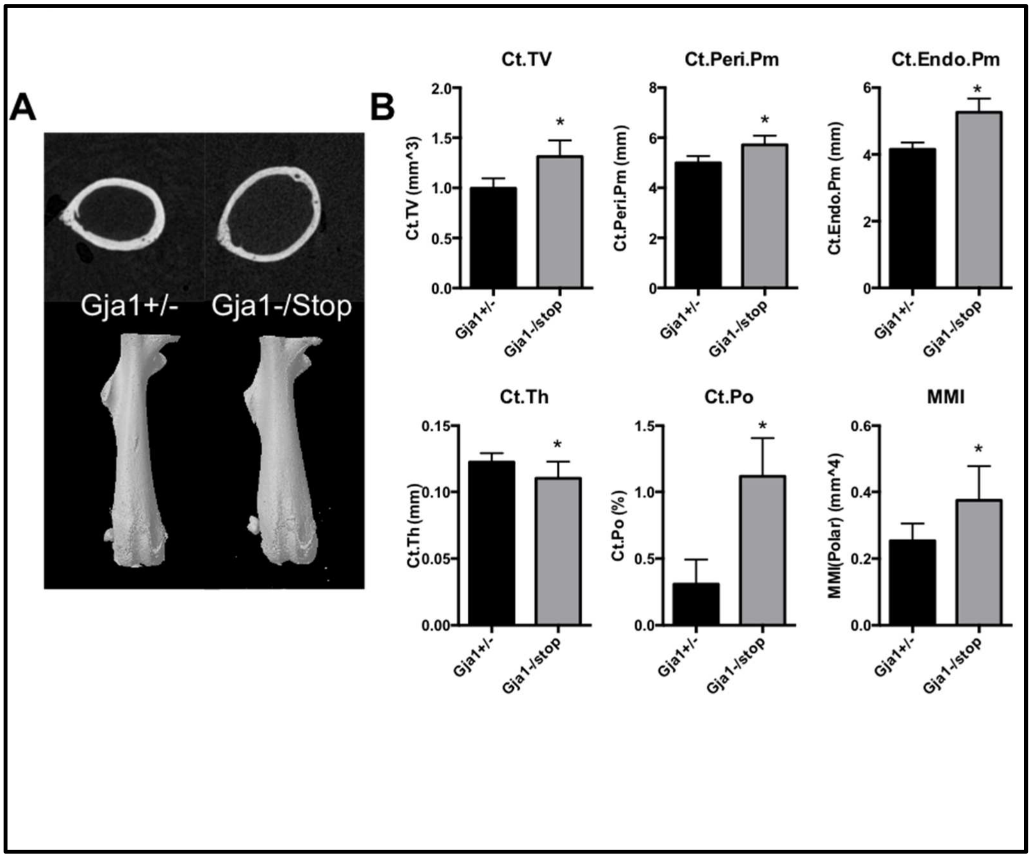

Figure 2.3. Truncation of Cx43 results in a cortical phenotype with increased cross-sectional area, increased cortical porosity, cortical thinning and marrow cavity expansion in 6-week-old, male *Gja1*$^{-/K258stop}$ mice. (A) Top, cross section through the femoral mid-diaphysis from a representative microCT slice from *Gja1*$^{+/-}$ and *Gja1*$^{-/K258stop}$ mice. Bottom, 3D reconstruction of intact femurs. (B) Quantification of the cortical phenotype at the femoral mid-diaphysis by microCT (*n*=11 for *Gja1*$^{+/-}$ and *n*=8 *for Gja1*$^{-/K258stop}$). Graphs depict mean±SD. * = $p<0.05$.

2.3.4 Altered bone formation rates in male Gja1$^{-/K258Stop}$ **mice**

Dynamic histomorphometric analysis of the femoral mid-diaphyseal cortical bone showed a nearly 2-fold increase in periosteal bone formation rate (bone formation rate = mineralizing surface * mineral apposition rate) without a concomitant change in mineral apposition rate (p=0.24) in mice expressing the truncated Cx43, suggesting an increase in mineralizing surface, i.e. the number of osteoblasts doing work (mineralizing surface), but not increased work of an individual osteoblast (mineral apposition rate) (**Figure 2.4A**).

Conversely, on the endosteal surface the bone formation rate was diminished but did not reach statistical significance (p=0. 10) in the *Gja1$^{-/K258stop}$* mice compared to control mice (**Figure 2.4B**). Analysis of serum type I collagen N-propeptide (P1NP), a marker of bone formation, was performed using a commercial ELISA. P1NP levels were increased in the *Gja1$^{-/K258stop}$* samples (**Figure 2.4C**). Static histomorphometry, an analysis of the cellular contribution to a skeletal phenotype, showed no difference in osteoblast number (characterized by plump, mature osteoblasts on the bone surface) per bone surface between groups, although it was slightly elevated in the *Gja1$^{-/K258stop}$* samples (**Figure 2.4D**). As osteocyte apoptosis has been implicated as one of the mechanisms of the effects of Cx43 on bone ([44,67]), empty and occupied osteocyte lacunae were counted in cortical bone for mice of each genotype. The percentage of occupied osteocyte lacunae was unaffected by Cx43 CT truncation, suggesting that osteocyte apoptosis did not contribute to the elaboration of the phenotype in this model (**Figure 2.4E**).

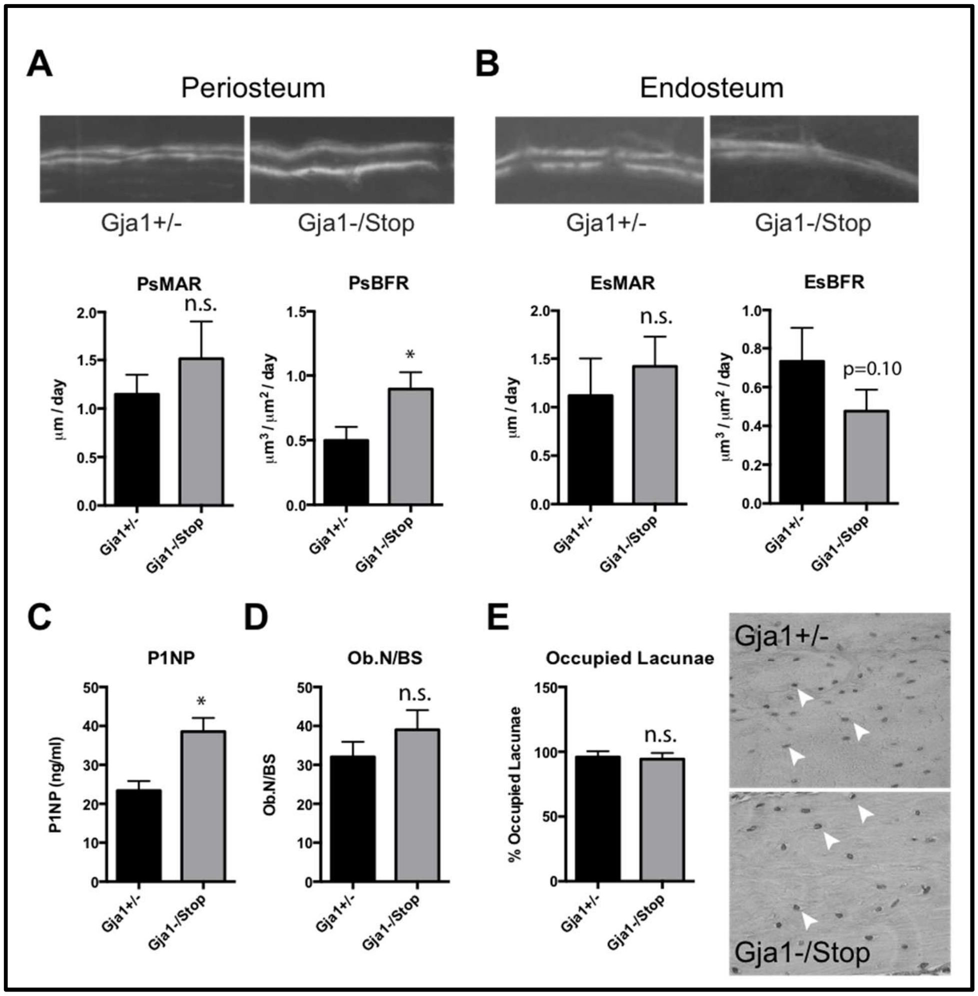

Figure 2.4. Exuberant periosteal bone apposition contributes to the cortical expansion of the mid-diaphysis in 6-week-old male *Gja1*$^{-/K258stop}$ mice. Calcein/Alizarin dual labeling and quantitation of the mineral apposition rate (MAR) and bone formation rate (BFR) is shown for each genotype at the (A) periosteal (Ps) and (B) endosteal (Es) surface of the femoral diaphysis. (*n*=3 animals per genotype, 3 sections per animal). (C) Quantification of serum levels of P1NP (*n*=4/genotype). (D) Static histomorphometry of osteoblast number per bone surface (*n*=5/genotype). (E) Quantification of occupied osteocyte lacunae observed in cortical bone from the indicated genotype (*n*= 3 animals and >1000 lacunae/genotype). A representative hematoxylin stained image of cortical bone is shown. White arrowheads point to occupied lacunae. Graphs depict mean±SD. * = $p<0.05$, n.s. = not significant.

2.3.5 Enhanced bone resorption in male Gja1$^{-/K258Stop}$ mice

Osteoblast-lineage specific Cx43 deletion has been shown to indirectly affect osteoclast-mediated bone resorption via the RANKL/OPG pathway, an effect that contributes to the expansion of the marrow cavity in those models ([33,42,44,46,67,84]). Accordingly, we looked at RANKL/OPG mRNA levels in RNA extracts from tibial extracts by quantitative real time RT-PCR (**Figure 2.5A**). In *Gja1$^{-/K258stop}$* mice, the relative expression of the gene encoding OPG was 68% of the levels in controls. Relative expression of the gene encoding RANKL was statistically unchanged between genotypes. As predicted by the increased RANKL/OPG ratio, the number of TRAP-positive osteoclasts per bone surface was increased 2.8-fold in the mice expressing the truncated Cx43 (**Figure 2.5B**). Similarly, the serum markers of bone turnover using a commercial ELISA for bone resorption (type I collagen C-telopeptide, CTX) was markedly increased in *Gja1$^{-/K258stop}$* mice (**Figure 2.5C**).

2.3.6 Signal transduction pathway activation is reduced in the Gja1$^{-/K258Stop}$ mice

To glean insights into the molecular mechanisms by which the Cx43 CT domain influences bone acquisition and remodeling, we examined the activation of the signaling proteins (i.e., PKCδ, ERK, and β-catenin) that physically associated with the Cx43 CT and have been shown to be impacted by Cx43 levels *in vitro*. As predicted, pPKCδ, pERK, and active β-catenin were reduced in protein extracts from *Gja1$^{-/K258stop}$* tibiae (**Figure 2.6A**). Consistent with decreased β-catenin activity, *Axin2* mRNA expression was decreased in the tibiae of *Gja1$^{-/K258stop}$* mice as compared to *Gja1$^{+/-}$* controls (**Figure 2.6B**). The mRNA expression of the Wnt/ β-catenin antagonist sclerostin (*Sost*) was

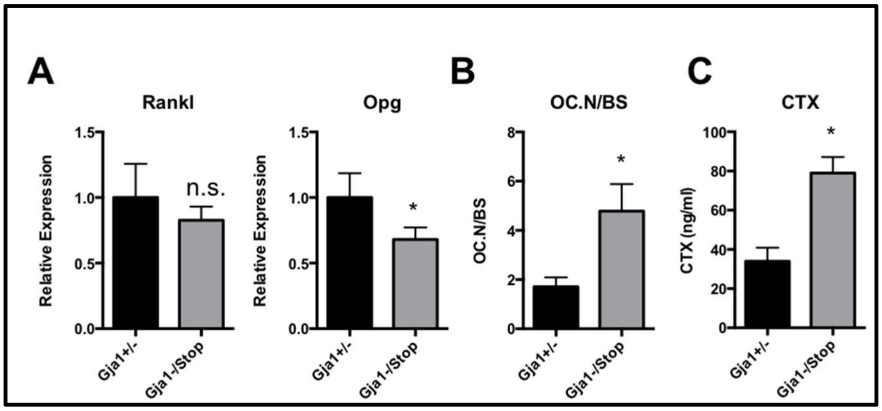

Figure 2.5. Cx43 truncation affects regulators of osteoclastogenesis, leading to increased osteoclast number and increased bone resorption. (A) qPCR from RNA isolated from tibia (marrow flushed) of the indicated genotype was performed for RANKL and OPG mRNA expression (n=7 for *Gja1*$^{+/-}$ and n=5 *for Gja1*$^{-/K258stop}$). (B) Static histomorphometry of osteoclast number per bone surface (N=5/genotype). (C) Quantification of serum levels of CTX (n=3 for *Gja1*$^{+/-}$ and n=4 *for Gja1*$^{-/K258stop}$). Graphs depict mean±SD. * = p<0.05, n.s. = not significant.

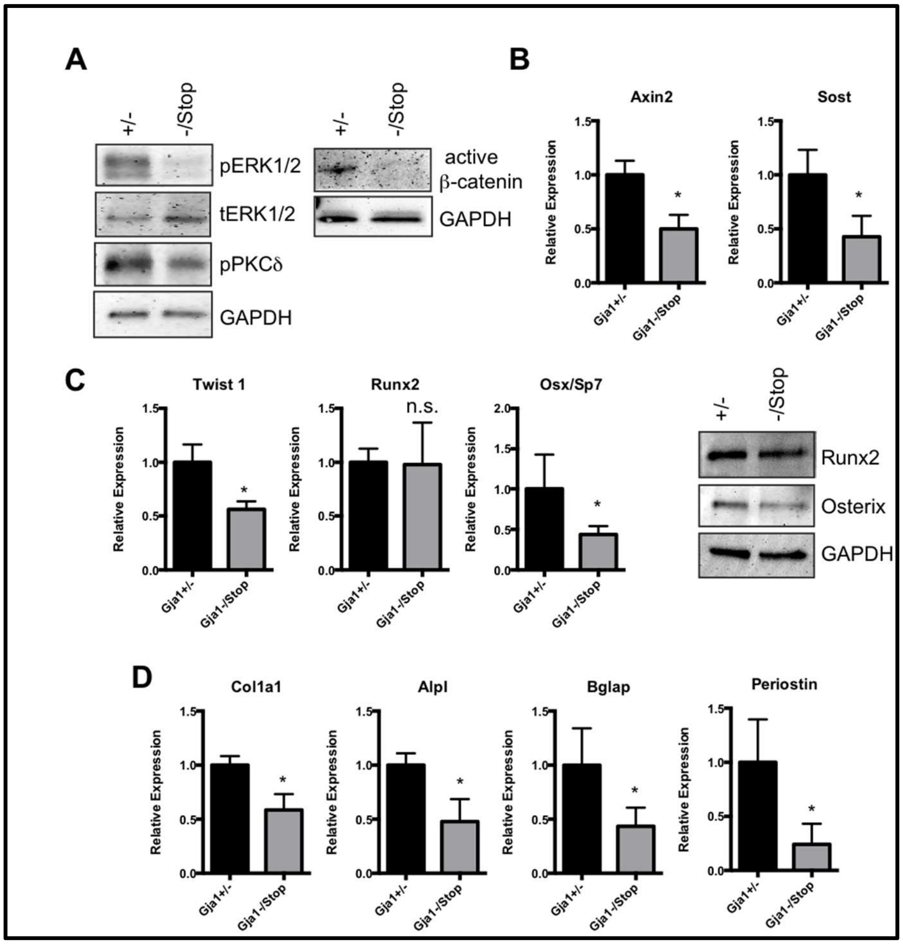

Figure 2.6. Cx43 truncation impairs signal cascade activation and osteoblast differentiation. (A.) Western blots were probed for indicated signaling proteins in tibial (marrow flushed) extracts of the indicated genotypes. qPCR from RNA isolated from tibia (marrow flushed) of the indicated genotype was performed for (B) Wnt/β-catenin related genes, (C) transcriptional regulators of osteoblastogenesis, and (D) osteoblast differentiation markers (*n*=7 for *Gja1*$^{+/-}$ and *n*=5 *for Gja1*$^{-/K258stop}$). Graphs depict mean±SD. * = p<0.05, n.s. = not significant.

unexpectedly decreased in these samples as well (**Figure 2.6B**). Next, we examined the expression of key transcriptional regulators of the osteoblast-lineage, *Twist1*, *Runx2* and Osterix/*Sp7*. The relative mRNA expression of *Twist1* and Osterix/*Sp7* were reduced, while *Runx2* levels were unaffected by truncation of the Cx43 CT domain (**Figure 2.6C**). Western blotting confirmed a downregulation of Osterix, but not Runx2, in primary BMSCs isolated from $Gja1^{-/K258stop}$ mice (**Figure 2.6C**). We were unable to detect Twist1 protein in these extracts (data not shown). Similarly, markers of osteoblast differentiation were uniformly reduced in the tibiae of $Gja1^{-/K258stop}$ mice (**Figure 2.6D**). In total, these data confirm that Cx43 and the Cx43 CT domain play a role throughout the osteoblast lineage, including the early stages of osteoblastogenesis.

2.3.7 Collagen processing and matrix maturation is disrupted in $Gja1^{-/K258Stop}$ **mice**

Cx43 gene deletion in cells of the osteoblast lineage has been shown to affect the expression of lysyl oxidase (gene name, *Lox*), an enzyme involved in collagen fiber cross-linking, and collagen organization ([33,43]). Similarly, *Lox* mRNA is reduced in tibial extracts from $Gja1^{-/K258Stop}$ mice (**Figure 2.7A**). In addition, the gene expression of the collagen-specific chaperone *Serpinh1*/Hsp47 is also reduced in these mice (**Figure 2.7A**). Western blotting of primary BMSCs isolated from $Gja1^{-/K258stop}$ and $Gja1^{+/-}$ mice confirmed the downregulation of Lox (proform and mature isoforms) and SerpinH1 proteins by truncation of the Cx43 CT domain (**Figure 2.7A**). Using picrosirius red staining in conjunction with polarized light microscopy to look at collagen fiber thickness and orientation, the collagen at the cortical bone in the femoral diaphysis of $Gja1^{-/K258stop}$ had thinner fibers and less organized orientation in comparison to the same anatomical

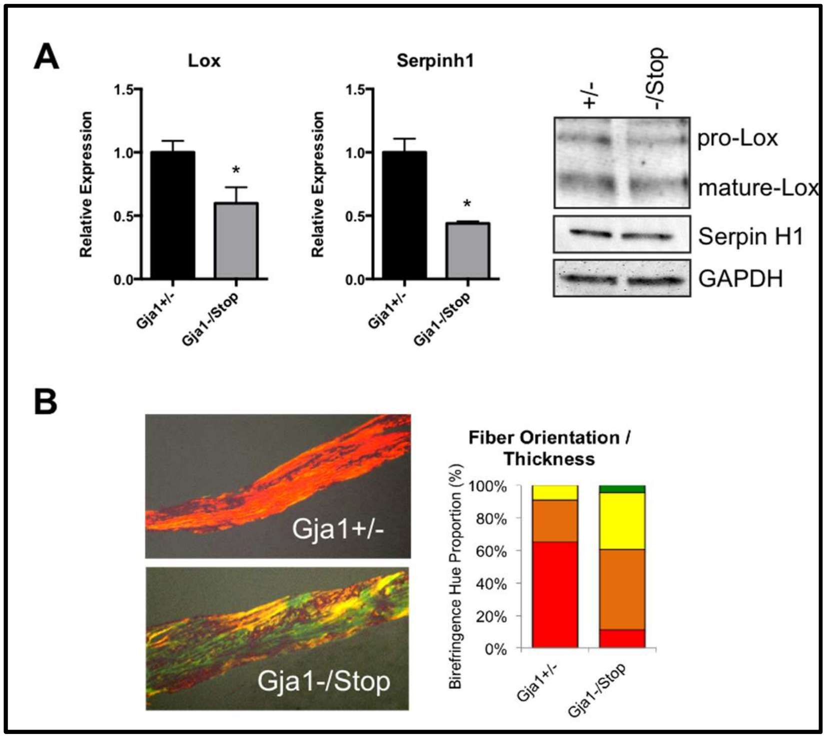

Figure 2.7. Cx43 truncation reduces mRNA expression of collagen processing factors and results in a disorganized, less mature collagen network in cortical bone. (A) qPCR from RNA isolated from tibia (marrow flushed) of the indicated genotype was performed for expression of collagen processing factors. Graphs depict mean±SD. * = $p<0.05$. (*n*=7 for *Gja1*$^{+/-}$ and *n*=5 *for Gja1*$^{-/K258stop}$). (B) Picrosirius red staining was performed and quantitated at the mid diaphyseal cortical bone, using a hue-range/color distribution method. A representative image of mid-diaphyseal cortical bone is shown. Quantification of fiber orientation and length is shown as a percentage of composition of birefringent hue (red, orange, yellow, green).

region in the *Gja1*$^{+/-}$ mice (**Figure 2.7B**). This was confirmed by quantification of the birefringence hue distribution, with red indicating thicker more cross-linked fibers and green indicating thinner, less cross-linked fibers ([89,90]). Orange and yellow colors indicate intermediate levels of thickness and orientation.

2.3.8 A cell autonomous defect in proliferation and signaling in osteoblasts from Gja1$^{-/K258Stop}$ **mice**

In order to establish if a cell autonomous defect in the osteoblast-lineage underlies the skeletal phenotype, bone marrow stromal cells (BMSCs) were isolated from mice of each genotype. Consistent with the increased osteoblast activity by P1NP and bone formation rate findings, cultured BMSCs from *Gja1*$^{-/K258stop}$ mice exhibited an accelerated rate of proliferation relative to controls (**Figure 2.8A**).

Indeed, cyclin D1 expression was increased in tibial extracts from the *Gja1*$^{-/K258stop}$ mice (**Figure 2.8B**). As was observed *in vivo*, the levels of pPKCδ, pERK, and active β-catenin were reduced in *Gja1*$^{-/K258stop}$ BMSCs in culture (**Figure 2.8C**). Finally, we determined mineralization capacity of primary cells from both genotypes. Increased alizarin red staining from *Gja1*$^{-/K258stop}$ BMSCs is apparent after 14 days under mineralizing conditions (**Figure 2.8D**).

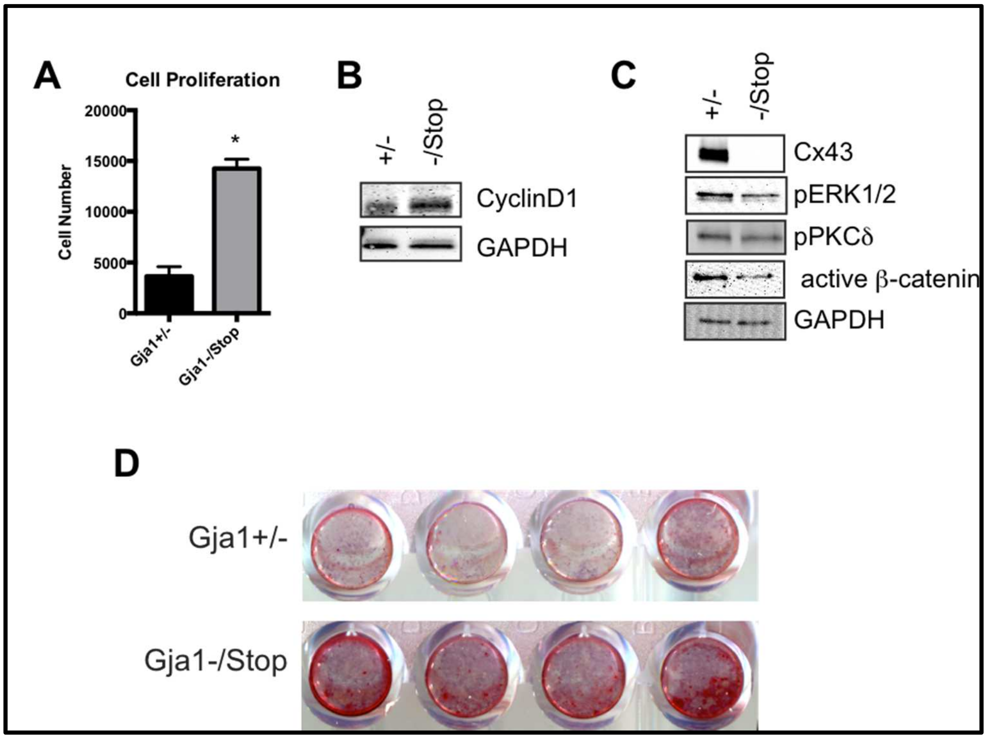

Figure 2.8. Truncation of Cx43 leads to cell autonomous defects in osteoblast proliferation, signaling and mineralization. (A) Cell proliferation on BMSCs after 48 hours in culture (*n*=6 wells per genotype). (B) Western blot on extracts from BMSCs cultured for 7 days in mineralization media and immunoblotted for indicated signaling proteins. (C) Alizarin Red S staining in replicate wells (*n*>4 wells per genotype) in BMSCs cultured for 14 days in mineralization media. Graphs depict mean±SD. * = p<0.05.

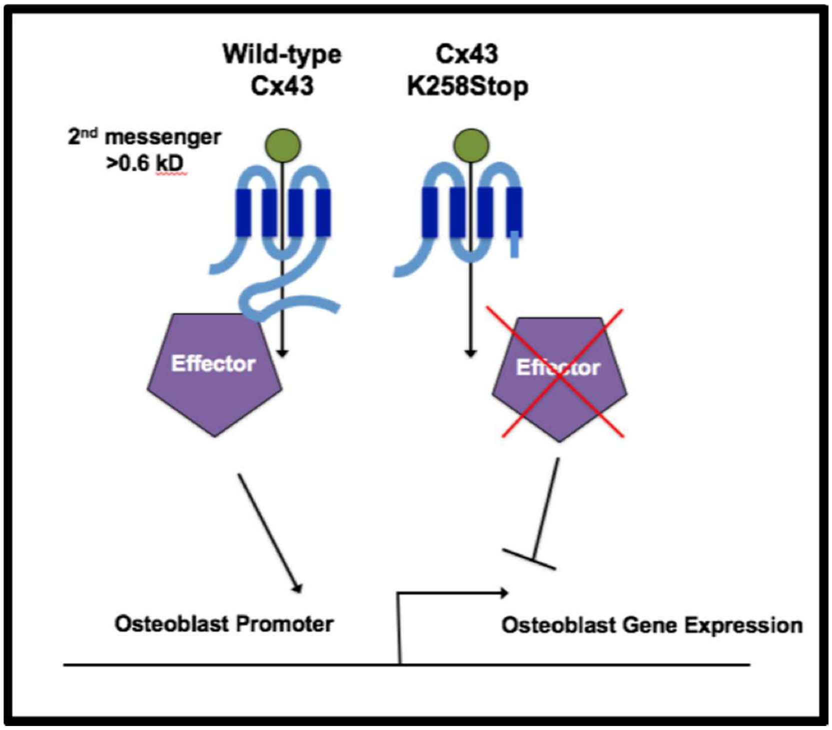

Figure 2.9. Proposed model of Cx43 CT's effects on osteoblasts. Cx43 is required for optimal signaling in osteoblasts, where the full length Cx43 can not only pass second messengers, but also recruit signaling effectors (i.e. ERK, PKC□). Conversely, the truncated form of Cx43 can only pass second messengers, but not recruit the signaling effectors needed to produce optimal signaling and osteoblast function.

4. *Discussion*

Our working model of Cx43 CT's effects on osteoblasts is that Cx43 is required for optimal signaling in osteoblasts, where the full length Cx43 can not only pass second messengers, but also recruit signaling effectors (i.e. ERK, PKCδ) (**Figure 2.9**). Conversely, the truncated form of Cx43 can only pass second messengers, but not recruit the signaling effectors needed to produce optimal signaling and osteoblast function.

This study demonstrates that the Cx43 CT binds signaling proteins and is required for efficient signaling and osteoblast differentiation *in vitro* and *in vivo*. We show, for the first time, that truncation of just the C-terminus of Cx43 in 6-week old male mice results in a skeletal phenotype, primarily in cortical bone, that closely copies the phenotype of osteoblast lineage-specific deletion of full length Cx43 ([33,40,43,44,84]). This strongly suggests that, at least in skeletal tissue, the Cx43 CT domain is functionally as important as the entire intact Cx43 protein. Among the shared features between the *Gja1*$^{-/K258stop}$ mice and most of the osteoblast-lineage specific Cx43 conditional knockout mice are the increased marrow cavity area, due to enhanced periosteal bone apposition and endosteal bone resorption; alterations in RANKL/OPG ratio; increased osteoclast number; and changes in *Lox* gene expression that affect collagen processing. The reduction in *Serpinh1* mRNA levels observed in *Gja1*$^{-/K258stop}$ mice have not been reported previously in Cx43 knockout models.

Decreased expression of this important collagen chaperone, which is implicated in osteogenesis imperfecta ([91–93]), may also contribute to the defective extracellular matrix and inferior material properties reported in other models of Cx43 deficiency ([33,34,43])

These data confirm a role for Cx43 and the Cx43 CT in the organization and maturation of the collagenous extracellular matrix of bone ([33,43,80]).

Additionally, we observed decreased expression of osteoblast differentiation markers *in vivo* and increased proliferation and mineralization capacity in *in vitro* cultures from *Gja1*$^{-/K258stop}$ mice. While the increases in mineralization and concomitant decreases in expression of differentiation markers seem paradoxical, these findings are consistent with previous reports ([33]). We speculate this may be due to a reciprocal role for Cx43 (and the Cx43 CT) in regulating early osteo-progenitor commitment and osteoblast differentiation. The control of progenitor cell commitment by Cx43 is supported by increases in BMSC proliferation rates, increases in Cyclin D1, and a loss of *Twist1* in *Gja1*$^{-/K258stop}$ cells. Twist1 maintains the osteo-progenitor pool in part by inhibiting the activity of Runx2, a key transcriptional regulator of early osteoblast differentiation ([94]). Thus, a reduction in *Twist1* mRNA may expand the committed osteoblast progenitor population. However, we and others have shown here and elsewhere ([12,33,73]), that Cx43 and the Cx43 CT domain influence the expression of Osterix/*Sp7*, a transcription factor required for osteoblast differentiation downstream of Runx2. We think this reciprocal regulation could lead to a bottleneck of osteoprogenitors that are unable to efficiently pass through terminal osteoblast differentiation. Such an expansion of the osteoprogenitor pool could account for the exuberant increase in periosteal bone formation observed here and in Cx43 conditional knockout models. Of course, there are limitations to extrapolating *in vitro* proliferation data to the *in vivo* context. Careful dissection of the osteo-progenitor pool by lineage tracking or other means *in vivo* will be required to confirm the details of this apparent bottleneck of early osteogenic differentiation.

A key aspect of these findings is that, while loss of the Cx43 CT nearly perfectly phenocopies the loss of the intact Cx43 in bone cells, these mice do not exhibit the developmental cardiovascular defect observed in the Cx43 global null ([35]). This implies that whatever signaling function the Cx43 CT plays, it is not universally obligated in all tissues or throughout development. Unlike the perinatal lethality observed in global Cx43 gene deletion (*Gja1*$^{-/-}$), *Gja1*$^{-/K258stop}$ mice show no significant overt phenotype, but present with increased myocardial infarct size and susceptibility to arrhythmias following experimentally induced coronary occlusion ([95]). Notably, we cannot exclude the possibility that the *Gja1 K258Stop* allele may function as a neomorph. *Gja1*$^{K258stop/K258stop}$ mice exhibit an unexpected epidermal barrier defect, that is present only in the homozygous mutants but not in *Gja1*$^{-/K258stop}$ or *Gja1*$^{+/K258stop}$ mice ([87]). However, the striking phenotypic overlap with osteoblast-lineage Cx43 conditional knockouts and the *Gja1*$^{-/K258stop}$ mice makes it unlikely that this is a unique neomorphic function of the Cx43 K258Stop protein. Similar to our findings in bone, *Gja1*$^{-/K258stop}$ phenocopies key aspects of Cx43 conditional knockout in neuronal tissue ([95]), indicating that the function of the Cx43 CT is important in a subset of tissues and is not exclusive to bone.

Multiple mechanisms have been proposed for how Cx43 deletion affects skeletal tissue, including signaling defects and disruption of osteocyte viability ([7,53,96,97]) Here, we report the impact of Cx43 CT truncation on signaling via ERK, PKCδ and β-catenin. Tissue extracts from cortical bone of male *Gja1*$^{-/K258stop}$ mice showed that Cx43 truncation resulted in reduced levels of pPKCδ, pERK, and active β-catenin, signaling effectors that bind to the Cx43 CT and play a role in osteoblast differentiation and function ([98–100]). While *in vitro* data suggested such a link ([12,72,75,77,78,86]), this is the first report of altered signaling in these pathways downstream of Cx43 CT truncation *in vivo*. These results are consistent with the requirement of the Cx43 CT as a docking platform for efficient signaling within interconnected bone cells. Cx43 containing gap junctions are present throughout bone, forming a functional syncytium of interconnected osteoblasts, osteocytes and progenitor cells. This network of cells is believed to rapidly and efficiently propagate signals among the coupled cells. Accordingly, it is intuitive that truncation of the Cx43 CT, which binds and locally recruits signaling proteins, would lead to reduced signaling. Further, the signals being passed among these cells are controlling the fate of signaling cascades known to be involved in both proliferation and maintenance of progenitors as well as differentiation through the osteoblast lineage, depending on the context of the cells and the signals passed.

Another mechanism contributing to the cortical phenotype of Cx43 deficiency is osteocyte apoptosis ([96]). Up to 30% unoccupied osteocyte lacunae have been observed in cortical bone of Cx43 conditional knockout mice ([44,47,67]). Despite the nearly identical cortical bone phenotype observed in the *Gja1*$^{-/K258stop}$ and Cx43 conditional knockout models, we did not detect any difference in empty lacunae between groups, suggesting that osteocytic apoptosis does not precede the phenotype, at least in male *Gja1*$^{-/K258stop}$ mice. Of course, this does not preclude a key role for osteocytes (viable or apoptotic) in the intercellular communication of bone remodeling signals. Indeed, osteocytes, osteoblasts and likely osteoprogenitors all form a functional syncytium of shared signals via intercellular communication through Cx43 ([53]).

Recently, a similar Cx43 truncation model was reported, in which the same *Gja1 K258Stop* allele was combined with osteocyte-specific deletion (*Dmp1*-Cre) of a floxed

Gja1 allele and performed in 4.5 month old female mice ([45]). These female $Gja1^{flox/K258Stop}$; *Dmp1-Cre* mice had a strong trabecular phenotype (decreased bone volume fraction, trabecular thickness, number and separation), but no statistically significant cortical phenotype; male mice were not examined in that study ([45]). On the surface, these data appear to directly contrast our findings, as 6-week-old male $Gja1^{-/K258stop}$ mice had no change in trabecular parameters and had striking changes in the cortical envelope in our study. However, based on this recent publication ([45]), we conducted a screen of 6 week old female $Gja1^{+/-}$ (*n*=3) and $Gja1^{-/K258stop}$ (*n*=4) mice. Similar to their findings, we found comparable trends in 6-week-old female $Gja1^{-/K258stop}$ mice in the trabecular and cortical compartments, where trabecular bone volume fraction, trabecular number and trabecular thickness approached significance (**Table 2**). These findings suggest the intriguing possibility that, beyond the disparate roles of Cx43 in the cortical and trabecular bone compartments, the effects of Cx43 on bone are sexually dimorphic. In female mice, estrogens are known to inhibit periosteal apposition and stimulate endocortical bone apposition; these effects may counteract the action of Cx43 to stimulate periosteal apposition and endocortical resorption ([101]). However, to systematically address the sexually dimorphic skeletal phenotype in these mice, studies should be conducted comparing estrogen replete and estrogen deficient mice. Importantly gender specific differences in bone are a result of numerous systemic factors, thus estrogen signaling alone is unlikely to fully account for this discrepancy ([102,103]).

			-/Stop		+/-		
			mean	sd	mean	sd	p-value
Tissue volume	TV	mm^3	4.74	0.46	3.83	0.32	0.117
Bone volume	BV	mm^3	0.40	0.16	0.46	0.06	0.196
Percent bone volume	BV/TV	%	8.54	3.46	12.06	0.99	0.098
Trabecular thickness	Tb.Th	mm	0.050	0.00 4	0.049	0.002	0.631
Trabecular number	Tb.N	1/mm	1.65	0.57	2.44	0.14	0.071
Trabecular separation	Tb.Sp	mm	0.32	0.04	0.25	0.01	0.130

			-/Stop		+/-		
			mean	sd	mean	sd	p-value
Tissue volume	TV	mm^3	1.13	0.12	1.02	0.01	0.365
Periosteal perimeter	Peri.Pm	mm	5.34	0.26	5.06	0.05	0.303
Endosteal perimeter	Endo.Pm	mm	4.82	0.29	4.31	0.11	0.125
Cortical thickness	Ct.Th	mm	0.099	0.004	0.106	0.009	0.221
Cortical porosity	Ct.Po	1/mm	0.58	0.35	0.25	0.08	0.139
MMI	MMI	mm^4	0.59	0.08	0.50	0.11	0.222

Table 2. Top, 6-week old female trabecular bone parameters at the distal femur by microCT (*Gja1*$^{-/Stop}$ *n*=4, Gja1$^{+/-}$ *n*=3). Bottom, 6-week old female cortical bone parameters at the femoral diaphysis by microCT.

In total, these data suggest that the Cx43 CT is required for optimal osteoblast signaling and gene expression, and that absence of the Cx43 CT in male mice results in a skeletal phenotype analogous to deletion of the entire Cx43 gene in osteoblasts. These data also imply that Cx43-containing gap junctions not only exchange signals, but also must recruit the appropriate effector molecules to the Cx43 CT in order to optimally affect cell function and bone acquisition.

5. ***Methods***

Materials

All chemicals and reagents were purchased from Sigma (St Louis, MO) unless indicated otherwise. The antibodies use in this study were: Sigma, anti-Cx43 (C6219); Cell Signaling Technology, total ERK (9102L), phospho-ERK (9101L), total PKC delta (2058S), phospho-PKCδ Thr505 (9374S), active β-catenin (8814S), CyclinD1 (2978S), Runx2 (8486S), anti-Rabbit HRP (7074S), anti-mouse HRP (7076S); BD Biosciences, total β-catenin (6310153); Agilent, FLAG (200470-2); Millipore, Osterix/Sp7 (AB3743), GAPDH (MAB374); Enzo Life Sciences, HSP47/SerpinH1 (ADI-SPA-470); Invitrogen, Lox (PA1-16953); Santa Cruz, Sp1 (sc-59). The flagged Tagged Cx43 CT construct, pCMV3XFLAGm43CT (aa 236-382), was a gift from Cecilia Lo (Addgene plasmid # 17664).

Cell Culture

UMR106 cells were obtained from the ATCC and were cultured as described (Gupta et al., 2016). Primary BMSCs were prepared from the long bones of mice of the indicated genotype as described (Buo et al., 2016). Briefly, bone marrow was flushed with sterile saline from long bones and pelleted at 500 x g for 10 minutes. The pellet was resuspended in αMEM containing 10% fetal bovine serum, penicillin (50 IU/ml), streptomycin (50 μg/ml) and gentamycin (50 μg/ml) and filtered through a 70 μm cell strainer. Cells were plated and grown to confluence. Cells were kept at 37°C in a humidified atmosphere of 95% air and 5% CO_2. Media was replaced every 2-3 days. For Alizarin Red S staining, confluent cultures of BMSCs were maintained for 14 days in mineralizing media, which contains ascorbic acid-2-phosphate (50 ng/mL) and glycerol-2-phosphate (10 μM). For western blotting, confluent cultures of BMSCs were maintained for 7 days in mineralizing media, which contains ascorbic acid-2-phosphate (50 ng/mL) and glycerol-2-phosphate (10 μM).Subsequently, the cells were rinsed three times in HBSS and fixed in 10% neutral buffered formalin prior to staining mineralized nodules with 1mg/ml Alizarin Red S (pH 4.2) solution, as described (Mbalaviele et al., 2005). For cell proliferation assays, freshly isolated BMSCs isolated from mice of each genotype were seeded at 5,000 cells/well in a 48 well plate and cultured in complete media for 48 hours. Cell number was quantitated using a CCK-8 colorimetric assay (Enzo Life Sciences, Farmingdale, NY, USA) according to the manufacturer's specifications in comparison to parallel wells of known cell numbers.

<u>Transient transfections, co-immunoprecipitations and western blotting</u>

UMR106 cells were transiently transfected using the Jetprime transfection reagent (Polyplus, New York, NY), as described (Gupta et al., 2016). Endotoxin free plasmid DNA was prepped using a Qiagen HI-Speed Maxi prep system, according to the manufacturer's specifications. Cells were lysed 48 hours post transfection with 1X cell lysis buffer (20 mM Tris (pH 7.5), 150 mM NaCl, 1% Triton X-100, 1X HALT phosphatase/protease inhibitor cocktail). Whole cell lysates (500 µg total proteins) were pre-cleared with protein A/G agarose beads at 4°C for 30 minutes. The cleared supernatants were incubated overnight at 4°C with 2 µg of the indicated antibodies (anti-ERK, anti-PKCδ, anti-β-catenin, anti-FLAG, anti-Cx43), followed by a 30-minute incubation at 4°C with protein A/G-agarose beads. After five washes in ice cold-PBS-T, the proteins were eluted from the beads by heating the samples for 5 minutes at 95°C in Laemmli 3x SDS buffer (62.5 mM Tris-HCl, 2%w/v SDS, 10% glycerol, 50 mM DTT, 0.01% w/v bromophenol blue). A fraction of the eluted proteins (bead fraction) and input fraction were analyzed by western blotting (as described below) with the indicated antibodies. Briefly, equal amounts of proteins were electrophoresed on 10% SDS-PAGE gels, blotted to PVDF membranes and probed with the indicated antibodies. Membranes were stripped and re-probed with GAPDH antibodies to ensure equal loading of proteins among lanes. All blots were repeated at least three times with independent cell cultures/tibial extracts. Representative data are shown for each.

Mouse colony

All animal studies were performed with approval by the Animal Care and Use Committee at the University of Maryland School of Medicine. *Gja1*$^{-/K258stop}$ mice on a C57BL/6 background were provided by Mario Delmar (NYU). *Gja1*$^{+/-}$ mice on a mixed (C57BL/6-C129/J) background were provided by Roberto Civitelli (Washington University in St Louis). Breeding colonies were maintained at the University of Maryland

School of Medicine. Littermates were used for all experiments. Mice were given *ad libitum* access to standard chow and water and were maintained on a 12 h light/dark cycle. For genotyping, DNA was extracted from tail snips prior to weaning, using Accustart genotyping mix (Quanta Bio, Gaithersburg, MD). PCR genotyping for the *Gja1*$^{+}$ and *Gja1*$^{-}$ alleles was carried out using allele specific PCR primers (Primer 1: CAC GTG AGC CAA GTA CAG GA; Primer 2: AGG TGG TGT CCA GAG CCT TA; Primer 3: AAT CCA TCT TGT TCA ATG GCC GAT C), as provided by the Jackson labs (stock number 002201). PCR genotyping for the *Gja1*$^{+}$ and *Gja1*^{K258Stop} alleles was carried out using allele specific PCR primers (Primer 1: GCA TCC TCT TCA AGT CTG TCT TCG; Primer 2: CAA AAC ACC CCC CAA CAA GGA ACC TAG), as described (Maass et al., 2004).

X-Ray Imaging

Lateral and AP radiographs (35 kV, 10 sec) were taken of the mice, post euthanasia using a Faxitron digital x-ray system, as described ([104]).

Protein extracts

For long bone extracts, tibiae were dissected from both genotypes and cleaned of soft tissue. Subsequently, the epiphyses were removed, the marrow cavity flushed with sterile saline, prior to lysis in a modified RIPA buffer (50 mM Tris (pH 8.0), 150 mM NaCl, 1.0% NP-40, 0.5% Sodium deoxycholate, 0.1% SDS, 10 mM $Na_4P_2O_7$, 10 mM 2-glycerolphosphate, 10 mM NaF, 10 mM EDTA, 1 mM EGTA, 1X HALT phosphatase/protease inhibitor cocktail. Samples homogenization was performed using 5 mm diameter stainless steel beads and a Qiagen tissue lyser LT at 50 MHz for up to 10 minutes or until the sample was completely homogenized. Samples were then centrifuged at max speed for 10 min at 4°C. The supernatant was used for protein expression analysis by western blotting. For BMSCs, cells were lysed in modified RIPA, as described ([105]).

Quantitative Real Time RT-PCR

Total RNA was isolated from tibial extracts (flushed of marrow) using TRIzol reagent and homogenizing the sample with 5 mm diameter stainless steel beads and a Qiagen tissue lyser LT at 50 MHz for up to 10 minutes. RNA (1 μg) was reverse transcribed and used for quantitative real time PCR (qPCR) as described ([12]). Genes were simultaneously normalized to *Gapdh*, *Rpl13* and *Hprt*. PCR primer sequences are as published and/or are available upon request ([12,62]).

MicroCT

Femurs were dissected from 6-week-old male $Gja1^{+/-}$ and $Gja1^{-/K258Stop}$ mice and fixed in 4% PFA for two to four days and then transferred to 70% ethanol. Three-dimensional microCT was performed on the femurs of each genotype using SkyScan 1172 (Bruker, Kontich, Belgium). The skeletal parameters assessed by microCT followed published nomenclature guidelines (Bouxsein et al., 2010). Bone morphology and microstructure were assessed at the mid-diaphysis for cortical parameters, including cortical bone volume (Ct.TV), periosteal perimeter (Ct.Peri.Pm), endosteal perimeter (Ct.Endo.Pm), cortical thickness (Ct.Th), cortical porosity (Ct.Po) and mean polar moment of inertia (MMI). Trabecular parameters were assessed at the distal femoral metaphysis for trabecular parameters, including the trabecular bone volume fraction (BV/TV), trabecular bone thickness (Tb.Th), trabecular number (Tb.N) and trabecular separation (Tb.Sp). Analysis was completed on 11 ($Gja1^{+/-}$) and 8 ($Gja1^{-/K258stop}$) animals for each genotype, respectively. Femurs were scanned with 2K resolution, 10-micron voxel size, 0.5 mm Al filter at 60kV and 167 µA. Trabecular bone was delineated manually in a region of interest 0.2 mm to 2.0 mm proximal to the distal femoral growth plate. For cortical bone parameters, transverse microCT scans were performed at the femoral diaphysis beginning at 56% of the femoral length (measured from the head of the femur) extending 0.6 mm distally.

ELISA

Serum was collected from animals, and serum CTX and P1NP levels were quantitated using IDS assay for P1NP production and RatLaps for CTX production, according to the manufacturer's specifications [Immunodiagnostic Systems Inc. [IDS Inc., Gaithersburg, MD, USA].

Bone Histomorphometry

Fixed femurs were decalcified in 14% EDTA (pH 8.0). Subsequently, the tissue was paraffin embedded and 5 µm serial, longitudinal sections were prepared. Sections were stained for tartrate-resistant acid phosphate using a leukocyte acid phosphatases (TRAP) kit (Sigma), as described ([106]). Osteoblasts and osteoclasts adjacent to the bone surface were quantified using the Bioquant Osteo measure histology software, as described ([40,107]). Sections were stained with hematoxylin and cortical occupied/empty lacunae were counted (N=3 animals per genotype; 1002 (*Gja1*$^{+/-}$) and 1015 (*Gja1*$^{-/K258stop}$) lacunae, respectively). Picrosirius red staining was performed on sections and allowed to air dry before imaging. Quantification of fiber thickness and orientation was completed using a hue range method ([89,90]). For dynamic parameters, 6-week-old mice of each genotype were injected with calcein (7.5 mg/kg body weight) and alizarin 3-methyl iminodiacetic acid (30 mg/kg body weight) at 7 and 2 days before euthanasia, respectively. Femoral bone formation rates were quantified by dynamic histomorphometry, as described ([108]). Following fixation, each femur was embedded in poly-(methyl methacrylate). 100 μm thick transverse sections were cut (Leco VC50) at the femoral midpoint, then polished to 30 μm and mounted on glass slides. Images of each section was generated for analysis using fluorescence microscopy (Olympus IX-71). Images were analyzed for endosteal (Es) and periosteal (Ps) bone formation rate (BFR/BS) and mineral apposition rate (MAR) as defined by the ASBMR Committee for Histomorphometry Nomenclature (Dempster et al., 2013).

<u>Statistics</u>

All data are displayed as means ± standard deviations. Unless stated otherwise, experiments were repeated at least three times ($n \geq 3$). For microCT and histological analysis, the reviewer was blinded as to the genotype of the mouse. Mean expression was compared between samples by a two-tailed t-test for unpaired samples. Data were statistically analyzed using GraphPad Prism 6 software. A p-value < 0.05 indicated statistical significance.

Chapter 3: Structure-Function Analysis of Connexins as Active Regulators of Signal Transduction in Osteoblasts

1. *Abstract*

Intercellular communication through connexin43 facilitates bone modeling and remodeling through an interconnected functional network made up of osteoblasts and osteocytes. While it is known that Cx43 binds numerous proteins and signaling molecules ("interactome"), the consequences of these interactions is unclear. Our recent work has demonstrated the requirement for the Cx43 C-terminus (CT) *in vivo* and *in vitro*, for optimal osteoblast signaling and gene expression, and that absence of the Cx43 CT in male mice results in a skeletal phenotype analogous to deletion of the entire Cx43 gene in osteoblasts. These data also implied that Cx43-containing gap junctions not only exchange signals, but also must recruit the appropriate effector molecules to the Cx43 CT in order to optimally affect cell function and bone acquisition.

Cx43 and Cx45 seem to have opposing functions in bone biology. We postulated that this may be due to differences in the signaling machinery each connexin recruits. Using chimeric connexin proteins composed of portions of both Cx43 and Cx45, we examined downstream signaling and gene expression in osteoblasts. By luciferase reporter assays, western blot analysis, and qPCR, we found that, in general, both the Cx43 pore and Cx43 tail are required for optimal osteoblast signaling and gene expression, as Cx45 overexpression was ineffective or inhibitory in all aspects, while Cx43 overexpression stimulated signaling and gene expression. The chimeras largely mimicked Cx45 or had an intermediate effect in all aspects of this study. Through co-immunoprecipitation, our data shows binding of ERK, CAMKII, and β-catenin to Cx43 but not to cCx45. In contrast, ZO-1 (zona-occludens-1) was found bound to both Cx43

and Cx45. In total, these data imply that each connexin can differentially regulate downstream signaling and gene expression from the gap junction by local recruitment of different signaling effector molecules to each connexin's CT in order to affect bone cell function and bone modeling.

2. ***Introduction***

In the present study, we wanted to further dissect the roles of signal protein docking to the CT (C-terminal) domain of connexins in bone cells and determine if this docking/tail function of the CT was unique to Cx43. For the purpose of this study, we define the **pore function** as the ability of connexins to transmit small molecules and second messengers. Likewise, we define the **tail function** as the ability of the C-terminus to locally recruit signaling molecules (refer to **Figure 1.3**, Chapter 1). This C-terminal domain is highly variable among various connexins and interacts with numerous signaling molecules to impact signaling and thus is likely to have connexins isotype specific functions ([13–15,77,78,86]).

My published data have shown that deletion of the Cx43 C terminus i*n vivo* mimics the phenotype of the Cx43 cKO phenotype in vivo, including alterations in cortical bone geometry, deficits in downstream signaling and osteoblast gene expression and altered collagen processing ([109]). This suggest that the tail function of Cx43 may be as important as the pore function, at least with respect to bone. The role of Cx45 in bone acquisition and function in vivo has not been extensively studied. Cx45 is required for development, and Cx45-deficent mouse embryos die at E9.5/10.5 due to disruptions in vascular development, which preclude the study of skeletal functions ([22]).

Cx43 and Cx45 form gap junctions with different pore sizes (<1kD;<0.3kD) and seem to have opposing functions in bone biology. While previous studies had suggested porosity was a driver of these differences, we postulated that differences in the signaling machinery each connexin locally recruits to the gap junction through CT interactions could also drive these observed opposing functions. Previous studies have shown that when over expressed, Cx45 altered coupling between cells and resulted in reduced permeability in comparison with Cx43 ([23,110]). Gene expression examination showed that altering the expression of Cx43 and Cx45 modulated expression of osteoblast genes. Cx43 increased expression while Cx45 decreased expression of genes associated with osteoblast differentiation ([111]). In addition to differing permeability between Cx43 and Cx45, a large number of signaling effectors have been shown to bind to the Cx43 C terminus ([14,77,78,86]). In contrast, none have been described for Cx45. These interactions with Cx43 are functionally important, as protein interactions with the Cx43 C terminus are necessary for optimal signaling and gene expression in osteoblasts ([12]). The un-conserved C-terminus of connexins can associate with a variety of signaling complexes ([14]), but the consequences of these interactions with Cx43 have not been studied in great detail.

Modulation of Cx43 expression impacts ERK, PKCδ, pCREB and β-catenin signaling pathways i*n vitro*, which influence osteoblast gene expression and cell function and cell survival ([73–76]). The regulation of signaling may involve assembly a specific subset of signaling effectors to the gap junction, as well as permitting the communication of a specific subset of second messengers though the gap junction pore. Three interactions between the Cx43 C-terminus and signaling effector molecules have been shown to affect the function of osteocytes and osteoblasts: PKCδ, β-arrestin, and α5β1 integrin ([77,78,86]). In MC3T3 osteoblasts, PKCδ transiently binds to the Cx43 C-terminal tail before translocating to the nucleus where it can regulate Runx2 transcriptional activity ([62,86]). In OB-6 cells, interactions between Cx43 tail and β-arrestin allow for the anti-apoptotic action of PTH by sequestering β-arrestin and allowing cAMP dependent cascades to be activated ([77]). Lastly, in MLO-Y4 osteocyte-like cells, the Cx43 C-terminus interacts with α5β1 integrin, which controls opening and closing of the hemichannels by causing a conformational change in the extracellular domain of the integrin in response to mechanical load ([78]).

Very few protein interactions with Cx45 have been described in any tissue, other than a ZO1 binding domain ([14]). While Cx43's "interactome" is somewhat characterized, it is not complete. These apparent discrepancies in CT-associated proteins suggested that in addition to having unique permeability characteristics, each connexin may assemble a unique interactome that can impact downstream signaling and ultimately affect bone cell function. This led us to test whether it was the **communication/pore** function, **the docking/tail** function, or both functions of Cx43 that dictates the opposing "bioactivity" of Cx43 and Cx45?

In this study, we examine the influence of each connexin's C-terminal tail on osteoblast signaling and function using UMR106 cells. We tested the hypothesis that both pore and tails functions of a connexin protein dictate its ability to optimally regulate downstream signaling from the gap junction. The interactome of C-termini within the connexin family allows for efficient signaling downstream of the gap junction through the local recruitment of effector molecules to the gap junction. To confirm the functional consequences of these interactions, we have generated chimeric connexins, which fuse the Cx43 pore with the Cx45 C-terminal tail (Cx43pore-Cx45tail, aka Cx43/45) and vice versa (Cx45pore-Cx43tail, aka Cx45/43). We compared full length Cx43 and Cx45 alongside the chimeras and examined downstream signaling and gene expression in osteoblasts.

3. <u>Results</u>

A model of the structures of Cx43 and Cx45 and the chimeric connexins, which fuse the Cx43 pore with the Cx45 C-terminal tail (Cx43pore-Cx45tail) and vice versa (Cx45pore-Cx43tail) are shown in **Figure 3.1A** and **Figure 3.1B**, respectively. Little is known about protein interactions with Cx45 in any tissue, and while Cx43's "interactome" is somewhat characterized, the total interactions with signaling molecules are not fully distinguished. A sequence alignment of the C terminal (CT) domains of mouse Cx43 (amino acids 234-382) and mouse Cx45 (amino acids 249-396) revealed limited homology between the two connexins tails, with only 17.5% identity (Figure 3.1C). Several important functional domains in the Cx43 CT are unconserved in Cx45 CT. Only the Cx43 CT contains a proline rich SH3 binding domain, ERK(1/2) /MAPK phosphorylation sites. Likewise, only one of four PKA phosphorylation sites found in the Cx43 CT are conserved in the Cx45 CT. Both proteins possess a ZO-1 binding site at the end of their C termini. While a microtubule(MT) binding domain has been described at the beginning of Cx43's CT sequence, a microtubule binding domain has not been established for Cx45, currently. Finally, our lab has defined a PKCδ binding domain in the Cx43 CT ([86]).

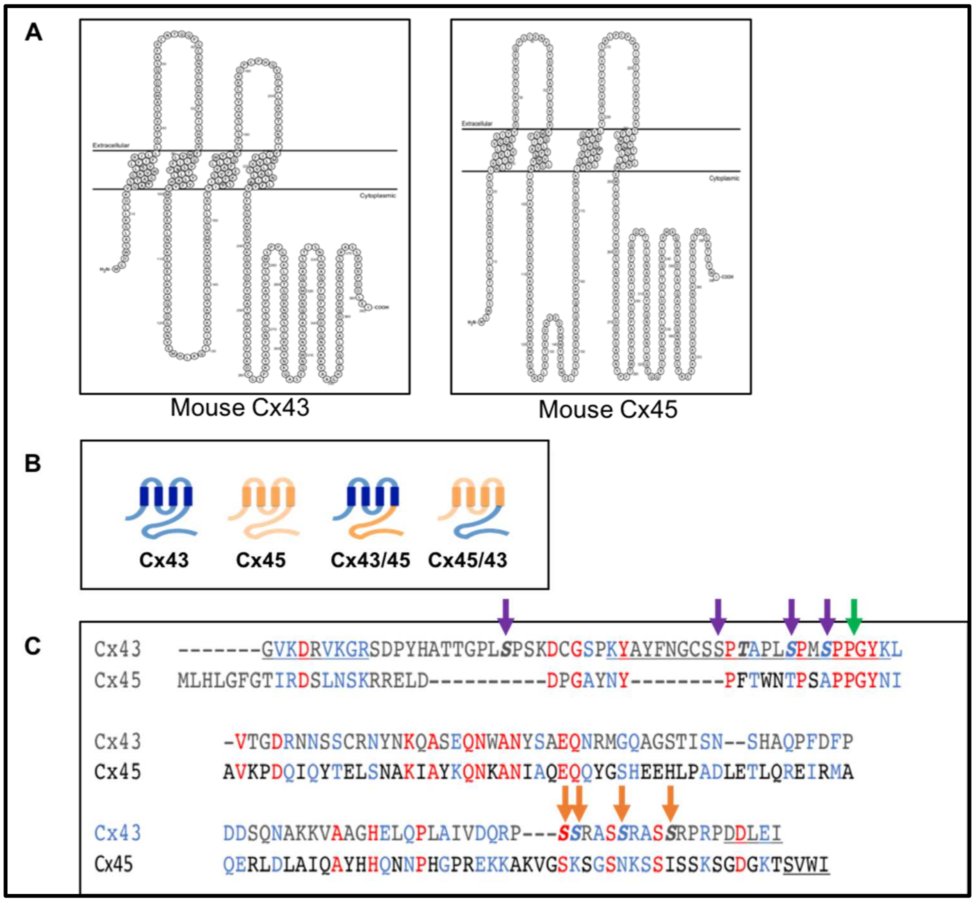

Figure 3.1. A. Complete structure of Mouse Cx43 and Mouse Cx45. B, **A schematic of the chimeric proteins compared with full length Connexin 43 and Connexin 45**. **C.** Sequence alignment of Cx43 and Cx45**.** 17.5% identity (:). 46.1% similarity(.). **Green arrow** – proline rich region, SH3 binding domain. **ZO1 binding site** – underlined at the end of both Cx sequences. **MT binding site** – underlined at the beginning of Cx43's CT sequence. **Purple arrow** – ERK(1/2)/MAPK phosphorylation sites. **Orange arrow** - PKA phosphorylation sites.

We confirmed of overexpression of both full length connexins by qPCR and western blots, as well as the chimeric constructs using C-terminal specific antibodies (**Figure 3.2A,B**). To confirm that the connexins chimeric constructs were functional, we used FRAP (fluorescence recovery after photo-bleaching) to test intercellular communication in comparison with the full length connexins. After loading the cells with Calcein AM (~682 Daltons), a cell was chosen in a cluster to photobleach, and the rate of recovery was measured. Full length Cx43 and the chimera with the pore of Cx43 (Cx43/45) had the same percent of recovery, while full-length Cx45 and the chimera with the pore of Cx45 (Cx45/43) prevented the intercellular communication of calcein. Calcein is around 0.6 kDa, which is over the limit of molecular mass efficiently passed by Cx45-containing gap junctions.

In order to understand the contribution of connexin domains to signaling cascade activation, we used several signaling pathway specific luciferase reporters/western blots to track signaling activation downstream of gap junctions following overexpression of wild type or chimeric connexins (**Figure 3.3**). Using a serum response element luciferase (SRE-Luc) reporter to examine MAPK signaling (**Figure 3.3A**), only full-length Cx43 increased SRE luciferase activity. Cx45 overexpression had the opposite effect, showing decreased SRE luciferase activity. With respect to MAPK signaling, the chimeric proteins were unable to mimic the effects of

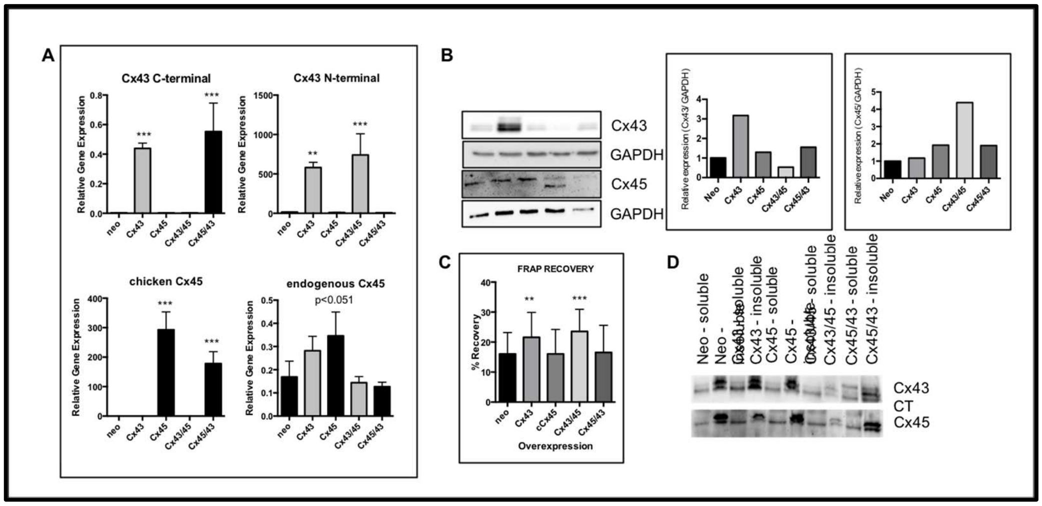

Figure 3.2. Gene expression analysis showing Cx43 and Cx45 overexpression following transfection of the experimental constructs. A. Real time PCR from UMR 106 cells confirms overexpression. B, western blots confirm protein expression. GAPDH was used as a loading control. C, FRAP results are shown as percent recovery. D. Fractionation confirms membrane localization. Graphs depicted as Mean +/- SD, * = p<0.05, ** = p<0.01, *** = p<0.001, **** = p<0.0001.

Cx43, supporting the notion that both the Cx43 pore and tail are required for efficient signaling in this pathway. Both the Cx43/45 and the Cx45/43 chimeras had similar inhibitory effects concerning MAPK signaling. These findings are supported by tracking MAPK activation by immunoblotting for p-p38 and p-ERK when the various constructs are overexpressed (**Figure 3.3B**). Cx43 overexpression stimulated both ERK and p38 phosphorylation. While none of the other connexin constructs stimulated both ERK and p38 pathways.

Similarly, using a cAMP/PKA-signaling luciferase (CRE-Luc) reporter (**Figure 3.3A**), only full-length Cx43 increased CRE luciferase activity. Cx45 overexpression had the opposite effect, shown by a reduction of CRE luciferase activity as compared to Cx43. The Cx43/45 had similar transcriptional activity to cCx45. In contrast, the Cx45/43 chimera increased CRE-Luc activity as compared to the empty vector, reaching almost the same level of activation as Cx43 overexpression. Immunoblot for p-CREB mimic the CRE-Luc reporter data (**Figure 3.3B**), in that the most robust activation of the pathway is when the Cx43 tail is present, be it in the full length Cx43 or in the Cx43/45 chimera. These data suggest that for cAMP-dependent signaling the pore of Cx43 may be sufficient to regulate downstream signaling independent of whether the tail of Cx43 or Cx45 are present.

Previously we have shown that Cx43 and Cx45 reciprocally regulate the activity of the master regulator of osteoblast differentiation, Runx2 ([69]). Using a pOSE2 (osteoblast specific element) luciferase reporter to look at Runx2 transcriptional activity (**Figure 3.3A**), only full-length Cx43 increased pOSE2 luciferase activity. Cx45 overexpression had the opposite effect, reducing pOSE2 luciferase activity. Our published data have shown that Runx2 activity is controlled by a combination of ERK1/2 and PKCδ acting downstream of Cx43 ([62,70]). With respect to PKCδ signaling, western blotting demonstrated that the chimeric proteins were unable to mimic the effects of Cx43, supporting the notion that both the Cx43 pore and tail are required for efficient PKCδ signaling.

Another key pathway involved in osteoblast function that we and others have linked to Cx43 function is β -catenin signaling ([109,112,113]). Using a Wnt/β -catenin signaling reporter (**Figure 3.3A),** only full-length Cx43 increased TOPflash luciferase activity. Cx45, Cx43/45 or Cx45/43 overexpression had the opposite effect, reducing TOPflash luciferase activity relative to empty vector transfected controls. These data were confirmed through an immunoblot for active β-catenin (**Figure 3.3B**), which clearly demonstrate connexin-dependent pathway activation.

We also investigated other pathways with roles in bone biology that had not yet been linked to gap junction regulation, using NFkB-Luc and GRE-Luc (Glucocorticoid response element) luciferase reporters (**Figure 3.4**).

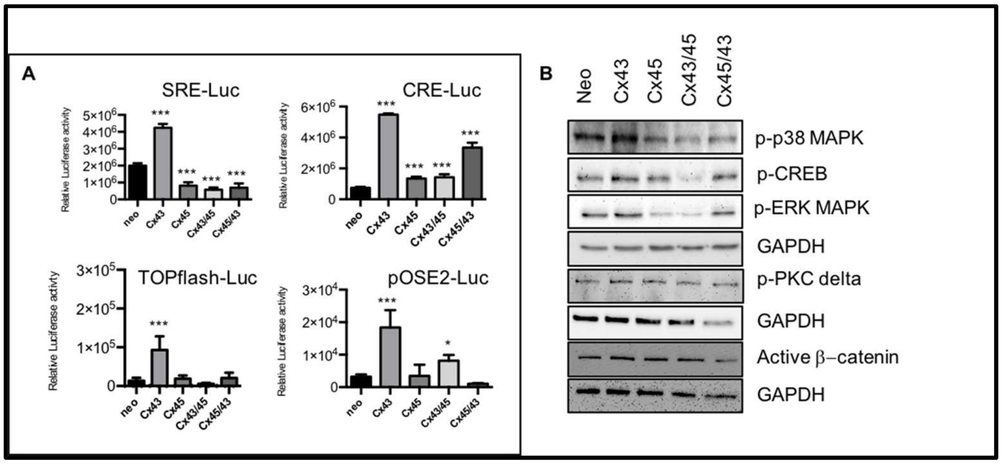

Figure 3.3. Overexpression of full length Cx43 leads to the most robust transcriptional activity even in the presence of different promoters. UMR106 cells were transfected with indicated plasmids and specific luciferase reporters. Data was collected 48 hours post transient transfection. We confirmed signaling pathway specific activation through western blots. Western blots were probed for indicated signaling proteins in UMR106 cells where the constructs were overexpressed. GAPDH was used as a loading control. Graphs depicted as Mean +/- SD, * = p<0.05, ** = p<0.01, *** = p<0.001, **** = p<0.0001.

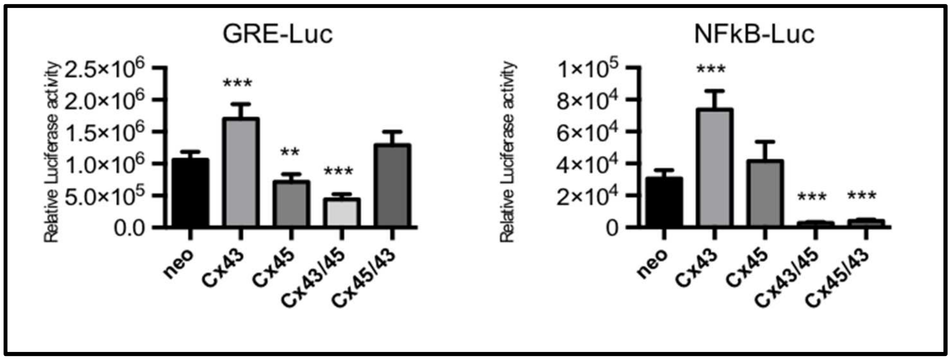

Figure 3.4. Overexpression of full length Cx43 leads to the most robust transcriptional activity even in the presence of different promoters. UMR106 cells were transfected with indicated plasmids and specific luciferase reporters. Data was collected 48 hours post transient transfection. Graphs depict mean±SD. * = $p<0.05$, ** = $p<0.01$, *** = $p<0.001$.

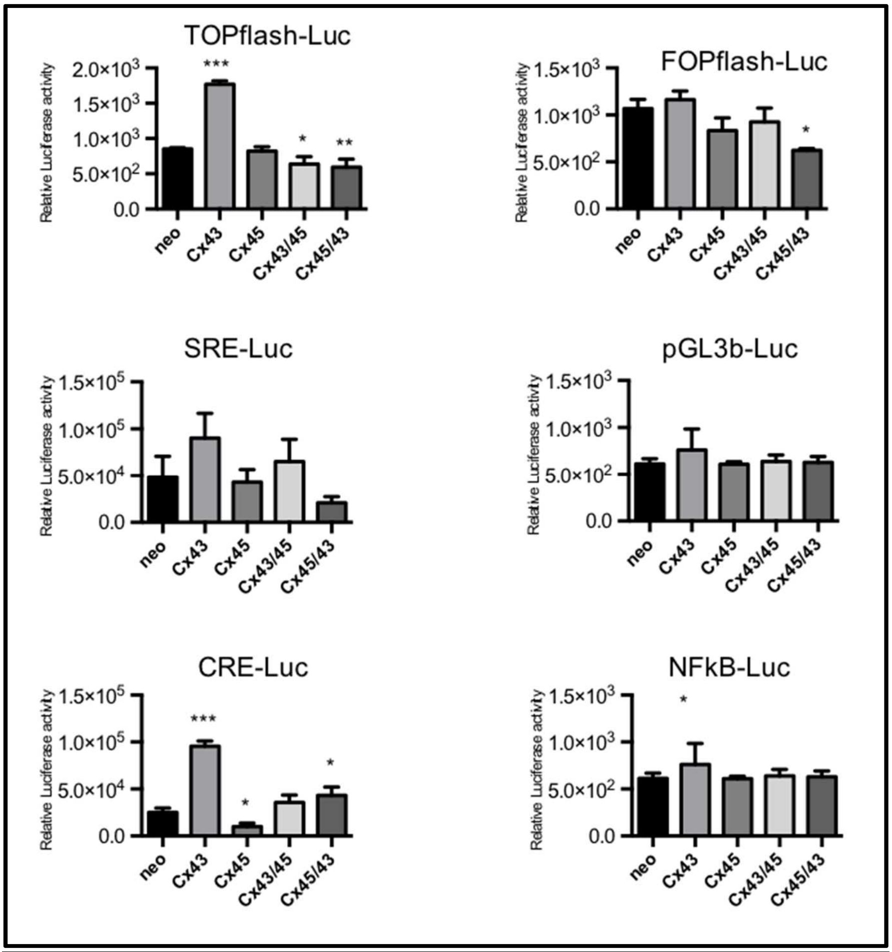

Figure 3.5. Overexpression of full length Cx43 leads to the most robust transcriptional activity even in the presence of different promoters. MC3T3 cells were transfected with indicated plasmids and specific luciferase reporters. Data was collected 48 hours post transient transfection. Graphs depict mean±SD. * = $p<0.05$, ** = $p<0.01$, *** = $p<0.001$.

These reporter constructs showed that only full length Cx43 increased NFkB-Luc and GRE-Luc activity. For NFkB signaling, both chimeras were unable to recapitulate the activity of full length Cx43. For glucocorticoid signaling, Cx45 was inhibitory and the 43/45 was even more inhibitory, as compared to an empty vector. We completed the same luciferase assays in another cell line, MC3T3 osteoblast like cells (**Figure 3.5**). These data show that in general, both the pore/communication and the docking/tail functions of Cx43 are required to stimulate signal pathway activation.

In order to understand the functional significance of connexin-dependent control of signaling pathways, we examined osteoblast gene expression in UMR106 where the full length and chimeric connexin constructs were overexpressed (**Figure 3.6**). In addition, we investigated the effects of overexpression of the chimeric constructs on collagen processing genes, as previous studies have reported the requirement for Cx43 in proper collagen processing ([33,109]). Similar to what we saw in our signaling outputs, in general Cx43 stimulated osteoblast gene expression, while Cx45 was generally ineffective at stimulating expression or was inhibitory. The chimeras were generally ineffective at stimulating gene expression associated with osteoblast differentiation in most contexts.

Specifically, an intact Cx43 stimulated the mRNA expression of osteoblast differentiation markers, Sp7/Osterix, Col1a1, and cell proliferation marker, CyclinD1 (**Figure 3.6**). Lox mRNA expression, which is an enzyme involved in collagen cross-linking was also increased with the overexpression of Cx43 as compared with other connexin constructs. Axin2 mRNA expression, which is a readout of Wnt/β-catenin signaling was also increased with the overexpression of Cx43 as compared with other

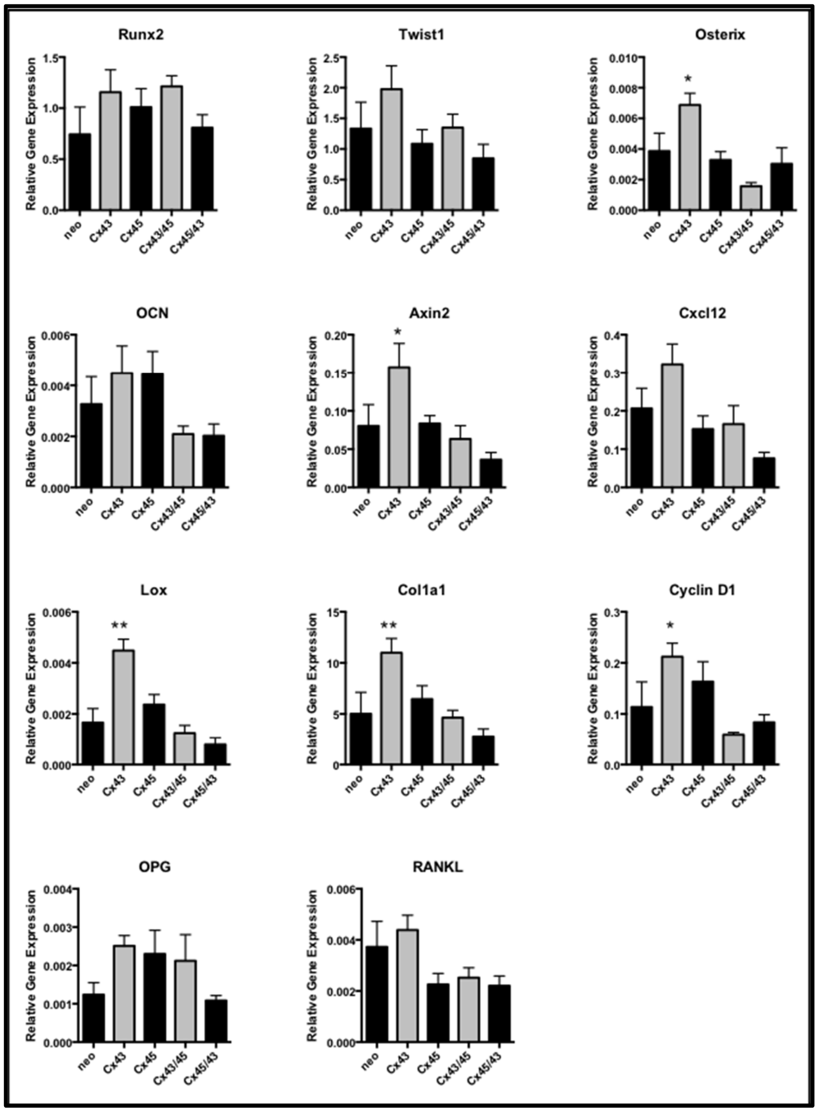

Figure 3.6. Quantitative RT-PCR analysis of the effect of chimeric connexin overexpression on osteoblast gene expression. qPCR from RNA isolated from UMR106 cells was performed for Wnt/β-catenin related genes, transcriptional regulators of osteoblastogenesis, and osteoblast differentiation markers, and collagen associated genes. (*n*=6). Graphs depict mean±SD. * = $p<0.05$, ** = $p<0.01$, *** = $p<0.001$.

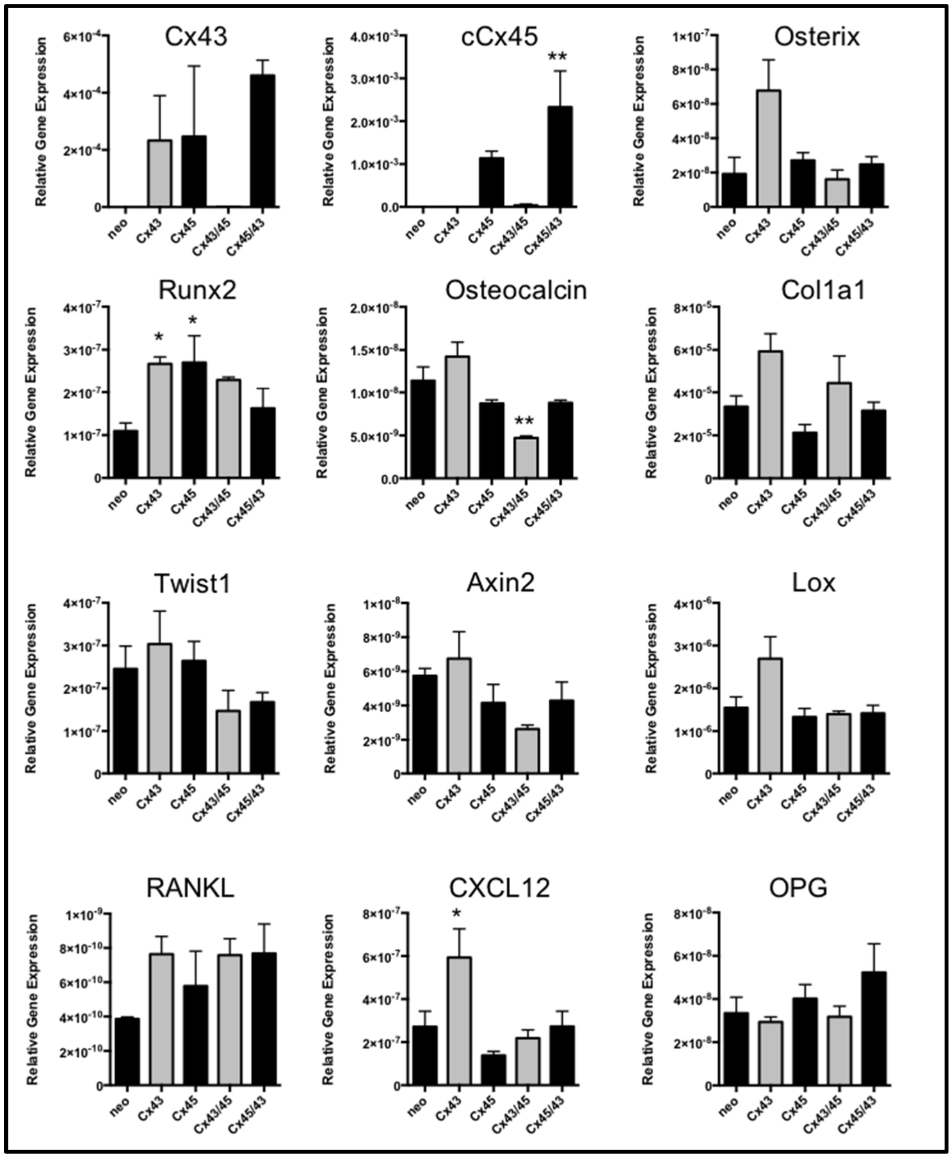

Figure 3.7. Quantitative RT-PCR analysis of the effect of chimeric connexin overexpression on osteoblast gene expression. qPCR from RNA isolated from MC3T3 cells was performed for Wnt/β-catenin related genes, transcriptional regulators of osteoblastogenesis, and osteoblast differentiation markers, and collagen associated genes. (*n*=6). Graphs depict mean±SD. * = $p<0.05$, ** = $p<0.01$, *** = $p<0.001$.

connexin constructs. In contrast, Cx45 attenuated the expression of most of these genes, while the chimeras were generally intermediate between the two or also just as inhibitory for gene expression as cCx45. In all cases, both the pore function (permeability) and tail function (signal recruitment) of Cx43 were required for optimal gene expression. We completed a preliminary screen of the same gene expression profile in MC3T3 osteoblast like cells (**Figure 3.7**).

Having established a requirement for Cx43 CTs, but not Cx45 CTs for most signaling pathways, we sought to clarify differences in interactomes between the Cx43 and Cx45 connexin tails (**Figure 3.8A**). To do this, we performed co-IPs (co-immunoprecipitations) in UMR106 osteoblast like cells. We overexpressed full length Cx43 and a Myc tagged-cCx45 and probed for interacting proteins. To confirm overexpression, we IPed Cx43 and the Myc-tag, respectively, and blotted with the same antibody. As a positive control, we confirmed association of Cx43 and Cx45 with ZO-1, which binds the CT of both connexins ([14,114]). We show robust binding of ERK1/2, CAMK2, and β-catenin to the overexpressed Cx43. In striking contrast, coIPs reveal little to none of the signaling proteins in complex with overexpressed Myc tagged-cCx45. To validate the co-IPs, we performed immunofluorescence to show co-detection with the signaling molecules and the Cx43 CT. By immunofluorescence, we observed that β-catenin and Cx43 co-localize together at the plasma membrane. To date, we have confirmed co-detection of only one downstream effector protein with Cx43 at the plasma membrane. Future experiments will be needed to confirm co-detection of Cx43 with other signaling molecules. (**Figure 3.8B**). In total, these data indicate connexin-specific interactomes are present, with most signaling complexes associated with Cx43, but not Cx45.

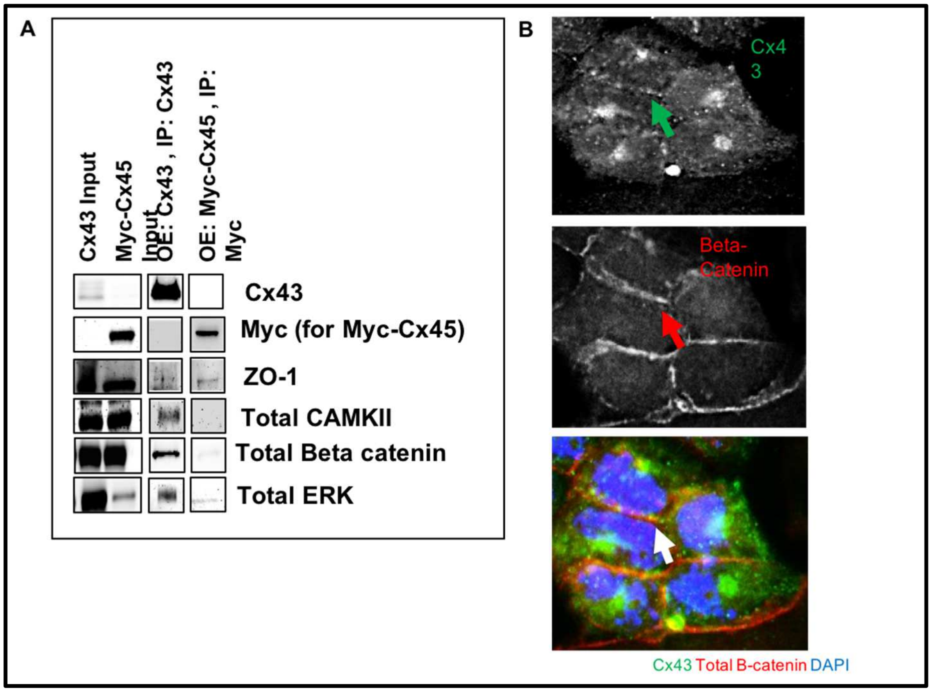

Figure 3.8. Cx43 and Cx45 have differential interactomes. A, Co-immunoprecipitations (co-IPs) were performed to assess protein–protein interactions between the indicated signaling proteins and the Cx43 CT and the Cx45 CT. UMR106 cells were transfected with a construct encoding Cx43 or Myc-tagged Cx45. (A) Input and bead fractions are shown for co-IPs performed with anti-ERK1/2, anti-CAMKII, anti-ZO-1, and anti-β-catenin antibodies and blotted with anti-Cx43 antibodies. Positive control co-IPs were also performed with anti-Cx43 and anti-Myc. **B**, Immunofluorescence was performed to show co-detection of Total b-catenin and Cx43 at the plasma membrane.

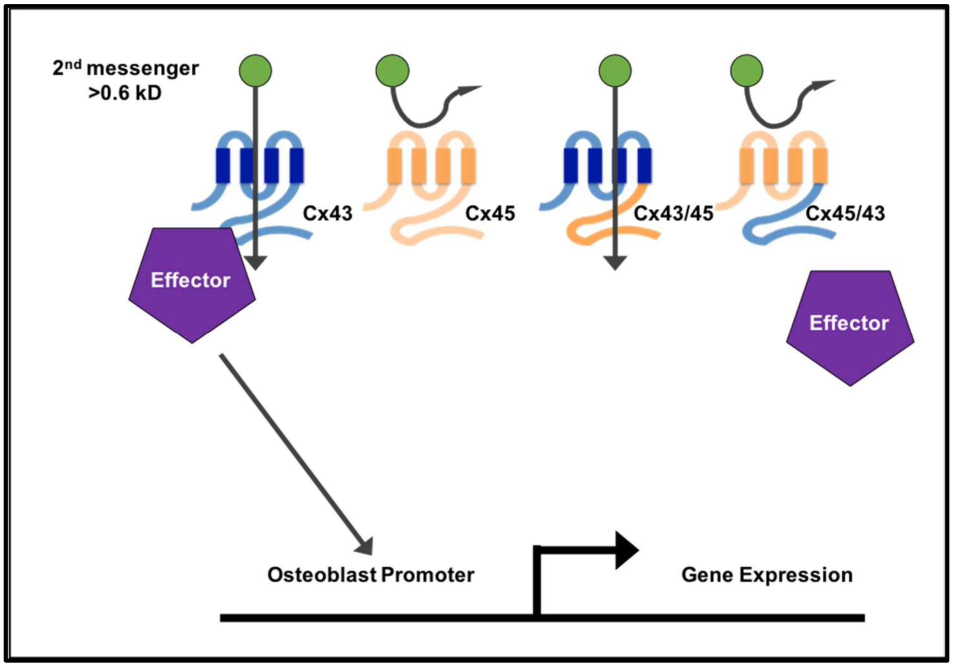

Figure 3.9. Schematic of the effects of chimeric connexins versus the full length connexins on downstream signaling and osteoblast function. Both pore and tail functions of Cx43 are required to elicit the optimal downstream signaling and osteoblast gene expression.

4. ***Discussion***

This is our working model of how the chimeric proteins affect downstream signaling and osteoblast function (**Figure 3.9**). Full length Cx43 can allow 2nd messengers to pass as well as to recruit appropriate effectors to the C terminus to permit optimal signaling and osteoblast gene expression. Cx45 doesn't allow passage of 2nd messengers larger than 0.3kD, attenuating signaling and gene expression. The Cx43/45 chimera can allow the passage of 2nd messengers, but cannot recruit the appropriate effector molecules, leading to a reduction of signaling and gene expression in comparison with full length Cx43. The Cx45/43 chimera cannot allow passage of some 2nd messengers, despite the ability to recruit effector molecules to the C terminus, also leading to a reduction of signaling and gene expression in comparison with full length Cx43.

The goal of this study was to explore the structure-function relationship by which Cx43 and Cx45 differentially affect osteoblasts. We found that, in general, both the Cx43 pore and Cx43 tail are required for optimal downstream signaling (e.g., MAPK, PKCδ and β-catenin, and pCREB) and osteoblast gene expression (e.g., COL1a1, Lox, Axin2, Osterix, and CyclinD1), as replacement of the Cx43 pore or tail domain with that of Cx45 was ineffective or inhibitory for connexin-dependent signaling and gene expression. By co-immunoprecipitation (co-IP), our data show that Cx43 complexes with ERK, CAMKII, and β-catenin. In contrast, co-IP of a myc-tagged Cx45 results in minimal co-association of these signaling proteins. As a positive control, IP of ZO-1 (zona-occuldens-1) confirms that the ability to IP Cx43 and myc-tagged Cx45, as previous studies have shown. These data show that Cx43 and Cx45 do, indeed, have different interactomes. Here, we showed that the pore/channel function and docking/tail function of Cx43 are required for its ability to optimally affect osteoblast signaling and gene expression.

The discrepancies between pathways for the transcriptional activity of the full length connexins versus the chimeras leads to a point of specificity for each second messenger. In some contexts, both channel/pore and docking/tail functions of Cx43 are required. For example, second messenger such as IP7 whose size is too large to diffuse through Cx45 channels and that activates PKCδ which is exclusively recruited to the Cx43 but not Cx45 channels, may require both the pore and tail functions of Cx43 to efficiently pass the second messenger and initiate downstream signal cascade activation. In contrast, in some contexts only pore function or tail function may be sufficient, such as cAMP/PKA signaling. Our data suggest that optimal cAMP communication and downstream PKA signaling absolutely require only the tail function of Cx43. However, either the pore of Cx43 or Cx45 provide functionality to his tail. This is likely because cAMP is small enough to pass through both Cx43 and Cx45 containing gap junctions, but without the Cx43 CT, the appropriate signaling effectors aren't recruited locally to the gap junction and downstream signaling does not occur.

The CT's role as a docking platform seems intuitive for the spatial control of downstream signaling. The local recruitment of signal machinery to the gap junction plaque will place these effectors where the concentrations of a communicated second messenger are highest, permitting efficient signaling from this microdomain. Additional studies are needed to survey and measure the local concentrations of second messengers at the gap junction plaque to prove this point. One of the ODDD mouse models ($Gja1^{Jrt/+}$) also exhibited reduced bone quality, both in the trabecular and cortical compartments, as the animals were aged up to 12 months. This is an intriguing result, showing Cx43 facilitates communication of both anabolic and catabolic signals ([115]). These findings underscore the importance of understanding which signals are being propagated through cells by gap junctions as well as the context in which those signals are being passed.

The findings in this study expand the known signaling pathways affected by Cx43 and deepen our understanding of how connexins participates in signaling in bone. This study may help us to understand the divergent effects of Cx43 in the context of different stimuli, such as different second messengers, hormones, growth factors, and mechanical load. Cx43 has been shown to be beneficial during mechanical loading in bone as well as deleterious in aging and disuse. Hormonally, PTH administration to Cx43 deficient mice lead to reduced bone anabolic responses as compared to control mice ([40]). As far as mechanical loading and unloading are concerned, several studies show that mechanical loading and unloading effects the endosteal and periosteal surfaces of long bones in opposite ways ([67,72,84]), and Cx43 ablation leads to an even more severe phenotype in bone. The cortical thinning and marrow cavity widening observed in Cx43 deficient mice resembles skeletal effects of aging and space flight ([116]). Cx43 ablation was also show to prevent cortical bone formation during unloading ([46]). In the cKO model of Gja1 deletion using the Col1α1 promoter, cortical bone was resistant to the effect of Botulinum Toxin Type A (Btx A) induced muscle paralysis in comparison with wild-type mice who did exhibit expansion of the marrow cavity as well as cortical thinning, due to increases in osteoclast activity ([117]). Cx43 is required throughout the entire osteoblast differentiation cascade, as differentiation markers such as Col1α1 and Osterix were increased when full length Cx43 is overexpressed. This is consistent with the convergence of Cx43 on Runx2 to promote osteoblastogenesis ([118]). The increase in cell proliferation marker, CyclinD1, is consistent with what was reported in an in vivo model of Cx43 CT truncation ([109]). These data also confirm the involvement of ERK/MAPK and PKCδ, and Wnt/β-catenin signaling pathways from previously published in vitro and in vivo work ([62,70,109]). The binding of CAMKII to Cx43 CT also confirms a previously published report of such interactions ([14]). The increase in Lox mRNA expression is consistent with previous finding, where Cx43 deletion or truncation was shown to reduce Lox gene expression ([33,43,109]).

In the current study, we only investigated basal signaling. It is likely that we would see a concomitant increase in transcriptional activity, downstream signaling, and osteoblast gene expression between different connexins using stimulations with fibroblast growth factor 2 (FGF2), Wnt3a, and parathyroid hormone (PTH), which have been shown to activate MAPK/ PKCδ, Wnt/β-catenin, and PKA signaling, repetitively ([12,62,70,98–100,119]). While *in vitro* data suggested such a link ([72,76–78,86]), these treatments could be used in future studies to see if effects of connexin expression on these signaling pathways are exacerbated by stimulating various signaling pathways.

One limitation of this study was the need for a functional Cx45 antibody, hence we used a Myc-tagged cCx45 construct for the co-immunoprecipitations because of difficulty finding an appropriate antibody for Cx45. While we did find a functional Cx45 antibody for western blotting, there is no Cx45 antibody functional for immunofluorescence. We also did not test the functionality of Cx45 containing gap junctions using FRAP. We do know they successfully made it to the plasma membrane through the membrane fractionation experiment and acted in a dominant negative way with respect to Cx43, but they were not tested for communication low molecular weight fluorophores such as neurobiotin, which is around 0.286 kDa.

Another limitation to this study was use of UMR106 and MC3T3 osteoblast cells which both have some endogenous connexin expression that may mildly confound our results. UMR106 cells have high endogenous Cx45 expression and lower Cx43 expression. Conversely, MC3T3 cells have higher endogenous Cx43 expression and lower amounts of Cx45 expression. However, given the reciprocal expression of these connexins in these two cell lines and yet consistency in our signaling findings, we feel that the effects we observe are only mildly influenced by the endogenous connexins. We did see similar results in the luciferase assays as well as gene expression in both cell lines, posing the idea that overexpression of the full length connexins and the chimeric connexins were able to overcome the endogenous expression. However, use of another cell line deficient in both Cx43 and Cx45 could strengthen the confirmation of our hypothesis. Primary cells deficient in both Cx43 and Cx45 would be the best model for continuing to delineate the functional aspects of each connexin's ability to differentially regulate transcriptional activity, downstream signaling, and osteoblast gene expression. Future studies using connexin deficient primary cells could confirm these results and make the data more translational.

In summary, the pore and tail of Cx43 are required for their ability to optimally affect transcriptional activity, downstream signaling, and mRNA expression of genes associated with osteoblast differentiation and function. All pathways and genes have been previously reported to be regulated by Cx43 abundance. The data presented in this study supports our hypothesis that gap junctions must not only communicate signals through the pore, but also be able to recruit the appropriate effector molecules to their C-terminus in order to optimally affect osteoblast function and the coordination of cells within the interconnected network of osteoblasts.

5. METHODS

Materials

All chemicals and reagents were purchased from Sigma (St Louis, MO) unless indicated otherwise.

Cell culture

MC3T3 clone 4 cells were obtained from the American Type Culture Collection [Manassas, VA (ATCC)] and were cultured in αMEM containing 10% fetal bovine serum (Benchmark), penicillin (50IU/ml), streptomycin (50µg/ml) and gentamycin (50µg/ml). Cells were used at passage < 15. Cultures were kept at 37°C in a humidified atmosphere of 95% air and 5% CO2. Media was replaced every 2-3 days.

UMR106 cells were obtained from the ATCC and were cultured in DMEM containing 10% fetal bovine serum (Benchmark), penicillin (50IU/ml), streptomycin (50µg/ml) and gentamycin (50µg/ml). Cells were used at passage < 15. Cultures were kept at 37°C in a humidified atmosphere of 95% air and 5% CO2. Media was replaced every 2-3 days ([109]).

Transient transfections and plasmid constructs

UMR106/MC3T3 cells were transiently transfected using the Jetprime transfection reagent (Polyplus, New York, NY), as described ([109,119]). Endotoxin free plasmid DNA was prepped using a Qiagen HI-Speed Maxi prep system, according to the manufacturer's specifications. The empty vector, pSFFV-neo, was provided by Dr. Gabriel Nunez (University of Michigan, Ann Arbor). The pSFFV-Cx43 plasmid, which contains the full length Cx43 coding sequence cloned downstream of the Spleen Focus Forming Virus promoter was provided by Dr. Thomas Steinberg (Washington University, St Louis). The pSFFV-cCx45 plasmid was gifted from cCx45 from Eric Beyer, University of Chicago Medical School.

Luciferase assays

Cells were plated at 50,000- 60,000 cells per well in a 48 well plate and allowed to adhere and become confluent. Cells were transiently transfected using the Jet prime system (Polyplus, New York, NY) according to manufacturer's directions at a 1:4 ratio of reagent to DNA. Total DNA volume was kept equal with empty vector. Whole cell extracts were obtained 48 hours post transfection by washing with HBSS (Hanks' balanced salt solution) and lysed in 1× Passive Lysis Buffer (Promega) with constant agitation for up to 20 minutes. Lysates were then added to a 96 well assay plate and read using the Berthold LB960 illuminometer system (Oak Ridge, TN).

Fractionation

Cells were transiently transfected and lysates were collected 48 hours post transfection in modified RIPA buffer (50 mM Tris(pH 8.0), 150 mM NaCl, 1.0% NP-40, 0.5% Sodium deoxycholate, 0.1% SDS, 10mM $Na_4P_2O_7$, 10 mM B-glycero - PO_4, 10mM NaF, 10mM

EDTA, 1mM EGTA). HALT phosphatase/protease inhibitor cocktail was added at 1:100 to the RIPA buffer prior to lysis. Lysates were centrifuged were centrifuged at 10,000 rpm for 10 minutes at 4 degrees C. the supernatant fraction was saved and the pellet was resuspended in Laemmli 5x SDS buffer (62.5 mM Tris-HCl, 2%w/v SDS, 10% glycerol, 50 mM DTT, 0.01% w/v bromophenol blue). Both the supernatant and pellet fractions were run side by side for each overexpression condition following western blotting techniques as previously described ([109]).

Western blotting

Whole cell extracts were obtained by washing confluent cultures of UMR 106 cells with HBSS (Hanks' balanced salt solution) and lysing with modified RIPA buffer (50 mM Tris(pH 8.0), 150 mM NaCl, 1.0% NP-40, 0.5% Sodium deoxycholate, 0.1% SDS, 10mM $Na_4P_2O_7$, 10 mM B-glycero - PO_4, 10mM NaF, 10mM EDTA, 1mM EGTA). HALT phosphatase/protease inhibitor cocktail was added at 1:100 to the RIPA buffer prior to lysis. The lysates were centrifuged at 10,000 rpm for 10 minutes at 4 degrees C and the supernatant was kept for protein analysis by western blotting. For all western blots, equal amounts of proteins were electrophoresed on 10% SDS-PAGE gels, blotted to PVDF membranes and probed with the indicated antibodies. The antibodies use in this study were: Sigma, anti-Cx43 (C6219); Cell Signaling Technology, total ERK (9102L), phospho-ERK (9101L), phospho-PKCδ Thr505 (9374S), active β-catenin (8814S), anti-Rabbit (7074S), anti-mouse (7076S), anti-Myc (71D10) (2278), total CAMKII (pan, D11a10, 3362), p-CREB (SER133) (8763); BD Biosciences, total β-catenin (6310153); Millipore, GAPDH (MAB374). Membranes were stripped and re-probed with GAPDH antibodies to ensure equal loading of proteins among lanes. All blots were repeated at least three times with independent cell cultures. Representative data are shown for each. Where indicated, the band intensities of western blots were quantitated with ImageJ (FIJI) image analysis software (NIH, Bethesda, MD). Data from multiple blots (a minimum of three) were normalized and averaged. ([73,109])

qPCR

Total RNA was isolated from cultured UMR106 and MC3T3 cells using TRIzol reagent, according to the manufacturer's directions. RNA (1 µg) was reverse transcribed and used for quantitative real time PCR (qPCR) as described ([12]). Genes were simultaneously normalized to *Rpl13* and *Hprt*. PCR primer sequences are as published and/or are available upon request([12,62,109]).

Co-IP

UMR106 cells were harvested 48 hours post transfection with 1X cell lysis buffer (20 mM Tris (pH 7.5), 150 mM NaCl, 1% Triton X-100,). HALT phosphatase/protease inhibitor cocktail was added at 1:100 to the 1X cell lysis buffer prior to lysis. Whole cell lysates (500 µg total proteins) were pre-cleared with protein A/G agarose beads at 4°C for 30 minutes. The cleared supernatants were incubated overnight at 4°C with 2 µg of the indicated antibodies, followed by a 30-minute incubation at 4°C with protein A/G-agarose beads. After five washes in ice cold-PBS-T or 1x cell lysis buffer, the proteins were eluted from the beads by heating the samples for 5 minutes at 95°C in Laemmli 3x SDS buffer (62.5 mM Tris-HCl, 2%w/v SDS, 10% glycerol, 50 mM DTT, 0.01% w/v bromophenol blue). A fraction of the eluted proteins (bead fraction) and supernatant (supe fraction) were then analyzed by western blotting (as described above) with the indicated antibodies ([62,70,109]).

Immunofluorescence

Cells were plated on coverslips and allowed to adhere. Methanol was used to fix and permeabilize the cells, followed by blocked for 1 hour in SUPER block (Thermo-Fisher). Primary antibodies were incubated overnight and washed 3 times with PBS-T(10x phosphate buffered saline, 1x MilliQ water, 1% Tween-20) Secondary antibodies were added, incubated for 2-4 hours, and washed several time with PBS-T, before mounting using PROLONG GOLD DAPI-containing mounting media (Thermo Fisher, P36930). Coverslips were allowed to dry at least 48 hours before imaging. Fluorescence was monitored using a Nikon Eclipse 50i microscope, a 40× Plan APO objective and Photometrics Coolsnap camera system. Antibodies used: Sigma, anti-Cx43 (C6219); BD Biosciences, total β-catenin (6310153)

FRAP – fluorescence recovery after photo-bleaching

The cells were plated on cover glass bottom culture dishes 72 hours before performing FRAP experiments. The cells were loaded at 37°C with calcein-AM (5 μM) for 30 minutes in DMEM media, then washed with Ringer solution for another 10 minutes to desterification of acetoxymethyl (AM) ester. The cells were kept in Ringer solution during imaging procedure. To perform the FRAP experiments, we used a confocal laser scanning microscope (A1R, Nikon Instruments, Japan) equipped with a 488-nm solid state laser (100 mW) for excitation and bleaching of calcein dye. The fluorescence emission was collected in 500 and 560 nm range and an 40X oil-immersion objective (NA 1.3) was used for the imaging. The laser output was controlled using a neutral-density filter (8 optical density) and the laser power was adjusted by software (NIS Elements, Nikon Instruments, Japan) to 2% for imaging and 20% for bleaching. 3 cells per image were randomly selected for photo-bleaching and images were acquired with 10 second intervals for 60 seconds followed by 20 second bleaching intervals. The fluorescence recovery was acquired for a 750 second period following the bleaching and normalized using pre-bleaching fluorescence intensity for each cell.

Statistics

All data are displayed as means ± standard deviations. Unless stated otherwise, experiments were repeated at least three times ($n \geq 3$). Mean expression was compared between samples by a one-way ANOVA compared to the empty vector. Data were statistically analyzed using GraphPad Prism 6 software. A p-value < 0.05 indicated statistical significance.

Chapter 4: Summary

1. Introduction

Osteoporosis, a disease of low bone mass, affects 200 million people worldwide, contributing to more than 8.9 million fractures annually and 19 million dollars in health related costs ([120]). The two most common types of osteoporosis are age/disuse induced osteoporosis and post-menopausal osteoporosis. Osteoporosis is related to the homeostatic balance of bone formation and bone resorption. When bone resorption by osteoclasts outweighs bone formation by osteoblasts, an overall catabolic response occurs leading to reduced bone mineral density and reduced bone quality. When the skeletal tissue becomes compromised, low energy bone fractures occur. Fractures commonly occur in the hip, spine, and wrist, although they can occur in other bones as well ([121]).

Intercellular communication by gap junctions plays an important role in achieving peak bone mass and determining bone quality ([53]). Through various studies, Cx43 has been shown to be required for the proper development and maintenance of the skeleton. Mutations in the gap junction protein, Cx43, result in diseases with skeletal anomalies, such as oculodentodigital dysplasia (ODDD) and craniometaphyseal dysplasia (CMD) ([28,29,31,32,82]). ODDD patients and mouse models exhibit broad, tubular bones, such as bones seen in aging and osteoporosis. In addition, connexin43 is required for the anabolic action of PTH on bone, and loss of connexin43 causes complex effects on both mechanical loading, aging and disuse. Thus, understanding Cx43's role in skeletal tissue and unraveling the ways in which gap junctional communicated signals regulated bone mass is imperative to developing potential therapies to combat diseases of skeletal fragility.

Cx43 has been shown to be beneficial during mechanical loading in bone as well as deleterious in aging and disuse ([116]). Hormonally, PTH administration to Cx43 deficient mice lead to reduced bone anabolic responses as compared to control mice ([40]). As far as mechanical loading and unloading are concerned, several studies show that mechanical loading and unloading effects the endosteal and periosteal surfaces of long bones in opposite ways ([67,72,84]), and Cx43 ablation leads to an even more severe phenotype in bone. The cortical thinning and marrow cavity widening observed in Cx43 deficient mice resembles skeletal effects of aging and space flight ([116]). Cx43 ablation was also show to prevent cortical bone formation during unloading ([46]). In the cKO model of Gja1 deletion using the Col1α1 promoter, cortical bone was resistant to the effect of Botulinum Toxin Type A (Btx A) induced muscle paralysis in comparison with wild-type mice who did exhibit expansion of the marrow cavity as well as cortical thinning, due to increases in osteoclast activity (35). One of the ODDD mouse models ($Gja1^{Jrt/+}$) also exhibited reduced bone quality, both in the trabecular and cortical compartments, as the animals were aged up to 12 months. This is an intriguing result, showing Cx43 facilitates communication of both anabolic and catabolic signals (33). These findings underscore the importance of understanding which signals are being propagated through cells by gap junctions as well as the context in which those signals are being passed.

Given the diverse roles, understanding the actual information communicated by gap junctions is important to fully understanding the role connexins play in the development and maintenance of skeletal tissue. Almost nothing is known about the specific second messengers communicated by gap junctions in bone. Our lab has shown that cAMP and inositol polyphosphates are efficiently passed through Cx43 containing gap junctions in bone cells ([61]). Likewise, the notion that Cx43 actively participates in signal is relatively novel. Here, we dramatically expand on these concepts as we establish a unique function for the Cx43 CT in bone. We expand the number of signaling complexes bound, showing for the first time the β-catenin complexes with the Cx43 CT. We define, for the first time, a unique interactome found with Cx43-conatining gap junctions which is not supported by Cx45. This concept of a unique C terminal interactome may reframe the interpretation of old data that was exclusively based on the idea that alteration in gap junction permeability is what drives the antagonistic action of Cx45 with respect to Cx43 in osteoblastogenesis. Furthermore, it is likely that diversity of signal complexes interactome may change in cell types, differentiation stage, and or disease. Understanding this diversity of recruitment of signaling machinery in future studies may provide even more specific details as to how Cx43 can cause and or be targeted for improving bone development and maintenance.

2. Major findings

2.1. <u>Central hypothesis</u>

The **<u>central hypothesis</u>** of this work is that in addition to having unique permeability, each connexin can assemble a unique "interactome" of locally recruited signaling machinery that can affect downstream signaling from the gap junction and ultimately, bone cell function.

2.2 Cx43 C terminal truncation, *in-vivo*

This work has overall shown that, in bone, the Cx43 CT is a docking platform for signaling machinery locally recruited to the gap junction for more efficient intercellular communication and these protein interactions are important contributors to the overall function of Cx43 in skeletal tissue. Cx43 truncation in mice lead to defective downstream signaling (ERK1/2/MAPK, PKCδ and β-catenin) and reduced osteoblast gene expression (Twist1, Osterix, Col1α1, Alkaline phosphatase, osteocalcin, and periostin). Altered collagen processing (Lox and Hsp47 mRNA expression, Picro-sirius red staining and quantification) was also apparent in this truncation model of Cx43CT, and a cortical bone phenotype resembling loss of the entire Cx43 protein in bone, through cortical thinning and increased marrow cavity area from Micro CT analysis ([109]).

Sexual dimorphic phenotypes have been shown in different models of Cx43 truncation, including the global truncation, *Gja1*$^{-/K258stop}$ model discussed in chapter 2. Female mice were more protected from the cortical phenotype seen in male *Gja1*$^{-/K258stop}$ mice. A similar Cx43 truncation model was recently reported, in which the same *Gja1 K258Stop* allele was combined with osteocyte-specific deletion (*Dmp1*-Cre) of a floxed *Gja1* allele and performed in 4.5 month old female mice ([45]). These female *Gja1*$^{flox/K258Stop}$; *Dmp1-Cre* mice had a strong trabecular phenotype, but no statistically significant cortical phenotype; male mice were not examined in that study ([45]). On the surface, these data appear to directly contrast the findings seen in male mice in chapter 2, as 6-week-old male *Gja1*$^{-/K258stop}$ mice had no change in trabecular parameters and had striking changes in the cortical envelope. However, based on this recent publication ([45]), a preliminary screen of 6 week old female *Gja1*$^{+/-}$ (*n*=3) and *Gja1*$^{-/K258stop}$ (*n*=4) mice was conducted, and we found comparable trends in 6 week old female *Gja1*$^{-/K258stop}$ mice in the trabecular and cortical compartments, where trabecular bone volume fraction, trabecular number and trabecular thickness approached significance (**see Table 2**). The protective effects of estrogen on cortical bone remodeling seems to be a well conserved evolutionary function of the hormone, estrogen, as females need to carry their offspring to term as well as be provide nutrients through milk, in the case of mammals.

Emerging data attribute some unique function to the Cx43 CT that may impact the interpretation of our data. In this study Cx43 was shown to be alternatively spliced, forming an C-terminal, truncated, 20kDa fragment that was found to be localized in the mitochondria along with helping traffic the full length 43kDa protein to the plasma membrane ([122,123]). Hypoxic stress has been shown to induce the expression of this smaller isoform ([124]). The smaller isoform was found to help transport mitochondria along the microtubule network within the cell, especially during oxidative stress. These data indicate an unexpected, non-canonical role of Cx43. It is unclear how loss of the 20kDa fragment may affect osteoblast function. It is possible that the Cx43 CT truncation model data is a result of loss of the smaller isoform. Further studies will be required to understand this alternate isoform's role in bone. In conclusion, this model of truncation of the Cx43 CT firmly established the requirement of the C terminus for Cx43's overall function in bone.

2.3 Cx43 CT functions:

The Cx43 CT is necessary to restrict endocortical osteoclast activity, restrain osteoprogenitor proliferation and to promote osteoblast differentiation. In the absence of the Cx43 CT, there is a bottle neck of early osteoprogenitors that fail to terminally differentiate ([109]). This leads to the increased, disorganized periosteal cortical bone apposition seen in our model of Cx43 CT truncation. Altered collagen processing (reduced mRNA expression of genes associated with collagen processing as well as defects in collagen orientation shown by Picro-sirius red staining and quantification) was also apparent in this truncation model of Cx43CT, Thus, the Cx43 CT is required for the proper export, organization, and maturation of collagen. This is important because of another disease, osteogenesis imperfecta, is a disease of brittle bones caused by collagen mutants. As mentioned previously, the conditional Cx43 knock out models also have brittle bones.

In our study, Cx43 CT was not required to support osteocyte survival. There is some controversy in the field regarding this point. A few publications in Cx43 deletion have reported increased osteocyte apoptosis, while others have not. Since our model of Cx43 CT deletion recapitulates the conditional knock out models and yet does not produce mass osteocyte apoptosis, our model suggests that osteocytic apoptosis is not a dominate factor driving the cortical phenotype in Cx43 deficiency shown by cortical thinning through periosteal expansion and endocortical resorption.

2.4 Cx43: unique functions in skeletal tissue

This unique, dual "pore and tail" function of Cx43 many not extrapolate to tissues other than bone. As stated previously, Cx43 global knock out mice die at birth due to a developmental cardiovascular defect of the ventricular outflow tract ([35,83]). In contrast to *Gja1*$^{-/-}$ mice ([35,83]), there is no lethal obstruction of the cardiac ventricular outflow tract in homozygous *Gja1*$^{K258Stop/K258stop}$ mice, though these mice die as a result of an unexpected postnatal epidermal barrier defect ([87]). This barrier defect is not present in Gja1-/K258stop mice. This is unlikely to be due to major differences in gap junction function, as in the *in vivo* model of Cx43 truncation, the resultant mutant Cx43 gap junctions traffic to the plasma membrane and form functional gap junctions with single channel properties similar to intact Cx43 containing gap junctions ([95]). However, the Cx43 K258Stop containing gap junction plaques were shown to be larger in size and fewer in number ([88]). Overall, these studies suggest a differential role for Cx43 concerning different tissues from bone, such as cardiac and skin, posing the possibility that this signaling/tail function of Cx43 is specific to skeletal tissue.

Cx45 is highly expressed in endothelial tissue of vasculature along with being expressed in bone. Cx45 has been shown to be required for development, as embryos die at E9.5/10.5 due to disruptions in vascular development, which preclude the study of bone acquisition ([22]). To date, conditional knock out models of Cx45 have not been published. Cx37, another connexin protein highly expressed in bone, is expressed in both osteoblasts and osteoclasts. However, Cx37 global knock out mice exhibit increases in overall bone mass due to defective osteoclast differentiation and no obvious defect in osteoblast function has been identified ([25]). It is possible that the connexins within the protein family, in general, contribute differently depending upon the context with which they are expressed, i.e. different tissues and different stages of differentiation.

This may be due to electrical vs chemical coupling between cells. Gap junctions have been portrayed as passive channels, whose only function is to efficiently pass small molecules, ions and second messengers between cells. Two separate, but complementary roles of gap junctions have been further distinguished in this thesis. The first is electrical coupling, which refers to depolarizing ions that are shared by cells in excitable tissues through gap junctions, such as in cardiac tissue. The second role is chemical coupling, which refers to the exchange of small molecules and nutrients through gap junctions for signaling purposes, not membrane depolarization, such as in skeletal tissue. The ability to efficiently recruit appropriate signaling machinery locally to the gap junction to allow for efficient downstream signaling in neighboring cells will be termed chemical coupling in this thesis. Electrically coupled systems like cardiac tissue, known to exhibit high endogenous Cx43 expression, may not need downstream signaling events to coordinate function among cells in the same way that chemically coupled systems like bone require for overall tissue function.

3. C terminal interactome of connexins

Having established that Cx43's C terminus is important for osteoblast differentiation and function as well as protection from the osteopenic skeletal phenotype seen in global and conditional knock out models of Cx43, we wanted to elucidate the molecular basis of the C terminus of connexins' function. To confirm the functional consequences of these interactions, chimeric connexins were generated, which fuse the Cx43 pore with the Cx45 C-terminal tail (Cx43pore-Cx45tail, aka Cx43/45) and vice versa (Cx45pore-Cx43tail, aka Cx45/43). We compared full length Cx43 and Cx45 alongside the chimeras and examined downstream signaling and gene expression in osteoblasts.

We found that, in general, both the Cx43 pore and Cx43 tail are required for optimal downstream signaling (e.g., MAPK, PKCδ and β-catenin, and pCREB) and osteoblast gene expression (e.g., COL1a1, Lox, Axin2, Osterix, and CyclinD1), as replacement of the Cx43 pore or tail domain with that of Cx45 was ineffective or inhibitory for connexin-dependent signaling and gene expression. By co-immunoprecipitation (co-IP), our data show that Cx43 complexes with ERK, CAMKII, and β-catenin. In contrast, co-IP of a myc-tagged Cx45 results in minimal co-association of these signaling proteins. These data suggest that Cx43 and Cx45 do, indeed, have different interactomes. These data infer that both channel and tails functions of a connexin protein dictate its ability to optimally regulate downstream signaling from the gap junction.

The data presented in chapter 3 lead to a new interpretation of the findings from previous in vitro studies portraying Cx45 as dominate negative in comparison with Cx43 ([110,111]). More importantly, these data may yield insights into why the connexin protein family has so many different members with overlapping permeability. The ability to appropriately recruit the local signaling machinery is required for efficient downstream signaling as well as the efficient communication of required second messengers. To effectively communicate a signal a gap junction must be able to both "share" the second messenger by having the appropriate permeability AND must also have locally recruited the appropriate signaling machinery to signal in response to the communicated second messenger. By mixing and matching permeabilities and signaling interactomes, each of the 21 different connexin proteins within this protein family can lead to very specific communication and responses to signals that can be fine-tuned and regulated by the specific connexin composition of a gap junction and the overall interactome in cells. This has implications beyond bone and skeletal tissue, in the case of other tissues where cell-cell communication is required for efficient tissue coordination.

3.1. <u>Project model</u>

Here is a summary of how Cx43 may be mediating signaling effects in cells (**Figure 4.1**). Whereby an individual cell may engage in growth factor receptor signaling, producing second messengers that initiate downstream cascades and ultimately induce Runx2/Osterix transcriptional activity and the expression of osteoblast genes. However, these second messengers may also pass through Cx43 gap junctions where they can impact the locally recruited signaling effector molecules which are bound to the CT domain, this induces efficient signal transduction activation in adjacent cells. Ultimately this coordinates cell function and increases the number of cells responding to an initial cue and a global osteogenic response. However, the repercussions of Cx43 C terminal deletion and/or replacement with Cx45 are as follows: Whereby an individual cell may engage in growth factor receptor signaling, producing second messengers that initiate downstream cascades and ultimately induce Runx2/Osterix transcriptional activity and the expression of osteoblast genes. However, despite the ability of these second messengers to pass through Cx43 gap junctions, in the absence of the Cx43 CT, the signaling effectors aren't locally recruited, and the passage of the second messengers doesn't efficiently activate downstream signaling in the neighboring cell. The replacement of Cx43 containing gap junctions with Cx45 containing gap junctions doesn’t allow for larger second messengers to be communicated to the neighboring cell. Again, with the substitution of Cx43 containing gap junctions with either chimera construct, effective signaling does not occur because of limitations on both the communication of important second messengers as well as the local recruitment of the appropriate signaling effector proteins. Ultimately, this results in reduced signal transduction activation and gene expression in adjacent cells. The mechanisms discovered from these studies are crucial to understanding how osteoblasts and osteocytes coordinate their function and how peak bone mass is achieved. The utility of this knowledge will impact therapies and strategies for controlling osteoblastogenesis,

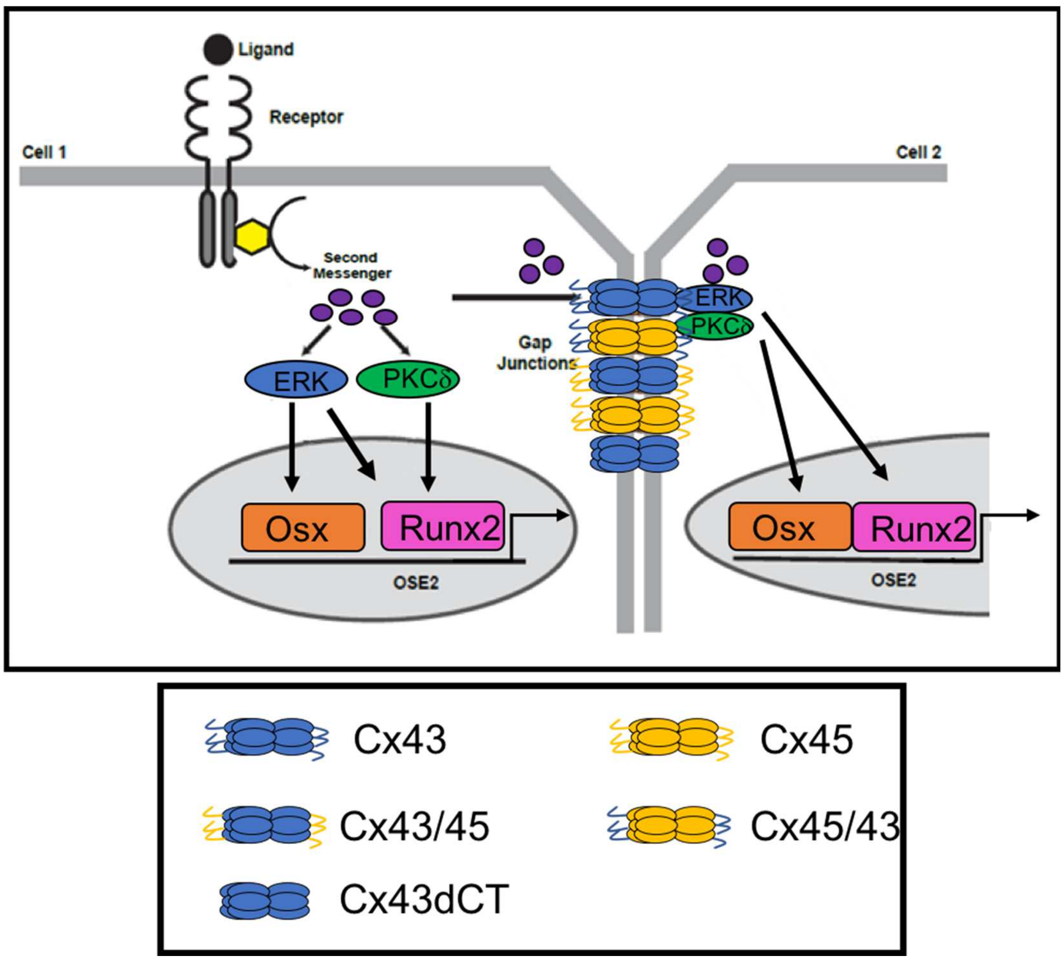

Figure 4.1. Thesis model schematic. Both pore and tail functions of Cx43 are required for optimal cell-cell communication of second messengers as well as signaling effector recruitment and gene expression. Gap junctions containing specific connexin monomers are labeled in the legend. (dCT= deltaCT, K258 truncation; only 3 C termini are shown for model simplicity.)

enhancing osteoblast responsiveness to anabolic cues, and the achievement and maintenance of peak bone mass.

3.2. __Future Directions__

Future studies could be done to investigate Cx43 and/or Cx45 as therapeutic targets to enhance bone quality or to modify specific interactions with Cx43 and/or Cx45 to shift homeostasis towards bone formation. Use of TAT-fusion proteins directed to sub-domains of the Cx43 CT, for example, could be a potential for disrupting the catabolic signals communicated through gap junctions in bone. Studies could use primary cells to directly add the fusion proteins as well as direct injection into in-vivo models to investigate the consequences of modifying specific interactions of signaling proteins with Cx43 and/or Cx45. Future studies could use CRISPR/Cas9 to disrupt these interactions *in vitro* and ultimately *in vivo* by creating point mutants or interaction domain deletions in the Cx43 CT that alter its interactome in a more refined way. FRET or anisotropy could be used as alternative methods to immunofluorescence to show protein proximity of Cx43 and Cx45 with signaling effector proteins and other protein interactions known to be important for overall cell function.

An uncertainty in the field currently is the effect of heteromeric and heterotypic gap junctions composed of multiple different connexin proteins influencing recruitment of the local signaling machinery. It's possible that all 6 C termini of one specific connexin are required for optimal recruitment and binding of signaling effectors. On the other hand, there is potential that only 3 C termini or even 1 C termini are the minimum requirement for recruitment. If, for example, only 1 Cx43 CT is required for recruitment of ERK1/2, Heterotypic gap junctions could potentially be able to contribute to optimal signaling. However, in the case of heteromeric gap junctions where one hemi-channel is composed of Cx45 monomers, the gap junction pore in total would still have different permeability characteristics, leading to differential ability to produce optimal coordination of signals and downstream signaling between cells.

Given the unexpected sexually dimorphic phenotype in the cortical bone of male and female mice lacking the Cx43 CT, further studies will also be needed to de-convolute the differences seen between sexes. An ovariectomized model of Cx43 truncation in females would be a nice model to investigate the protective role of estrogen in cortical bone maintenance.

The interactome of Cx43 is still incomplete, and we do not know if other connexins expressed at lower levels in bone influence Cx43's ability to recruit signaling machinery. Further, it is unclear if other connexins expressed in bone (e.g., Cx37, Cx40, Cx45 and Cx46) also recruit signaling machinery to their C terminus, or if this function is unique to Cx43. Mapping of all interactions with Cx43 and investigating the functional relevance of these unknown interactions in bone would be the first steps to elucidating the complete role of connexins on downstream signaling, osteoblast gene expression and overall cell function. Bio-ID, which is an agnostic, mass-spec based approach could be performed to investigate putative binding sites of both the Cx43 and Cx45 C-termini. BioID is used to screen for physiologically relevant protein interactions and the method uses a promiscuous biotin ligase to biotinylate proteins based on proximity ([125]).

These studies are important for establishing a better understanding of how gap junctions, as a protein family, regulate bone quality and have implications in diseases of skeletal fragility, such as osteoporosis. The potential impact of this work, is that understanding these interactions and the coordination of signals among bone cells will allow us to develop therapeutic interventions that can enhance or suppress signals being communicated by gap junctions to enhance bone mass and improve bone quality.

References

1. Rosen, Clifford J., Bouillon, Roger, Compston, Juliet E., Rosen V. *Primer on the Metabolic Bone Diseases and Disorders of Mineral Metabolism*. 8th ed. (Rosen, Clifford J., Bouillon, Roger, Compston, Juliet E., Rosen V., ed.). Ames, IA: John Wiley & Sons, Inc.; 2013.
2. Plotkin LI, Bellido T. Osteocytic signalling pathways as therapeutic targets for bone fragility. *Nat Rev Endocrinol*. 2016;12(10):593-605. doi:10.1038/nrendo.2016.71
3. Prideaux M, Findlay DM, Atkins GJ. Osteocytes: The master cells in bone remodelling. *Curr Opin Pharmacol*. 2016;28:24-30. doi:10.1016/j.coph.2016.02.003
4. Bonewald LF. The amazing osteocyte. *J Bone Miner Res*. 2011;26(2):229-238. doi:10.1002/jbmr.320
5. Otto F, Thornell AP, Crompton T, et al. Cbfa1, a candidate gene for cleidocranial dysplasia syndrome, is essential for osteoblast differentiation and bone development. *Cell*. 1997;89(5):765-771. doi:10.1016/S0092-8674(00)80259-7
6. Nakashima K, Zhou X, Kunkel G, et al. The novel zinc finger-containing transcription factor Osterix is required for osteoblast differentiation and bone formation. *Cell*. 2002;108(1):17-29. doi:10.1016/S0092-8674(01)00622-5
7. Buo AM, Stains JP. Gap junctional regulation of signal transduction in bone cells. *FEBS Lett*. 2014;588(8):1315-1321. doi:10.1016/j.febslet.2014.01.025
8. Gaietta G, Deerinck TJ, Adams SR, et al. Multicolor and electron microscopic imaging of connexin trafficking. *Science (80-)*. 2002;296(5567):503-507. doi:10.1126/science.1068793
9. Söhl G, Willecke K. Gap junctions and the connexin protein family. *Cardiovasc Res*. 2004;62(2):228-232. doi:10.1016/j.cardiores.2003.11.013
10. Solan JL, Lampe PD. Specific Cx43 phosphorylation events regulate gap junction turnover in vivo. In: *FEBS Letters*. Vol 588. ; 2014:1423-1429. doi:10.1016/j.febslet.2014.01.049
11. Koval M, Molina SA, Burt JM. Mix and match: Investigating heteromeric and heterotypic gap junction channels in model systems and native tissues. In: *FEBS Letters*. Vol 588. ; 2014:1193-1204. doi:10.1016/j.febslet.2014.02.025
12. Hebert C, Stains JP. An intact connexin43 is required to enhance signaling and gene expression in osteoblast-like cells. *J Cell Biochem*. 2013;114(11):2542-2550. doi:10.1002/jcb.24603
13. Hervé J-C, Derangeon M. Gap-junction-mediated cell-to-cell communication. *Cell Tissue Res*. 2013;352(1):21-31. doi:10.1007/s00441-012-1485-6
14. Hervé J-C, Derangeon M, Sarrouilhe D, Giepmans BNG, Bourmeyster N. Gap junctional channels are parts of multiprotein complexes. *Biochim Biophys Acta - Biomembr*. 2012;1818(8):1844-1865. doi:10.1016/j.bbamem.2011.12.009
15. Palatinus JA, Rhett JM, Gourdie RG. The connexin43 carboxyl terminus and cardiac gap junction organization. *Biochim Biophys Acta*. 2012;1818(8):1831-1843. doi:10.1016/j.bbamem.2011.08.006
16. Civitelli R, Beyer EC, Warlow PM, et al. Connexin43 Mediates Direct

Intercellular Communication in Human Osteoblastic Cell Networks. *Clin Invest*. 1993;91(5):1888-1896. doi:10.1172/JCI116406

17. Schirrmacher K, Schmitz I, Winterhager E. Characterization of gap junctions between osteoblast-like cells in culture. *Calcif tissue …*. 1992. http://www.springerlink.com/index/N0P8061146K61852.pdf%5Cnpapers2://publication/uuid/4668F8DC-D269-42D5-9D02-59966EC7EC57.
18. Elfgang C, Eckert R, Lichtenberg-Frate H, et al. Specific permeability and selective formation of gap junction channels in connexin-transfected HeLa cells. *J Cell Biol*. 1995;129(3):805-817. doi:10.1083/jcb.129.3.805
19. Jones SJ, Gray C, Sakamaki H, et al. The incidence and size of gap junctions between the bone cells in rat calvaria. *Anat Embryol (Berl)*. 1993;187(4):343-352. doi:10.1007/BF00185892
20. Brink PR, Valiunas V, Gordon C, Rosen MR, Cohen IS. Can gap junctions deliver? *Biochim Biophys Acta - Biomembr*. 2012;1818(8):2076-2081. doi:10.1016/j.bbamem.2011.09.025
21. Lemcke H, Steinhoff G, David R. Gap junctional shuttling of miRNA - A novel pathway of intercellular gene regulation and its prospects in clinical application. *Cell Signal*. 2015;27(12):2506-2514. doi:10.1016/j.cellsig.2015.09.012
22. Kruger O, Plum A, Kim JS, et al. Defective vascular development in connexin 45-deficient mice. *Development*. 2000;127(19).
23. Steinberg TH, Civitelli R, Geist ST, et al. Connexin43 and connexin45 form gap junctions with different molecular permeabilities in osteoblastic cells. *EMBO J*. 1994;13(4):744-750. http://www.ncbi.nlm.nih.gov/pubmed/8112289. Accessed December 5, 2016.
24. Koval M, Harley JE, Hick E, Steinberg TH. Connexin46 is retained as monomers in a trans-Golgi compartment of osteoblastic cells. *J Cell Biol*. 1997;137(4):847-857. doi:10.1083/jcb.137.4.847
25. Pacheco-Costa R, Hassan I, Reginato RD, et al. High bone mass in mice lacking Cx37 because of defective osteoclast differentiation. *J Biol Chem*. 2014;289(12):8508-8520. doi:10.1074/jbc.M113.529735
26. Schilling AF, Filke S, Lange T, et al. Gap junctional communication in human osteoclasts in vitro and in vivo. *J Cell Mol Med*. 2008;12(6A):2497-2504. doi:10.1111/j.1582-4934.2008.00275.x
27. Ilvesaro J, Nen KVN, Tuukkanen J. Bone-Resorbing Osteoclasts Contain Gap-Junctional Connexin-43*. *J Bone Miner Res*. 2000;15(5):909-926. doi:10.1359/jbmr.2000.15.5.919
28. Paznekas WA, Boyadjiev SA, Shapiro RE, et al. Connexin 43 (GJA1) mutations cause the pleiotropic phenotype of oculodentodigital dysplasia. *Am J Hum Genet*. 2003;72(2):408-418. doi:10.1086/346090
29. Hu Y, Chen I-P, de Almeida S, et al. A novel autosomal recessive GJA1 missense mutation linked to Craniometaphyseal dysplasia. *PLoS One*. 2013;8(8):e73576. doi:10.1371/journal.pone.0073576
30. Roscoe W, Veitch GIL, Gong X-Q, et al. Oculodentodigital dysplasia-causing connexin43 mutants are non-functional and exhibit dominant effects on wild-type connexin43. *J Biol Chem*. 2005;280(12):11458-11466. doi:10.1074/jbc.M409564200

31. Flenniken AM, Osborne LR, Anderson N, et al. A Gja1 missense mutation in a mouse model of oculodentodigital dysplasia. *Development*. 2005;132(19).
32. Dobrowolski R, Sasse P, Schrickel JW, et al. The conditional connexin43G138R mouse mutant represents a new model of hereditary oculodentodigital dysplasia in humans. *Hum Mol Genet*. 2008;17(4):539-554. doi:10.1093/hmg/ddm329
33. Watkins M, Grimston SK, Norris JY, et al. Osteoblast connexin43 modulates skeletal architecture by regulating both arms of bone remodeling. *Mol Biol Cell*. 2011;22(8):1240-1251. doi:10.1091/mbc.E10-07-0571
34. Lecanda F, Warlow PM, Sheikh S, Furlan F, Steinberg TH, Civitelli R. Connexin43 deficiency causes delayed ossification, craniofacial abnormalities, and osteoblast dysfunction. *J Cell Biol*. 2000;151(4):931-944. http://www.ncbi.nlm.nih.gov/pubmed/11076975. Accessed November 30, 2016.
35. Reaume a G, de Sousa P a, Kulkarni S, et al. Cardiac malformation in neonatal mice lacking connexin43. *Science*. 1995;267(5205):1831-1834. doi:10.1126/science.7892609
36. Misu A, Yamanaka H, Aramaki T, et al. Two different functions of Connexin43 confer two different bone phenotypes in zebrafish. *J Biol Chem*. 2016;291(24):12601-12611. doi:10.1074/jbc.M116.720110
37. Hoptak-Solga AD, Klein KA, DeRosa AM, White TW, Iovine MK. Zebrafish short fin mutations in connexin43 lead to aberrant gap junctional intercellular communication. *FEBS Lett*. 2007;581(17):3297-3302. doi:10.1016/j.febslet.2007.06.030
38. Iovine MK, Higgins EP, Hindes A, Coblitz B, Johnson SL. Mutations in connexin43 (GJA1) perturb bone growth in zebrafish fins. *Dev Biol*. 2005;278(1):208-219. doi:10.1016/j.ydbio.2004.11.005
39. Sims K, Eble DM, Iovine MK. Connexin43 regulates joint location in zebrafish fins. *Dev Biol*. 2009;327(2):410-418. doi:10.1016/j.ydbio.2008.12.027
40. Chung DJ, Castro CHM, Watkins M, et al. Low peak bone mass and attenuated anabolic response to parathyroid hormone in mice with an osteoblast-specific deletion of connexin43. *J Cell Sci*. 2006;119(20).
41. Grimston SK, Brodt MD, Silva MJ, Civitelli R. Attenuated response to in vivo mechanical loading in mice with conditional osteoblast ablation of the connexin43 gene (Gja1). *J Bone Miner Res*. 2008;23(6):879-886. doi:10.1359/jbmr.080222
42. Watkins MP, Norris JY, Grimston SK, et al. Bisphosphonates improve trabecular bone mass and normalize cortical thickness in ovariectomized, osteoblast connexin43 deficient mice. *Bone*. 2012;51(4):787-794. doi:10.1016/j.bone.2012.06.018
43. Bivi N, Nelson MT, Faillace ME, Li J, Miller LM, Plotkin LI. Deletion of Cx43 from osteocytes results in defective bone material properties but does not decrease extrinsic strength in cortical bone. *Calcif Tissue Int*. 2012;91(3):215-224. doi:10.1007/s00223-012-9628-z
44. Bivi N, Condon KW, Allen MR, et al. Cell autonomous requirement of connexin 43 for osteocyte survival: consequences for endocortical resorption and periosteal bone formation. *J Bone Miner Res*. 2012;27(2):374-389. doi:10.1002/jbmr.548
45. Pacheco-Costa R, Davis HM, Atkinson EG, Katchburian E, Plotkin LI, Reginato RD. Osteocytic connexin 43 is not required for the increase in bone mass induced

by intermittent PTH administration in male mice. *J Musculoskelet Neuronal Interact*. 2016;16(1):45-57.
46. Lloyd SA, Loiselle AE, Zhang Y, Donahue HJ. Connexin 43 deficiency desensitizes bone to the effects of mechanical unloading through modulation of both arms of bone remodeling. *Bone*. 2013;57(1):76-83. doi:10.1016/j.bone.2013.07.022
47. Lloyd SA, Loiselle AE, Zhang Y, Donahue HJ. Evidence for the role of connexin 43-mediated intercellular communication in the process of intracortical bone resorption via osteocytic osteolysis. *BMC Musculoskelet Disord*. 2014;15(1). doi:10.1186/1471-2474-15-122
48. Komori T. Mouse Models for the Evaluation of Osteocyte Functions. *J bone Metab*. 2014;21:55-60. doi:10.11005/jbm.2014.21.1.55
49. Tatsumi S, Ishii K, Amizuka N, et al. Targeted Ablation of Osteocytes Induces Osteoporosis with Defective Mechanotransduction. *Cell Metab*. 2007;5(6):464-475. doi:10.1016/j.cmet.2007.05.001
50. Li M, Hasegawa T, Hogo H, et al. Histological examination on osteoblastic activities in the alveolar bone of transgenic mice with induced ablation of osteocytes. *Histol Histopathol*. 2013;28(3):327-335. doi:10.14670/HH-28.327
51. Moriishi T, Maruyama Z, Fukuyama R, et al. Overexpression of Bcl2 in osteoblasts inhibits osteoblast differentiation and induces osteocyte apoptosis. *PLoS One*. 2011;6(11). doi:10.1371/journal.pone.0027487
52. Jahani M, Genever PG, Patton RJ, Ahwal F, Fagan MJ. The effect of osteocyte apoptosis on signalling in the osteocyte and bone lining cell network: A computer simulation. *J Biomech*. 2012;45(16):2876-2883. doi:10.1016/j.jbiomech.2012.08.005
53. Stains JP, Civitelli R. Connexins in the skeleton. *Semin Cell Dev Biol*. 2016;50:31-39. doi:10.1016/j.semcdb.2015.12.017
54. Grimston SK, Watkins MP, Stains JP, Civitelli R. Connexin43 modulates post-natal cortical bone modeling and mechano-responsiveness. *Bonekey Rep*. 2013;2(November):1-8. doi:10.1038/bonekey.2013.180
55. Lloyd SA, Loiselle AE, Zhang Y, Donahue HJ. Shifting paradigms on the role of connexin43 in the skeletal response to mechanical load. *J Bone Miner Res*. 2014;29(2):275-286. doi:10.1002/jbmr.2165
56. Ellison D, Mugler A, Brennan MD, et al. Cell–cell communication enhances the capacity of cell ensembles to sense shallow gradients during morphogenesis. *Proc Natl Acad Sci*. 2016;113(6):E679-E688. doi:10.1073/pnas.1516503113
57. Henriksen Z, Hiken JF, Steinberg TH, Jørgensen NR. The predominant mechanism of intercellular calcium wave propagation changes during long-term culture of human osteoblast-like cells. *Cell Calcium*. 2006;39(5):435-444. doi:10.1016/j.ceca.2006.01.012
58. Geneau G, Defamie N, Mesnil M, Cronier L. Endothelin1-induced Ca2+ mobilization is altered in calvarial osteoblastic cells of Cx43+/- mice. In: *Journal of Membrane Biology*. Vol 217. ; 2007:71-81. doi:10.1007/s00232-007-9024-1
59. Jørgensen NR, Geist ST, Civitelli R, Steinberg TH. ATP- and gap junction-dependent intercellular calcium signaling in osteoblastic cells. *J Cell Biol*. 1997;139(2):497-506. doi:10.1083/jcb.139.2.497

60. Ishihara Y, Kamioka H, Honjo T, Ueda H, Takano-Yamamoto T, Yamashiro T. Hormonal, pH, and calcium regulation of connexin 43-mediated dye transfer in osteocytes in chick calvaria. *J Bone Miner Res*. 2008;23(3):350-360. doi:10.1359/jbmr.071102
61. Gupta A, Anderson H, Buo AM, Moorer MC, Ren M, Stains JP. Communication of cAMP by connexin43 gap junctions regulates osteoblast signaling and gene expression. *Cell Signal*. 2016;28(8). doi:10.1016/j.cellsig.2016.04.014
62. Niger C, Luciotti MA, Buo AM, Hebert C, Ma V, Stains JP. The regulation of runt-related transcription factor 2 by fibroblast growth factor-2 and connexin43 requires the inositol polyphosphate/protein kinase Cδ cascade. *J Bone Miner Res*. 2013;28(6):1468-1477. doi:10.1002/jbmr.1867
63. Genetos DC, Kephart CJ, Zhang Y, Yellowley CE, Donahue HJ. Oscillating fluid flow activation of gap junction hemichannels induces ATP release from MLO-Y4 osteocytes. *J Cell Physiol*. 2007;212(1):207-214. doi:10.1002/jcp.21021
64. Romanello M, Pani B, Bicego M, D'Andrea P. Mechanically induced ATP release from human osteoblastic cells. *Biochem Biophys Res Commun*. 2001;289(5):1275-1281. doi:10.1006/bbrc.2001.6124
65. Cherian PP. Mechanical Strain Opens Connexin 43 Hemichannels in Osteocytes: A Novel Mechanism for the Release of Prostaglandin. *Mol Biol Cell*. 2005;16(7):3100-3106. doi:10.1091/mbc.E04-10-0912
66. Siller-Jackson AJ, Burra S, Gu S, et al. Adaptation of connexin 43-hemichannel prostaglandin release to mechanical loading. *J Biol Chem*. 2008;283(39):26374-26382. doi:10.1074/jbc.M803136200
67. Xu H, Gu S, Riquelme MA, et al. Connexin 43 channels are essential for normal bone structure and osteocyte viability. *J Bone Miner Res*. 2015;30(3):436-448. doi:10.1002/jbmr.2374
68. Thi MM, Islam S, Suadicani SO, Spray DC. Connexin43 and Pannexin1 channels in osteoblasts: Who is the "hemichannel"? *J Membr Biol*. 2012;245(7):401-409. doi:10.1007/s00232-012-9462-2
69. Lima F, Niger C, Hebert C, Stains JP. Connexin43 potentiates osteoblast responsiveness to fibroblast growth factor 2 via a protein kinase C-delta/Runx2-dependent mechanism. *Mol Biol Cell*. 2009;20(11):2697-2708. doi:10.1091/mbc.E08-10-1079
70. Niger C, Buo AM, Hebert C, Duggan BT, Williams MS, Stains JP. ERK acts in parallel to PKCδ to mediate the connexin43-dependent potentiation of Runx2 activity by FGF2 in MC3T3 osteoblasts. *Am J Physiol Cell Physiol*. 2012;302(7):C1035-44. doi:10.1152/ajpcell.00262.2011
71. Stains JP, Civitelli R. Gap junctions regulate extracellular signal-regulated kinase signaling to affect gene transcription. *Mol Biol Cell*. 2005;16(1):64-72. doi:10.1091/mbc.E04-04-0339
72. Bivi N, Pacheco-Costa R, Brun LR, et al. Absence of Cx43 selectively from osteocytes enhances responsiveness to mechanical force in mice. *J Orthop Res*. 2013;31(7):1075-1081. doi:10.1002/jor.22341
73. Niger C, Lima F, Yoo DJ, et al. The transcriptional activity of osterix requires the recruitment of Sp1 to the osteocalcin proximal promoter. *Bone*. 2011;49(4):683-692. doi:10.1016/j.bone.2011.07.027

74. Stains JP, Lecanda F, Screen J, Towler DA, Civitelli R. Gap junctional communication modulates gene transcription by altering the recruitment of Sp1 and Sp3 to connexin-response elements in osteoblast promoters. *J Biol Chem*. 2003;278(27):24377-24387. doi:10.1074/jbc.M212554200
75. Plotkin LI, Manolagas SC, Bellido T. Transduction of cell survival signals by connexin-43 hemichannels. *J Biol Chem*. 2002;277(10):8648-8657. doi:10.1074/jbc.M108625200
76. Plotkin LI, Aguirre JI, Kousteni S, Manolagas SC, Bellido T. Bisphosphonates and estrogens inhibit osteocyte apoptosis via distinct molecular mechanisms downstream of extracellular signal-regulated kinase activation. *J Biol Chem*. 2005;280(8):7317-7325. doi:10.1074/jbc.M412817200
77. Bivi N, Lezcano V, Romanello M, Bellido T, Plotkin LI. Connexin43 interacts with βarrestin: a pre-requisite for osteoblast survival induced by parathyroid hormone. *J Cell Biochem*. 2011;112(10):2920-2930. doi:10.1002/jcb.23208
78. Batra N, Burra S, Siller-Jackson AJ, et al. Mechanical stress-activated integrin α5β1 induces opening of connexin 43 hemichannels. *Proc Natl Acad Sci U S A*. 2012;109(9):3359-3364. doi:10.1073/pnas.1115967109
79. Pacheco-Costa R, Davis HM, Sorenson C, et al. Defective cancellous bone structure and abnormal response to PTH in cortical bone of mice lacking Cx43 cytoplasmic C-terminus domain. *Bone*. 2015;81:632-643. doi:10.1016/j.bone.2015.09.011
80. Hammond MA, Berman AG, Pacheco-Costa R, Davis HM, Plotkin LI, Wallace JM. Removing or truncating connexin 43 in murine osteocytes alters cortical geometry, nanoscale morphology, and tissue mechanics in the tibia. *Bone*. 2016;88:85-91. doi:10.1016/j.bone.2016.04.021
81. Kelly JJ, Simek J, Laird DW. Mechanisms linking connexin mutations to human diseases. *Cell Tissue Res*. 2015;360(3):701-721. doi:10.1007/s00441-014-2024-4
82. Laird DW. Syndromic and non-syndromic disease-linked Cx43 mutations. *FEBS Lett*. 2014;588(8):1339-1348. doi:10.1016/j.febslet.2013.12.022
83. Ya J, Erdtsieck-Ernste EBHW, de Boer PAJ, et al. Heart Defects in Connexin43-Deficient Mice. *Circ Res*. 1998;82(3).
84. Zhang Y, Paul EM, Sathyendra V, et al. Enhanced osteoclastic resorption and responsiveness to mechanical load in gap junction deficient bone. *PLoS One*. 2011;6(8):e23516. doi:10.1371/journal.pone.0023516
85. Solan JL, Lampe PD. Connexin43 phosphorylation: structural changes and biological effects. *Biochem J*. 2009;419(2):261-272. doi:10.1042/BJ20082319
86. Niger C, Hebert C, Stains JP. Interaction of connexin43 and protein kinase C-delta during FGF2 signaling. *BMC Biochem*. 2010;11(1):14. doi:10.1186/1471-2091-11-14
87. Maass K, Ghanem A, Kim J-S, et al. Defective epidermal barrier in neonatal mice lacking the C-terminal region of connexin43. *Mol Biol Cell*. 2004;15(10):4597-4608. doi:10.1091/mbc.E04-04-0324
88. Maass K, Shibayama J, Chase SE, Willecke K, Delmar M. C-terminal truncation of connexin43 changes number, size, and localization of cardiac gap junction plaques. *Circ Res*. 2007;101(12):1283-1291. doi:10.1161/CIRCRESAHA.107.162818

89. Bauman TM, Nicholson TM, Abler LL, et al. Characterization of fibrillar collagens and extracellular matrix of glandular benign prostatic hyperplasia nodules. *PLoS One*. 2014;9(10). doi:10.1371/journal.pone.0109102
90. Rich L, Whittaker P. Collagen and Picrosirius Red Staining : a Polarized Light Assessment of Fibrillar Hue and Spatial Distribution. *Braz J Morphol Sci*. 2005;22(2):97-104. http://jms.org.br/PDF/v22n2a06.pdf.
91. Christiansen HE, Schwarze U, Pyott SM, et al. Homozygosity for a Missense Mutation in SERPINH1, which Encodes the Collagen Chaperone Protein HSP47, Results in Severe Recessive Osteogenesis Imperfecta. *Am J Hum Genet*. 2010;86(3):389-398. doi:10.1016/j.ajhg.2010.01.034
92. Drögemüller C, Becker D, Brunner A, et al. A missense mutation in the SERPINH1 gene in Dachshunds with osteogenesis imperfecta. *PLoS Genet*. 2009;5(7). doi:10.1371/journal.pgen.1000579
93. Kojima T, Miyaishi O, Saga S, Ishiguro N, Tsutsui Y, Iwata H. The retention of abnormal type I procollagen and correlated expression of HSP 47 in fibroblasts from a patient with lethal osteogenesis imperfecta. *J Pathol*. 1998;184(2):212-218. doi:10.1002/(SICI)1096-9896(199802)184:2<212::AID-PATH996>3.0.CO;2-Z
94. Miraoui H, Marie PJ. Pivotal role of Twist in skeletal biology and pathology. *Gene*. 2010;468(1-2):1-7. doi:10.1016/j.gene.2010.07.013
95. Cina C, Maass K, Theis M, Willecke K, Bechberger JF, Naus CC. Involvement of the Cytoplasmic C-Terminal Domain of Connexin43 in Neuronal Migration. *J Neurosci*. 2009;29(7):2009-2021. doi:10.1523/JNEUROSCI.5025-08.2009
96. Plotkin LI. Connexin 43 hemichannels and intracellular signaling in bone cells. *Front Physiol*. 2014;5 APR. doi:10.3389/fphys.2014.00131
97. Plotkin LI, Bellido T. Beyond gap junctions: Connexin43 and bone cell signaling. *Bone*. 2013;52(1):157-166. doi:10.1016/j.bone.2012.09.030
98. Ge C, Xiao G, Jiang D, Franceschi RT. Critical role of the extracellular signal–regulated kinase–MAPK pathway in osteoblast differentiation and skeletal development. *J Cell Biol*. 2007;176(5):709-718. doi:10.1083/jcb.200610046
99. Kobayashi Y, Uehara S, Koide M, Takahashi N. The regulation of osteoclast differentiation by Wnt signals. *Bonekey Rep*. 2015;4. doi:10.1038/bonekey.2015.82
100. Tu X, Joeng KS, Nakayama KI, et al. Noncanonical Wnt signaling through G protein-linked PKCdelta activation promotes bone formation. *Dev Cell*. 2007;12(1):113-127. doi:10.1016/j.devcel.2006.11.003
101. Callewaert F, Venken K, Kopchick JJ, et al. Sexual dimorphism in cortical bone size and strength but not density is determined by independent and time-specific actions of sex steroids and IGF-1: Evidence from pubertal mouse models. *J Bone Miner Res*. 2010;25(3):617-626. doi:10.1359/jbmr.090828
102. Callewaert F, Sinnesael M, Gielen E, Boonen S, Vanderschueren D. Skeletal sexual dimorphism: Relative contribution of sex steroids, GH-IGF1, and mechanical loading. *J Endocrinol*. 2010;207(2):127-134. doi:10.1677/JOE-10-0209
103. Manolagas SC, O’Brien CA, Almeida M. The role of estrogen and androgen receptors in bone health and disease. *Nat Rev Endocrinol*. 2013;9(12):699-712. doi:10.1038/nrendo.2013.179

104. Gupta RR, Kim H, Chan Y-K, et al. Axial strain enhances osteotomy repair with a concomitant increase in connexin43 expression. *Bone Res*. 2015;3:15007. doi:10.1038/boneres.2015.7
105. Gupta A, Niger C, Buo AM, Eidelman ER, Chen RJ, Stains JP. Connexin43 enhances the expression of osteoarthritis-associated genes in synovial fibroblasts in culture. *BMC Musculoskelet Disord*. 2014;15(1). doi:10.1186/1471-2474-15-425
106. Nanjundaiah SM, Venkatesha SH, Yu H, Tong L, Stains JP, Moudgil KD. Celastrus and its bioactive celastrol protect against bone damage in autoimmune arthritis by modulating osteoimmune cross-talk. *J Biol Chem*. 2012;287(26):22216-22226. doi:10.1074/jbc.M112.356816
107. Castro CHM. Targeted expression of a dominant-negative N-cadherin in vivo delays peak bone mass and increases adipogenesis. *J Cell Sci*. 2004;117(13):2853-2864. doi:10.1242/jcs.01133
108. Tomlinson RE, Silva MJ. HIF-1α regulates bone formation after osteogenic mechanical loading. *Bone*. 2015;73:98-104. doi:10.1016/j.bone.2014.12.015
109. Moorer MC, Hebert C, Tomlinson RE, Iyer SR, Chason M, Stains JP. Defective signaling, osteoblastogenesis and bone remodeling in a mouse model of connexin 43 C-terminal truncation. *J Cell Sci*. 2017;130(3). doi:10.1242/jcs.197285
110. Koval M, Geist ST, Westphale EM, et al. Transfected connexin45 alters gap junction permeability in cells expressing endogenous connexin43. *J Cell Biol*. 1995;130(4):987-995. http://www.ncbi.nlm.nih.gov/pubmed/7642714. Accessed November 30, 2016.
111. Lecanda F, Towler DA, Ziambaras K, et al. Gap junctional communication modulates gene expression in osteoblastic cells. *Mol Biol Cell*. 1998;9(8):2249-2258. http://www.ncbi.nlm.nih.gov/pubmed/9693379. Accessed November 30, 2016.
112. Grimston SK, Fontana F, Watkins M, Civitelli R. Heterozygous deletion of both sclerostin (Sost) and connexin43 (Gja1) genes in mice is not sufficient to impair cortical bone modeling. *PLoS One*. 2017;12(11). doi:10.1371/journal.pone.0187980
113. Mbalaviele G, Sheikh S, Stains JP, et al. ??-catenin and BMP-2 synergize to promote osteoblast differentiation and new bone formation. *J Cell Biochem*. 2005;94(2):403-418. doi:10.1002/jcb.20253
114. Laing JG, Manley-Markowski RN, Koval M, Civitelli R, Steinberg TH. Connexin45 Interacts with Zonula Occludens-1 and Connexin43 in Osteoblastic Cells. *J Biol Chem*. 2001;276(25):23051-23055. doi:10.1074/jbc.M100303200
115. Zappitelli T, Chen F, Moreno L, et al. The G60S connexin 43 mutation activates the osteoblast lineage and results in a resorption-stimulating bone matrix and abrogation of old-age-related bone loss. *J Bone Miner Res*. 2013;28(11):2400-2413. doi:10.1002/jbmr.1965
116. Ruff C, Hayes W. Subperiosteal expansion and cortical remodeling of the human femur and tibia with aging. *Science (80-)*. 1982;217(4563):945-948. doi:10.1126/science.7112107
117. Grimston SK, Goldberg DB, Watkins M, Brodt MD, Silva MJ, Civitelli R. Connexin43 deficiency reduces the sensitivity of cortical bone to the effects of

muscle paralysis. *J Bone Miner Res*. 2011;26(9):2151-2160. doi:10.1002/jbmr.425
118. Buo AM, Tomlinson RE, Eidelman ER, Chason M, Stains JP. Connexin43 and Runx2 Interact to Affect Cortical Bone Geometry, Skeletal Development, and Osteoblast and Osteoclast Function. *J Bone Miner Res*. 2017;32(8):1727-1738. doi:10.1002/jbmr.3152
119. Gupta A, Anderson H, Buo AMAM, Moorer MCMC, Ren M, Stains JPJP. Communication of cAMP by connexin43 gap junctions regulates osteoblast signaling and gene expression. *Cell Signal*. 2016;28(8):1048-1057. doi:10.1016/j.cellsig.2016.04.014
120. Facts and Statistics | International Osteoporosis Foundation. https://www.iofbonehealth.org/facts-statistics.
121. National Osteoporosis Foundation. https://www.nof.org/patients/what-is-osteoporosis/). Published 2017.
122. Fu Y, Zhang SS, Xiao S, et al. Cx43 isoform GJA1-20k promotes microtubule dependent mitochondrial transport. *Front Physiol*. 2017;8(NOV):1-12. doi:10.3389/fphys.2017.00905
123. Basheer W, Shaw R. The “tail” of Connexin43: An unexpected journey from alternative translation to trafficking. *Biochim Biophys Acta - Mol Cell Res*. 2016;1863(7):1848-1856. doi:10.1016/j.bbamcr.2015.10.015
124. Ul-Hussain M, Olk S, Schoenebeck B, et al. Internal ribosomal entry site (IRES) activity generates endogenous carboxyl-terminal domains of Cx43 and is responsive to hypoxic conditions. *J Biol Chem*. 2014;289(30):20979-20990. doi:10.1074/jbc.M113.540187
125. Roux KJ, Kim DI, Burke B, Roux KJ, Kim DI, Burke B. BioID: A Screen for Protein-Protein Interactions. In: *Current Protocols in Protein Science*. Hoboken, NJ, USA: John Wiley & Sons, Inc.; 2013:19.23.1-19.23.14. doi:10.1002/0471140864.ps1923s74